NOTICE

The quality of this microform is heavily dependent upon the quality of the original thesis submitted for microfilming. Every effort has been made to ensure the highest quality of reproduction possible.

If pages are missing, contact the university which granted the degree.

Some pages may have indistinct print especially if the original pages were typed with a poor typewriter ribbon or if the university sent us an inferior photocopy.

Reproduction in full or in part of this microform is governed by the Canadian Copyright Act, R.S.C. 1970, c. C-30, and subsequent amendments.

AVIS

La qualité de cette microforme dépend grandement de la qualité de la thèse soumise au microfilmage. Nous avons tout fait pour assurer une qualité supérieure de reproduction.

S'il manque des pages, veuillez communiquer avec l'université qui a conféré le grade.

La qualité d'impression de certaines pages peut laisser à désirer, surtout si les pages originales ont été dactylographiées à l'aide d'un ruban usé ou si l'université nous a fait parvenir une photocopie de qualité inférieure.

La reproduction, même partielle, de cette microforme est soumise à la Loi canadienne sur le droit d'auteur, SRC 1970, c. C-30, et ses amendements subséquents.

Effect of Oil Contamination on the Properties of Sand

by

Faouzi Ben Amor

Thesis submitted to the School of Graduate Studies
as partial fulfillment of the requirements
for the degree of M.A.Sc. in
Civil Engineering

UNIVERSITY OF OTTAWA
OTTAWA, CANADA, 1990.

NOTICE

The quality of this microform is heavily dependent upon the quality of the original thesis submitted for microfilming. Every effort has been made to ensure the highest quality of reproduction possible.

If pages are missing, contact the university which granted the degree.

Some pages may have indistinct print especially if the original pages were typed with a poor typewriter ribbon or if the university sent us an inferior photocopy.

Reproduction in full or in part of this microform is governed by the Canadian Copyright Act, R.S.C. 1970, c. C-30, and subsequent amendments.

AVIS

La qualité de cette microforme dépend grandement de la qualité de la thèse soumise au microfilmage. Nous avons tout fait pour assurer une qualité supérieure de reproduction.

S'il manque des pages, veuillez communiquer avec l'université qui a conféré le grade.

La qualité d'impression de certaines pages peut laisser à désirer, surtout si les pages originales ont été dactylographiées à l'aide d'un ruban usé ou si l'université nous a fait parvenir une photocopie de qualité inférieure.

La reproduction, même partielle, de cette microforme est soumise à la Loi canadienne sur le droit d'auteur, SRC 1970, c. C-30, et ses amendements subséquents.

ISBN 0-315-60598-7

UNIVERSITÉ D'OTTAWA
UNIVERSITY OF OTTAWA

Summary

Oil contamination of soils is frequently occuring specially in recent years. This may be for, example, due to an oil spill from a tanker or a leakage from a pipeline. In most cases, investigations were carried out to find the effect of oil contamination on the groundwater conditions or animal life. However, oil contamination might also affect the geotechnical properties of soils.

Considering that oil is capable of altering the frictional resistance of all surfaces, it may be expected that the angle of internal friction of sand also change if oil penetrates its pores. The experimental part of the present research is an attempt to find out how much the behaviour of sand is affected by oil contamination.

Laboratory experiments have been performed on clean and oil contaminated sand samples. The results of a series of conventional triaxial compression tests showed that oil contamination resulted in a significant reduction in the angle of internal friction. Furthermore, the behaviour of an interface between sand and two different structural materials was investigated. Oil contamination of the interface resulted in a relatively small changes of the interface friction angle.

Practical examples were used to illustrate the effect of oil contamination. The bearing capacity and sliding resistance of a retaining wall, and the factor of safety of a slope were evaluated for both clean and oil contaminated sands.

The effect of oil contamination may be modelled using advanced mathematical models for soils. Lade's work hardening model which was modified to compensate for plastic strains resulting from proportional loading Evgin (1981), has been used in this study. The modified model has been coded in a computer program, KLADE. The model parameters for both clean and oil contaminated sand were

determined and predictions were made for the soil behaviour in tests using the computer program.

Acknowledgement

I wish to express my gratitude tc Dr. E. Evgin for his patiency, continuous encouragement and invaluable suggestions throughout the research and would like to thank my colleague Ameir Altaee for his help and generosity.
I would like to express my sincere thanks to the Tunisian government for providing financial support.

The financial support for this research provided by EMR Research Agreement Program (Contract No. 90.9.237, Contract Officier: S. Lord) is greatly appreciated.

Dedication

This thesis is dedicated to my fiancée Vicky Duford.

Nomonclature

Symbol	Definition
K_1, RLK1	stress level at failure
K_{ur}, RLKUR	modulus number
σ_3, SIGMA3	confining pressure
σ_n	normal stress
I_1, I_2, I_3	stress invarients
W_p	plastic work
W_c	work from collapse strains
f_p, RLFP	stress level related to the cone
f_c, RLFC	stress level related to the cap
f_t, RLFT	threshold stress level
ν, MU	Poisson's ratio
p_a, PA	atmospheric pressure
f	yield function
g	plastic potential function
PNEW	new state of stress vector
PRE	old state of stress vector
CURFP	current value of f_p
CURFC	current value of f_c
P.W.P	pore water pressure
M and l	work hardening parameters
C and p	plastic collapse parameters
A, RLA	work hardening parameter
r_f, RF	failure ratio
λ	proportionality constant
ϕ	internal friction angle
δ	interface angle

Contents

List of Tables

List of Figures

Chapter 1

Introduction

In the last 15 years, there has been considerable research into the effect of petroleum in the environment. Most of this work has focused on the problem of marine crude oil spills and some literature now exists on this topic as reviewed recently by the National Academy of Sciences (1985). Current research is reported in the *Oil Spill Conference Proceedings* (American Petroleum Institute, 1985), in the proceedings of the Arctic Marine Oilspill Technical Seminar (Environment Canada, 1985), and journals such as Oil and Petrochemical Pollution.

It has become increasingly apparent that the regimes in which oil is most harmfull and persistent are from active microbial oxidation and from photolysis (as occurs on the sea surface). More attention is thus being devoted to cleaning oil incorporated into sediments of shorelines. A particular recent concern has been related to the incidents in which petroleum fractions have become incorporated into soils, have undergone some vertical and horizontal migration as a bulk oil phase, and have additionally migrated in air and groundwater phases resulting in more widespread contamination of drinking water supplies (Feenstra and Cherry,

1988). In many cases, indoor basement atmospheres have been contaminated causing additional risk of fire and explosion.

There are several sources of oil contamination: leaking underground storage tanks, pipelines, landfill sites and dumps, periodic spillage at industrial and refueling facilities, and accidental spills during transportation. One of the most dramatic oil spills happened recently in Valdez, Alaska 1989 where the oil tanker Exxon Valdez poured millions of gallons of crude oil into Alaska's Prince William Sound for almost two weeks, creating a deadly slick covering more than 2,590 square kilometers.

The mechanism of oil contamination and its rate of dissipation has been addressed by Mackay (1987) who showed that the rate of the oil going through the unsaturated soil zone by replacing the air and possibly some water is primarly controlled by:

1. the viscosity of oil (a low-viscosity gasoline moving rapidly, a high-viscosity fuel oil moving slowly)
2. the porosity or permeability of the soil (a loose sandy soil being very permeable and a clay almost impermeable)
3. the moisture of the soil as a secondary influence

Although subsurface migration of oil and other petroleum products has been addressed by many researcher, the effect of the presence of oil on the engineering properties and particularly mechanical behaviour of soils has not yet been given any importance. Therefore, in the current design practice it is probably assumed that the properties of the soil remain unchanged during the lifetime of the structure.

The shear strength of a soil is related to the angle of internal friction. Considering that oil is capable of altering the frictional resistance of any surface, it is likely that the internal friction of soils will also change if oil is allowed to go into the pores. However, to what extent the oil will alter the shear strength and deformation characteristics of a soil has to be determined experimentally. There are many variables in such an investigation, notably: soil type, permeability, density, insitu stresses, type of oil, viscosity, temperature, rate of testing, percentage of saturation, etc.

Viscous effects due to oil contamination might be significant in the behaviour of sand. A material which is a frictional type may start behaving as a viscous type, however in the present research such effect was not investigated.

If oil contamination affects the strength and deformation properties of soils then this has to be considered in the design of the structures where a spill is possible. In order to analyze the effect of changes in soil properties on the behaviour of soil structures, a mathematical model simulating the stress-strain response of the soil is required. There are many soil models developed for the purpose of predicting soil behaviour, such as, Roscoe and Burland (1968), Chang and Duncan (1970), Lade (1972), Lade (1977), Prevost (1986), Bardet (1986), etc.

Lade's model in its modified form (Evgin, 1981) has been chosen in the present research because it incorporates the most important aspects of soil behaviour.

1.1 Objectives of Research

The main objectives of this study are:

1. to determine the effect of oil contamination on the properties of sand.

2. to investigate the effect of oil contamination on the behaviour of the interfaces between sand and different structural materials.

3. to model mathematically the stress strain behaviour of clean and oil contaminated sand.

4. to investigate the effect of oil contamination on the behaviour of some engineering structures.

1.2 Scope of Research

1. Perform a series of undrained, drained conventional triaxial compression tests on sand.

2. Perform isotropic compression tests on sand.

3. Perform a series of direct shear tests to study the behaviour of interfaces between an oil contaminated sand and different engineered materials.

4. Implement Lade's modified model into a computer program.

5. Calculate changes in the factor of safety against sliding instability of a slope where a part of the ground is contaminated.

6. Investigate the effect of oil contamination on the stability of a retaining wall.

7. Make simulations of soil behaviour using the modified version of Lade's model.

Chapter 2

Experimental Investigation

2.1 Introduction

Considering that oil is capable of altering the frictional resistance of any surface, it is likely that the internal friction of soils will also change if oil is allowed to go into the pores. However, to what extent the oil will alter the shear strength and deformation chacteristics of a soil has to be determined experimentally. A series of triaxial compression tests were carried out on cohesionless soil as part of this investigation. The results of drained and undrained triaxial tests on both oil saturated (contaminated) and water saturated (clean) sands are presented in this chapter. Comparisons are then made in terms of stress strain and strength properties.

2.2 Testing Program

2.2.1 Type of Materials

a) *Sand*

The soil used in these experiments is a factory crushed quartz sand designed as silica-24. The grain size distribution, Figure 2.1, shows that the sand is fine to medium. It is composed of angular particules with a specific gravity of 2.65. The maximum and minimum void ratios are $e_{max} = 1.13$ and $e_{min} = 0.42$, determined by following the ASTM standards, designation D2049.

b) *Oil*

The oil used in the experiments is a Motomaster grade 50 heavy duty motor oil. The density of the oil is $0.927 g/cm^3$ and its viscosity is 455 mPa.s at a temperature of 24°C as measured in the laboratory. This type of oil was chosen because it has properties representative of crude oil that may be encountered in oil spills.

2.2.2 Type of Tests

Four series of tests were carried out using standard triaxial testing equipment. In the first series, the samples were saturated with water, consolidated isotropically and sheared up to about 20% axial strain. In the second series, the samples were saturated with oil and tested with similar procedure. In the third series, samples were saturated with oil, consolidated isotropically and sheared under undrained conditions. In the final series of tests, the samples were saturated with water and tested in undrained conditions. Three different confining pressures were applied and two different densities were used in most cases. A constant rate of axial strain, 0.3 mm/min, was used throughout the testing program. In drained tests

on oil saturated samples, a pore pressure transducer was used to ensure that the strain rate was slow enough to prevent the development of excess pore pressure. In addition to the tests described above, four isotropic compression tests were performed using both clean and contaminated sands in loose and dense states.

2.2.3 Sample Preparation

$50mm$ diameter and $100mm$ long cylindrical samples were used. All samples were prepared in dry condition using a raining device, (Derradji-Aouat, 1988). Different densities were obtained by varying the height of sand fall. The density of the loose samples in different experiments varied between $1.38g/cm^3$ and $1.42g/cm^3$. The density of the dense samples was between $1.68g/cm^3$ and $1.72g/cm^3$. Full saturation with oil or water was achieved in three stages. First, the air in the dry sample was replaced with carbon dioxide. Subsequently, the oil or water was allowed to pass through the sample at a very slow rate. Finally, the back pressure and cell pressure were increased an equal amount simultaneously to achieve full saturation. A back pressure up to 310 kPa was necessary in some cases. The B value was used as a measure of the degree of saturation, (Bishop and Henkel, 1962). The saturation process took about three hours. A degree of saturation, almost 100%, was reached before any load increment was applied on the sample. In undrained tests, the pore pressure was measured with a pore pressure transducer which was deaired before each test. In drained tests, the volume change was measured with a burette and kerosene system. In tests with oil saturated samples, an intermediate pot was placed between soil sample and the volume change measuring device to obtain an oil-water interface which served as a storage space and prevented the oil from mixing with the kerosene. Enlargement of drainage openings was necessary to accelerate the flow of oil. In addition, a thin wire mesh was used instead of a regular porous stone.

2.3 Experimental Results

2.3.1 Drained Tests

The results of experiments on loose clean sand under drained test conditions are provided in Figure 2.2. The results of similar tests where loose samples were saturated with oil are shown in Figure 2.3 for the same confining pressures. Comparisons between these two figures indicate that the effect of oil contamination is to decrease the strength and increase the volumetric strains. The behaviour of the loose sand in the hydrostatic compression tests is shown in Figure 2.4. It appears that the presence of oil does affect the compressibility of the loose sand under hydrostatic compression. Figure 2.5 shows the stress strain response of the clean dense sand in the drained triaxial test. The confining pressures used in these tests are 138, 276, and 414 kPa. Test data related to the oil contaminated dense sand are presented in Figure 2.6. Figures 2.5 and 2.6 indicate that the strength of the dense sand decrease when the soil is saturated with oil. There is little difference in the volumetric strains developed in clean sand and contaminated dense sand during shearing. The hydrostatic compression curves are given in Figure 2.7 for the dense samples saturated with water and oil. An increase in the compressibility is evident when the dense sand is contaminated.

2.3.2 Undrained Tests

The undrained behaviour of loose sand in its clean and contaminated states is presented in Figure 2.8 for a confining pressure of 138 kPa. The pore pressure in oil contaminated loose sand is higher than that of clean sand. The peak pore pressure was reached at different axial strain levels in clean and oil contaminated

loose sands as can be seen in Tables B.17 and B.18 of Appendix B. Figure 2.9 shows the experimental results of undrained tests on dense sand. These tests were conducted using a confining pressure of 276 kPa. No significant change is caused by oil contamination on the pore pressure response of dense sand.

2.4 Analysis of Experimental Data

The experimental data was analyzed to obtain the internal friction angle and the initial tangent modulus of both clean and oil contaminated sands. These results are summarized in Table I.

Membrane penetration effect may take place but this effect was assumed to be the same for both clean and oil contaminated samples.

The internal friction angle for dense sand was obtained using the peaks of the stress strain curves. For loose samples, there was no peak. The state of stress at the end of the test, at about 20 % axial strain, was used to obtain the angle of internal friction. In order to find an average friction angle from tests with three confining pressures, the K_f-line was used (Bishop and Henkel, 1962). For the calculation of the initial tangent modulus, a second degree polynomial was first used to obtain a best fit to the deviatoric stress versus axial strain data. Then the derivative of the polynomial at the origin gave the initial tangent modulus.

Table 2.1: Summary of soil parameters

		clean sand		contaminated sand	
		Dense	Loose	Dense	Loose
internal friction angle (degrees)		41.5	32.2	35.3	26.2
initial tangent modulus (MPa) for	σ_3=138 kPa	62	19	100	6
	σ_3=276 kPa	93	28	167	14
	σ_3=414 kPa	116	38	250	23

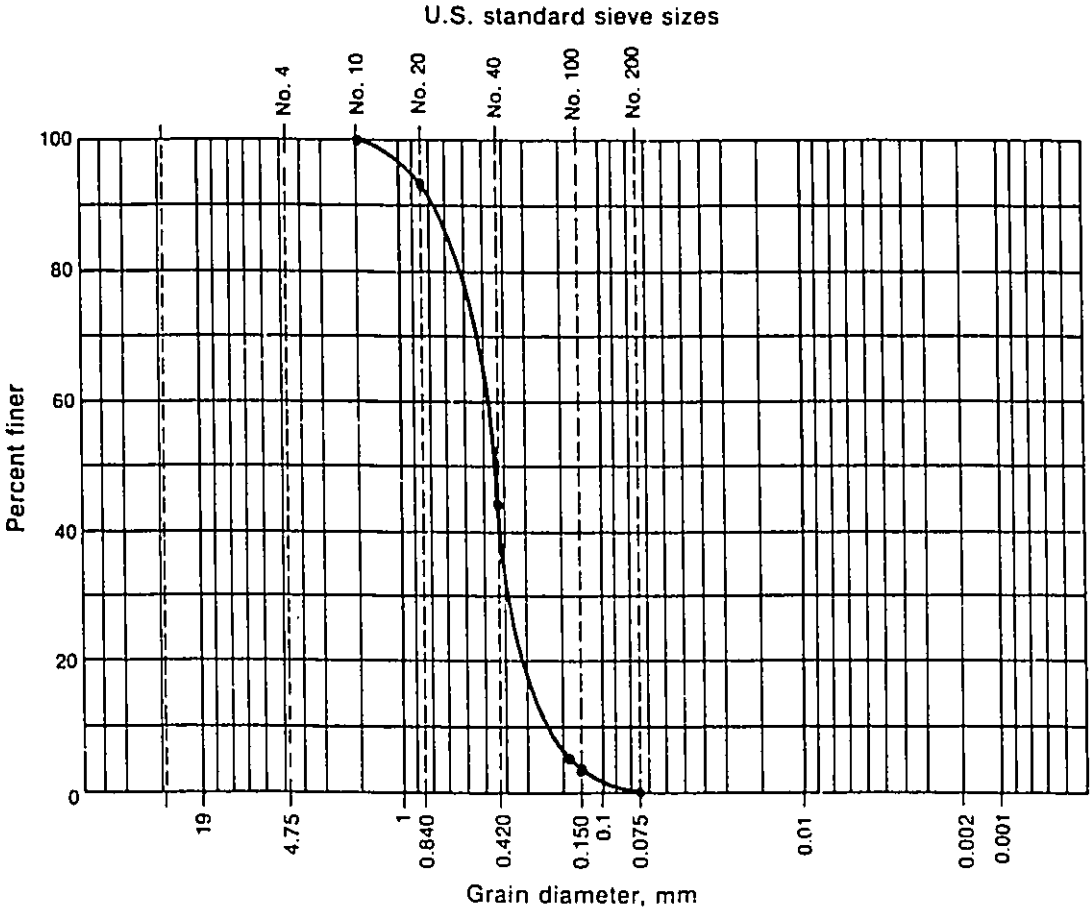

Figure 2.1: Grain size distribution of crushed quartz sand

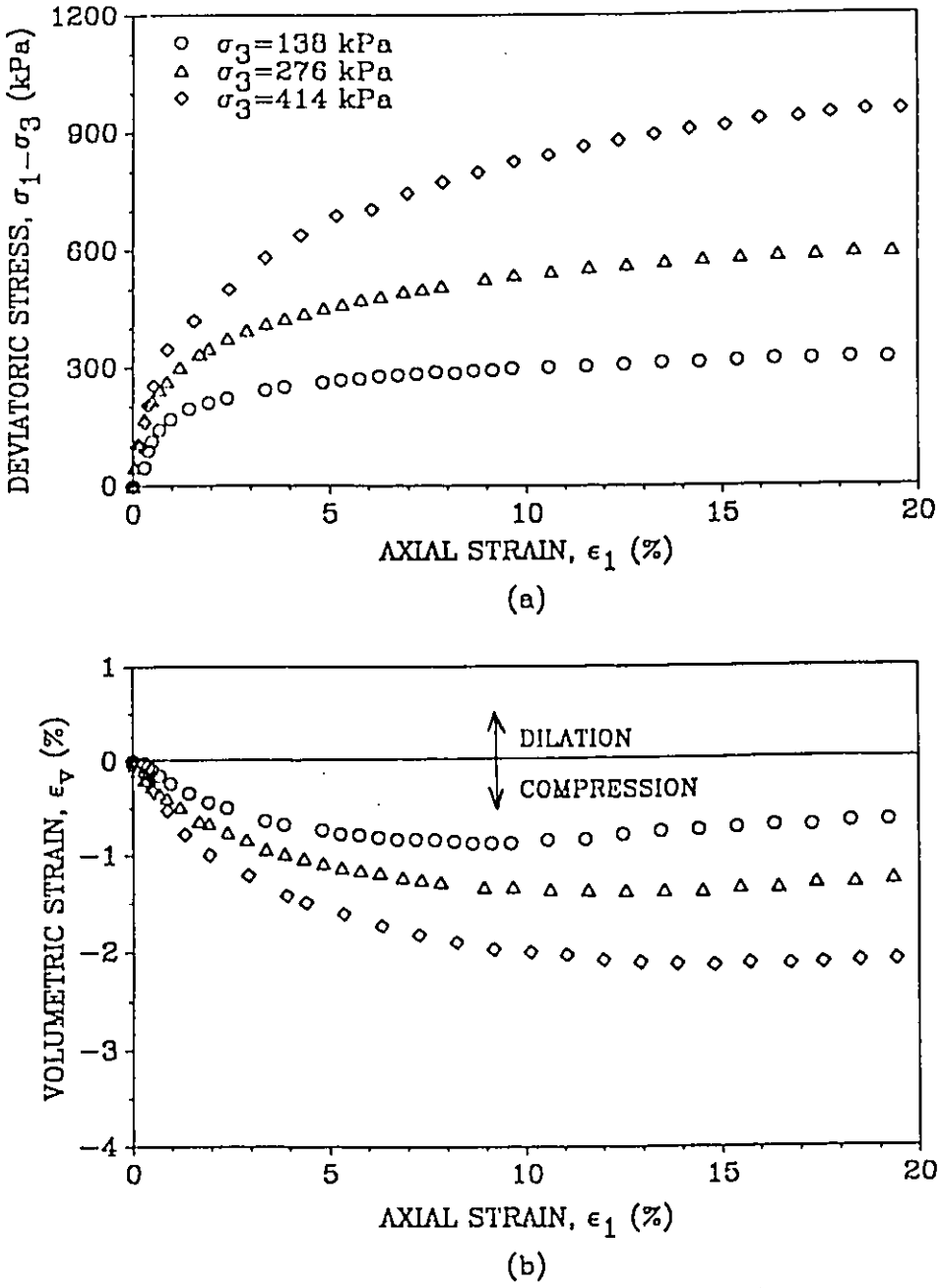

Figure 2.2: Drained triaxial test results for clean loose sand (a) deviatoric stress versus axial strain; (b) volumetric strain versus axial strain.

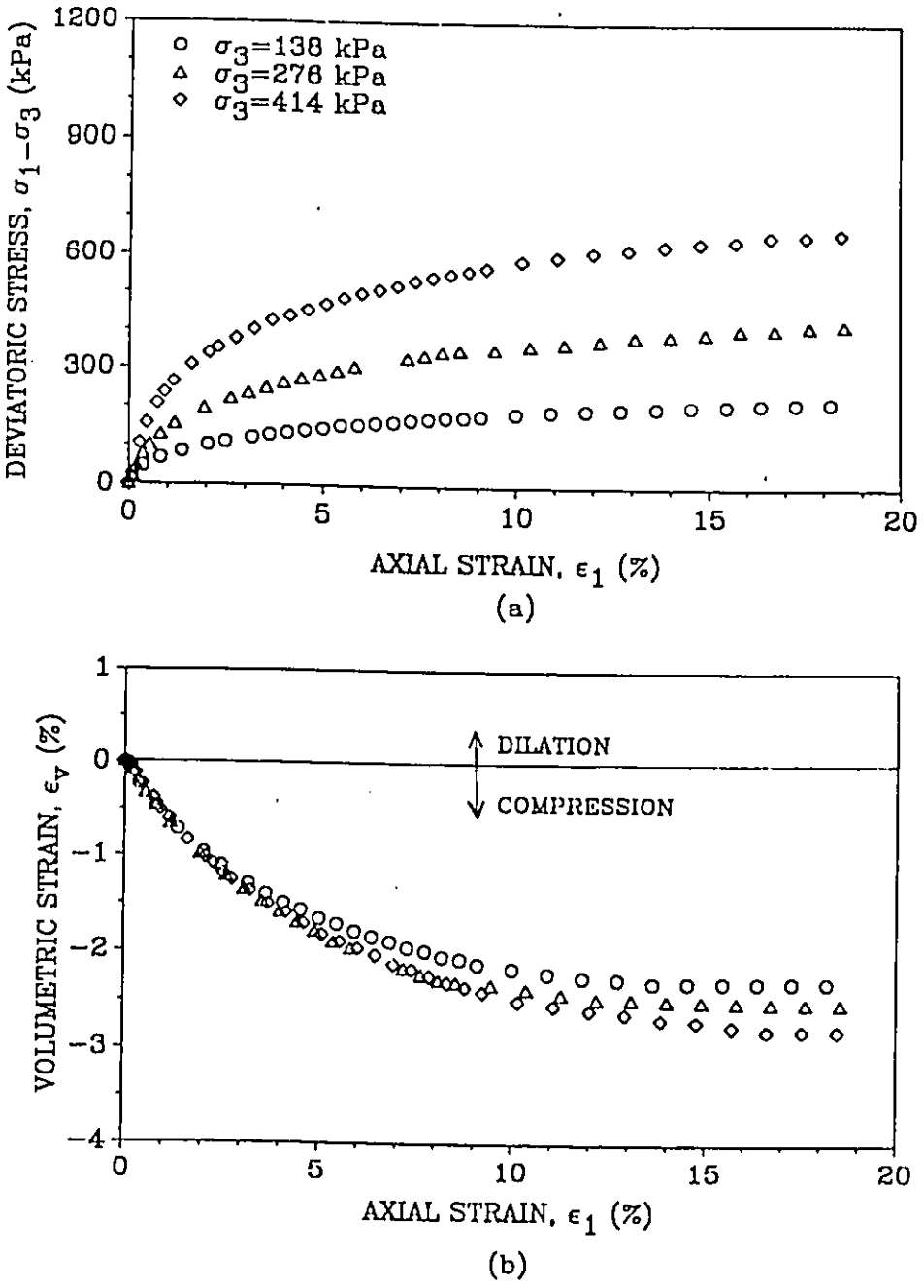

Figure 2.3: Drained triaxial test results for oil contaminated loose sand: (a) deviatoric stress versus axial strain; (b) volumetric strain versus axial strain.

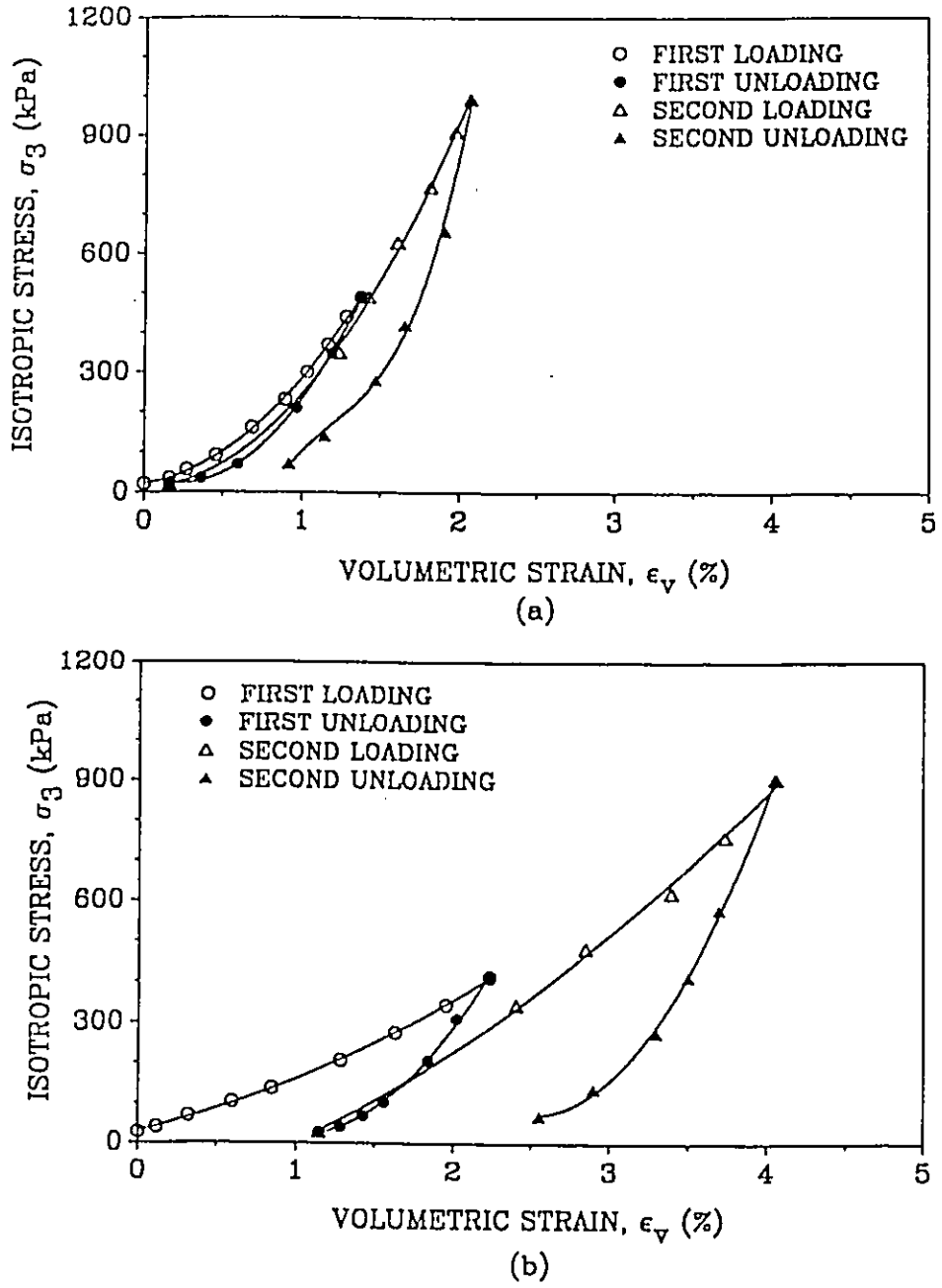

Figure 2.4: Isotropic compression tests on loose: (a) clean sand; (b) oil contaminated sand.

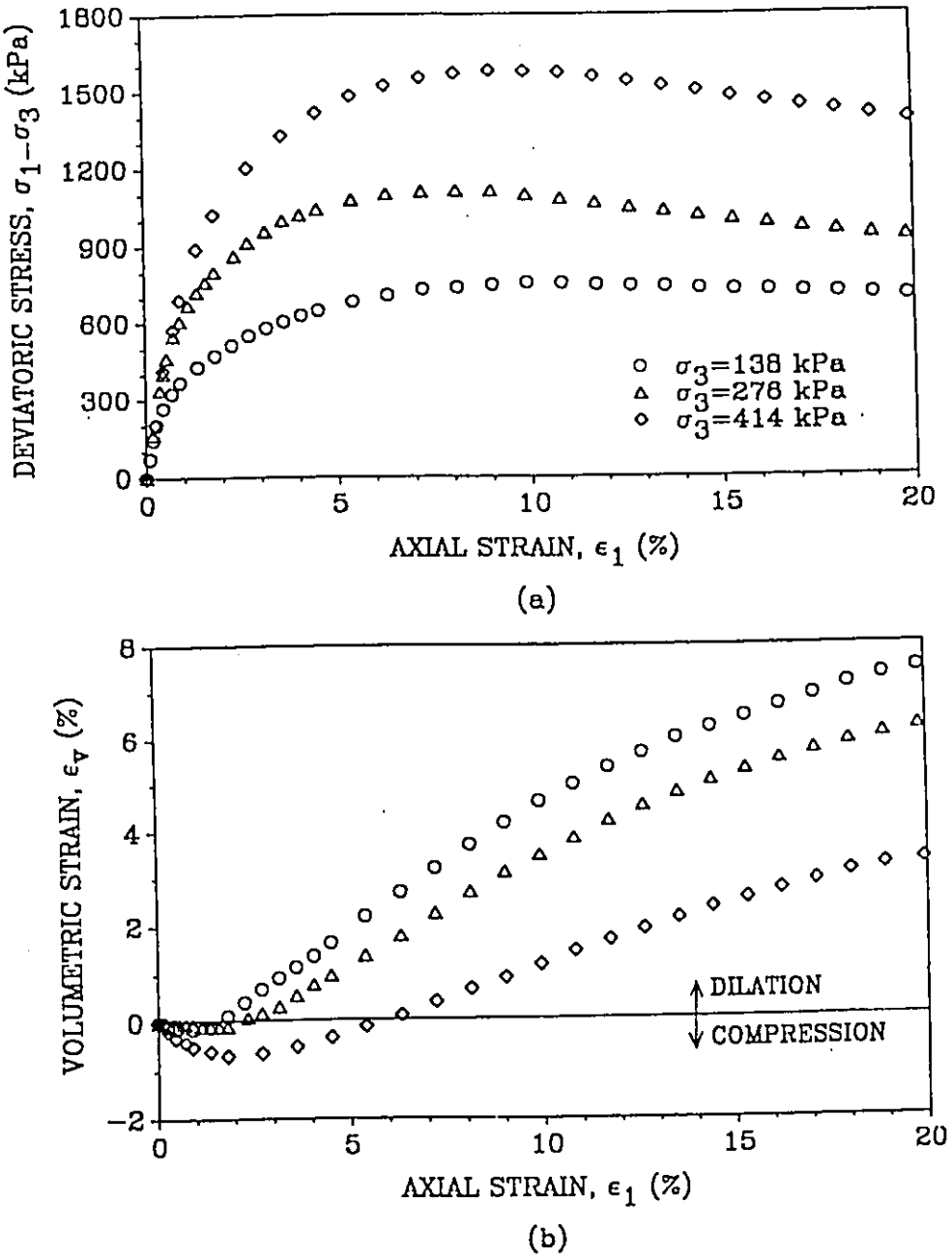

Figure 2.5: Drained triaxial test results for clean dense sand: (a) deviatoric stress versus axial strain; (b) volumetric strain versus axial strain.

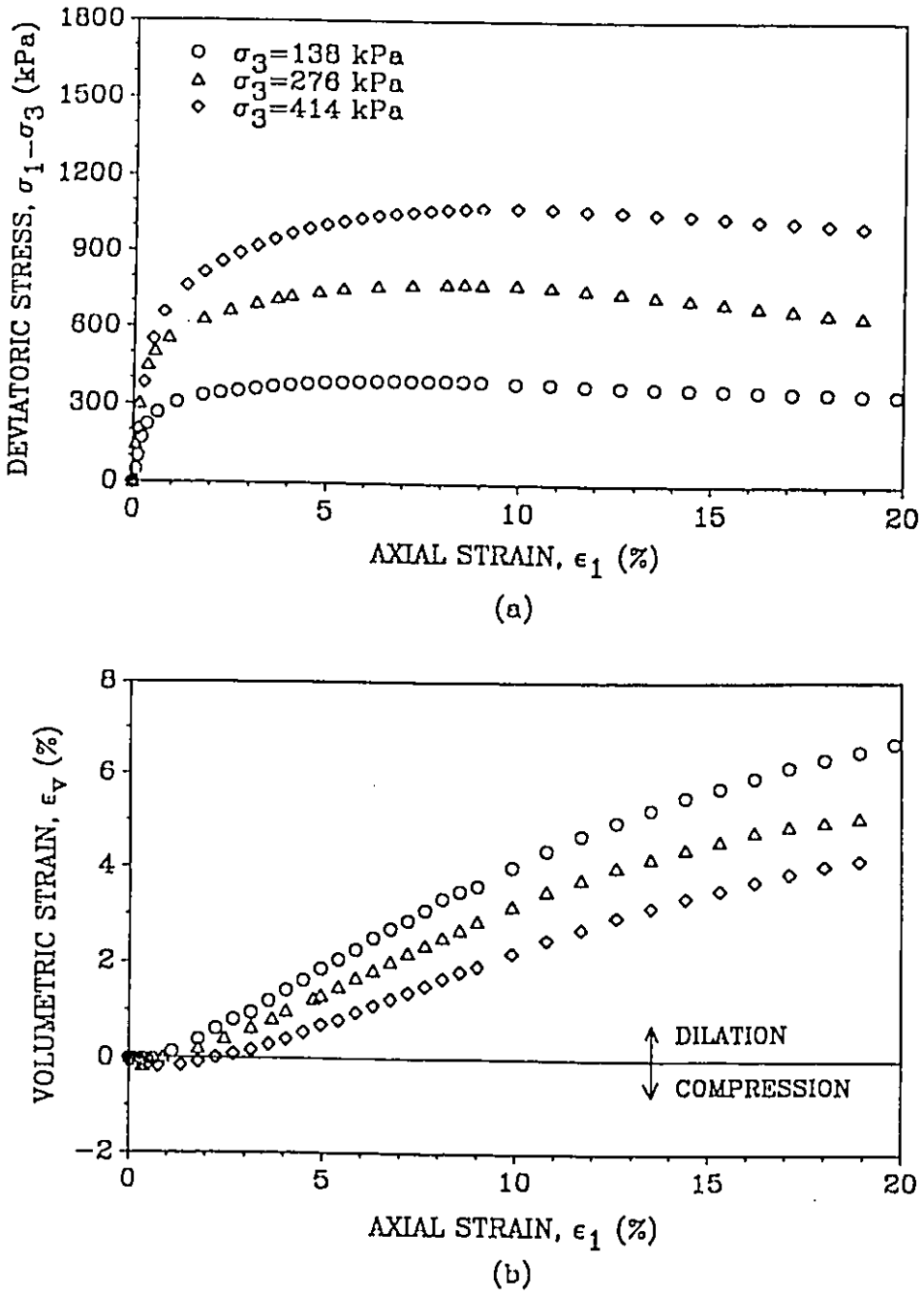

Figure 2.6: Drained triaxial test results for oil contaminated dense: (a) deviatoric stress versus axial strain; (b) volumetric strain versus axial strain.

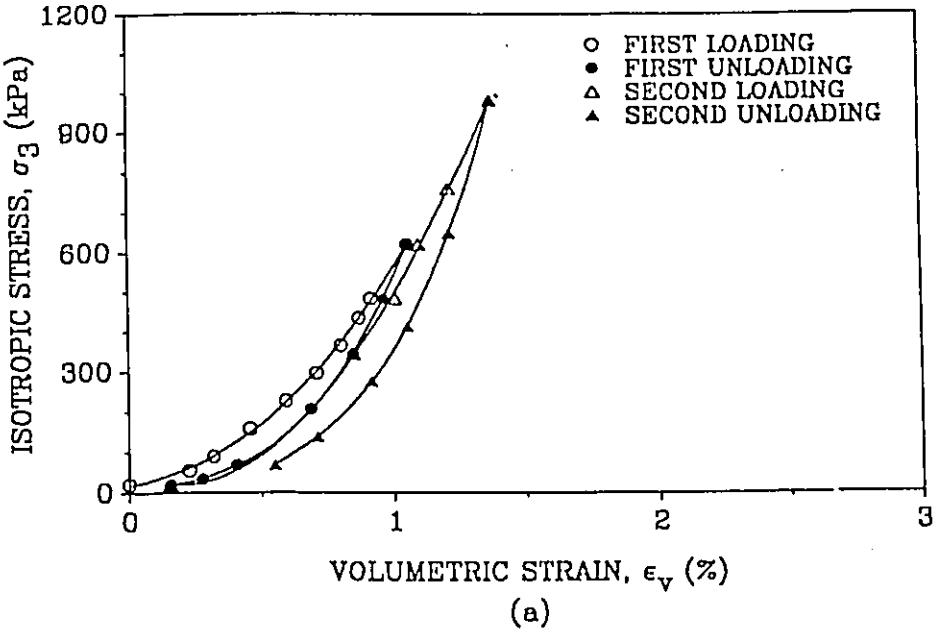

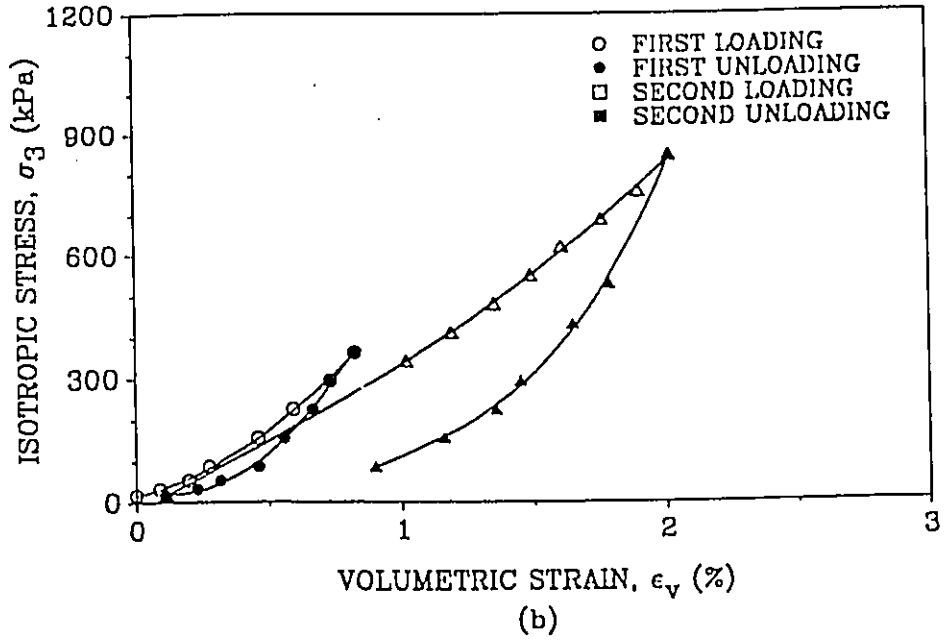

Figure 2.7: Isotropic compression tests on dense sand (a) clean; (b) oil contaminated.

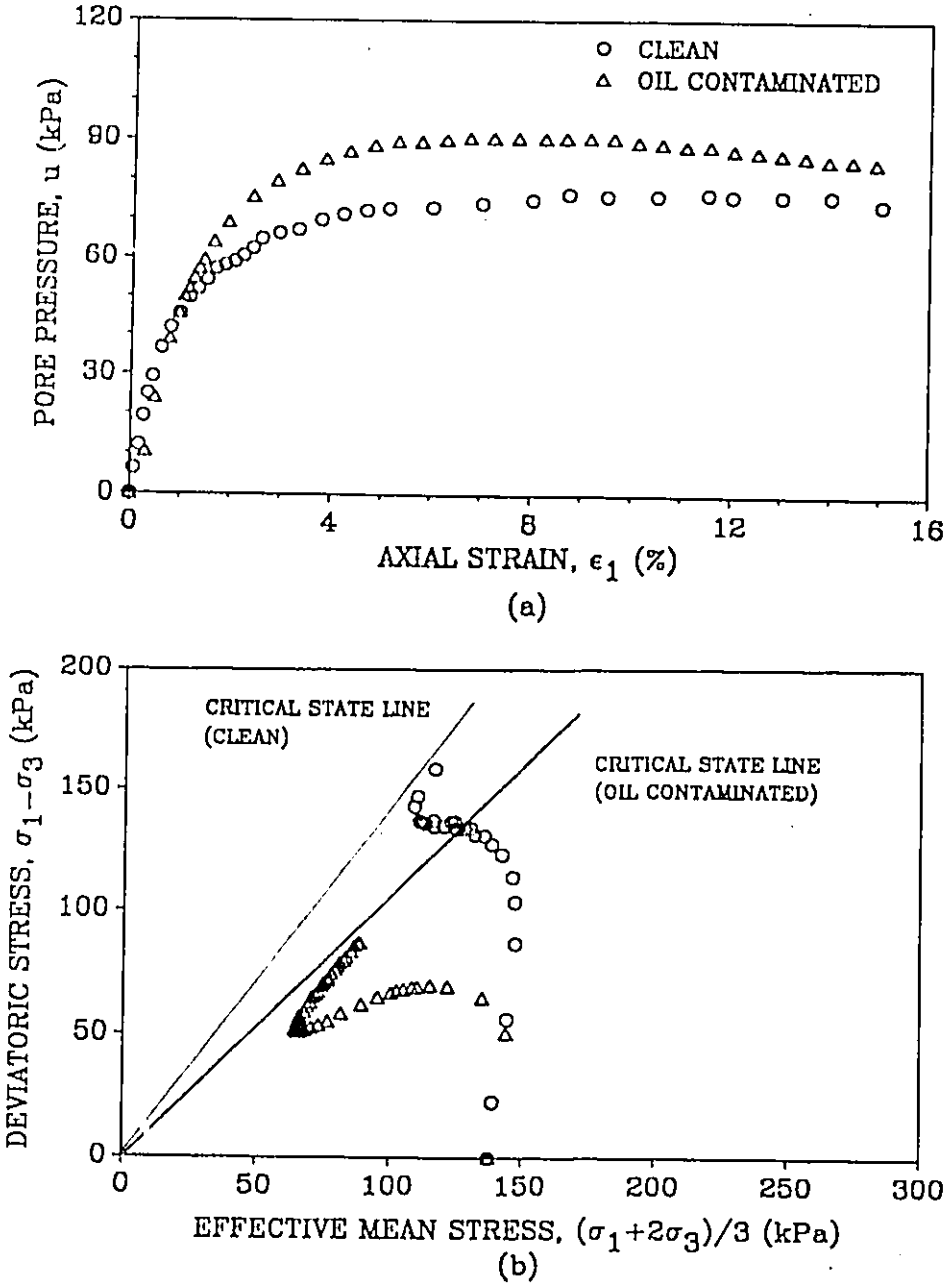

Figure 2.8: Undrained triaxial test results for loose clean sand and loose oil contaminated sand: (a) pore pressure versus axial strain; (b) deviatoric stress versus effective mean stress.

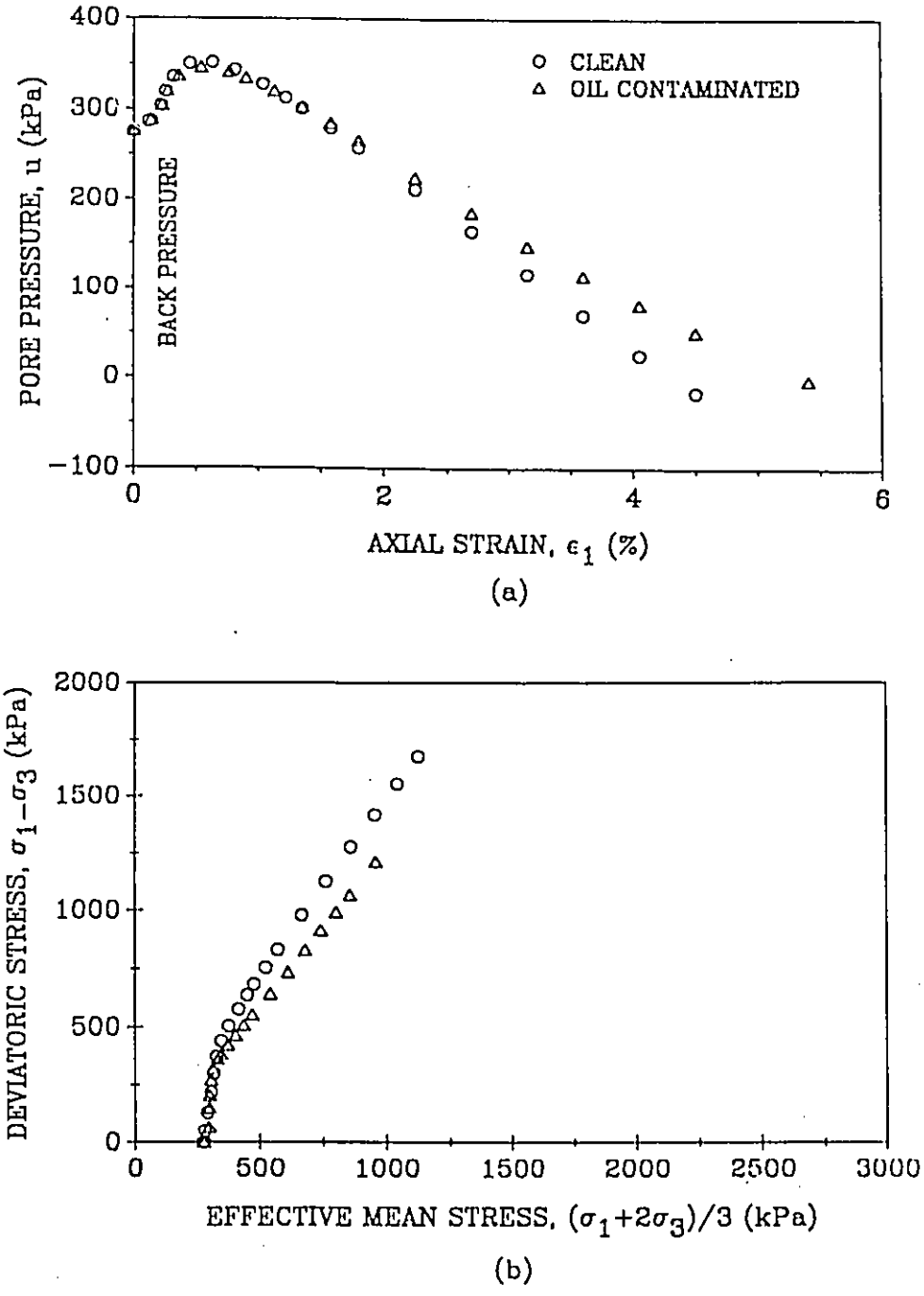

Figure 2.9: Undrained triaxial test results for dense clean sand and dense oil contaminated sand: (a) pore pressure versus axial strain; (b) deviatoric stress versus effective mean stress.

Chapter 3

Interface Behaviour

3.1 Introduction

Knowledge of the strength and stress-deformation behaviour of the interfaces between the soil and structure is important in the analysis and design involving soil-structure interaction. The most common of these problems relate to the evaluation of earth pressures on retaining structures and the prediction of the compression or uplift capacity of piles.

Soil-structure interface behaviour has been addressed by a number of investigators, among them Potyondy (1961), U.S. Army Eng. (1962), Clough (1969), Clemence (1973), Brumund and Leonards (1973), Kulhawy and Peterson (1979), and Acar et al. (1982). Most of the above named researchers have performed laboratory tests in order to investigate soil-structure interface behaviour. Research in this area has been focused on the limiting boundary conditions of smooth or rough surface for the structural material.

A rough surface was defined as the one prepared by pouring concrete directly against the soil or on a rough ground surface. A smooth surface was prepared by pouring concrete against a steel or glass plate. Brumund and Leonards (1973) concluded that when the structural surface is rough, shearing occurs in the sand rather than along the interface. This phenomenon takes place when the interface friction angle is greater than the soil friction angle. Clemence (1973), in turn, defined a rough surface as one where the size of the grains or surface projections are greater than the average grain size (D_{50}) of the soil placed against the surface. Wu (1976) stated that the usual approach is to assume that the interface friction angle ranges from one half to two third of the soil friction angle for smooth concrete interfaces. Kulhawy conducted 178 interface sand-concrete tests and stated that interface roughness can be quantified by using a relative roughness (R_R).

It is also important to characterize the stress deformation behaviour of the interfaces, particularly for use in finite element soil-structure interaction studies. Clough (1969), has demonstrated that the stress deformation behaviour of interfaces can be described effectively with a normal stiffness and a shear stiffness, as described by Goodman, Taylor and Brekke (1968). These stiffnesses are defined as the stresses per unit displacement in the normal and tangential (shear) directions to the interface.

Clough (1969), demonstrated that the shear stiffness is both nonlinear and normal stress-dependent. He also showed that the nonlinear behaviour may be descibed by a hyperbolic relationship.

Regardless of their differences, all investigators agreed, in general, that the interface friction angle depends on:

1. angularity and grain size distribution of the soil

2. moisture content of the soil

3. type of interface material and its texture

4. normal stress on the interface

A summary of the results of some previous investigations for interface behaviour is presented in Table 3.1. In this chapter, the experimental results of the present work are presented to illustrate the effect of oil contamination on the strength and stress-deformation behaviour of sand-concrete and sand-steel interfaces. The testing was conducted so that the eventual failure plane was forced to develop along the interface. Two different interface materials with different roughnesses were used. Only the loose sand was employed in both clean and oil contaminated conditions.

3.2 Testing Procedure

The stress-deformation and strength behaviour of soil-concrete and soil-steel interfaces was investigated in a laboratory testing program. The variables included: soil type (clean or oil contaminated sand), normal stress acting on the interface, and type of interface material. Altogether fifteen tests were performed.

All tests were conducted in a Wykeham-Farrance strain-controlled direct shear machine using a 38 mm deep, 50 mm square shear box. The cohesionless soil used was a crushed quartz sand obtained from the same batch as the sand used for the triaxial tests. The gradation curve of the sand is given in Figure 2.1. The same type of oil as for the triaxial tests was used to saturate the sand.

For testing, the sand was prepared at a loose state obtained by pluvial deposition,

Kolbuszewski (1948). The density of the sand ranged from 1.35 g/cm^3 to 1.40 g/cm^3. Two different types of interfaces were tested. The first interface was between the soil and a block of mortar prepared by mixing sand and Portland cement. The finished surface was polished to obtain a clean level interface. The second interface had a steel block whith a surface intentially made smooth. Nonetheless, the surface roughness of the concrete and the steel differed considerably.

The testing procedures were similar to the conventional direct shear testing, with the major difference being in the set-up of the samples. The shear box was assembled in the testing machine, with the concrete or the steel block in the bottom half, as shown in Figure 3.1. Sand was placed in the top half of the box by pluvial deposition. Since the testing program was aimed at establishing the effect of oil contamination on the behaviour of the interfaces, the test procedure was the same for both clean and oil contaminated sand. Oil contamination was achieved by submerging the shear box in oil contained in the load cart. Three normal stresses were applied for each particular case. The effect of deformation rate during the test was also taken into consideration. The shear displacement rate used was 0.30 mm per minute which is considered low, Kulhawy and Peterson (1979). The deformation rate used in testing the interfaces was the same as the rate used for the triaxial tests which resulted in no pore pressure generation in drained tests.

3.3 Experimetal Results

The results of interface tests by Acar et al. (1982), presented in Figure 3.2, show the variation of friction angle with normal stress for different materials.

The primary purpose of the experiments in the present study was to investigate the effect of oil contamination on the frictional behaviour of the interfaces. The

experimental data are plotted in the form of shear stress-horizontal displacement curves in Figures 3.3, 3.4, 3.5, 3.6, and 3.7. The maximum shear resistance versus normal stress plots gave the interface friction angle, δ. The results are presented in Table 3.2 and Figure 3.8.

The interface friction angle δ varied by about 1.5^0 as a result of oil contamination in sand-concrete interface, while almost no change in the interface friction angle was obtained in the case of sand-steel interface.

Table 3.1: Results of some previous investigations for interface behaviour

Reference	Test Type	Soil	Interface	Moisture Content, w %	Normal Stress σ (kg/cm^2)	Relative Density (D_r) or Dry Unit, Weight (γ_d)	Test Area (mm^2)	Soil Friction Angle, ϕ (Degrees)	Interface Friction Angle, δ (Degrees)	$\frac{\delta}{\phi}$
Potyondy	Direct Shear	Sand	Smooth Concrete	Dry	47.8-143.5	D_r=66%	3600	44.0	39.0	0.89
			Rough Concrete	Dry	47.8-143.5	D_r=66%		44.0	43.2	0.98
			Smooth Concrete	Saturated	47.8-143.5	D_r=66%	9000	38.0	34.0	0.89
		Rock Flour	Smooth Concrete	Dry	47.8-143.5	Dense		39.6	39.3	1.00
			Rough Concrete	Dry	47.8-143.5	Dense		39.8	39.6	1.00
			Smooth Concrete	Saturated	191.3-382.4	Dense		31.2	30.5	0.98
U. S. Army Engineers Southern Division	Direct Shear	Sand	Mortar	9.1	47.5-287.2	γ_d = 1378kg/m^3	5100	32.0	25.3	0.79
			Mortar	9.1	47.5-287.2	γ_d = 1402kg/m^3	5100	31.0	31.8	1.03
			Mortar	9.3	47.5-287.2	γ_d = 1714kg/m^3	5800	33.3	26.7	0.86
			Mortar	17.4	47.5-287.2	γ_d = 1570kg/m^3	5800	35.3	32.5	0.92
			Mortar	19.1	47.5-287.2	γ_d = 1602kg/m^3	5800	31.3	31.0	0.99
		Silty Sand	Mortar	15.7	47.5-287.2	γ_d = 1602kg/m^3	5800	33.7	35.5	1.01
Clough	Direct Shear	Poorly Graded Sand	Smooth Concrete	Saturade	44.8-223.8	γ_d = 1634kg/m^3	2500	40.0	33.0	0.83
Clemence	Direct Shear	River Sand	Smooth Concrete	Dry	10.3-23.4	D_r=65%	3160	38.2	30.4	0.80
			Rough Concrete	Dry	10.3-23.4	D_r=45%	3160	38.2	38.2	1.00
			Rough Concrete	Dry	10.3-23.4	D_r=75%	3160	42.6	42.9	1.00
Brumund and Leonards	Annular Shear	Poorly Graded Quartz Sand	Smooth Mortar	Dry	9.0-86.1	D_r=90%	22,580	40.0	31.0	0.78
			Teflon Coated Smooth Mortar	Dry	9.0- 86.1	D_r=90%	22,580	40.0	18.3	0.46
			Graphite Coated Smooth Mortar	Dry	9.0-86.1	D_r=90%	22,580	40.0	17.7	0.44
			Rough Mortar	Dry	9.0-86.1	D_r=90%	22,580	48.0	37.2	0.93
		Crushed	Smooth Mortar	Dry	9.0-86.1	D_r=90%	22,580	48.0	46.4	0.97
		Quartz Sand	Teflon Coated Smooth Mortar	Dry	9.0-96.1	D_r=90%	22,580	48.0	23.7	0.62
			Graphite Coated Smooth Mortar	Dry	9.0-86.1	D_r=90%	22,580	48.0	31.4	0.65
			Rough Mortar	Dry	9.0-86.1	D_r=90%	22,580	48.0	48.0	1.0

Table 3.2: Summary results on interfaces

Type of test	Friction angle
Direct shear	30.0
Interface concrete and clean sand	27.3
Interface concrete and oil contaminated sand	25.9
Interface steel and clean sand	20.0
Interface steel and oil contaminated sand	20.3

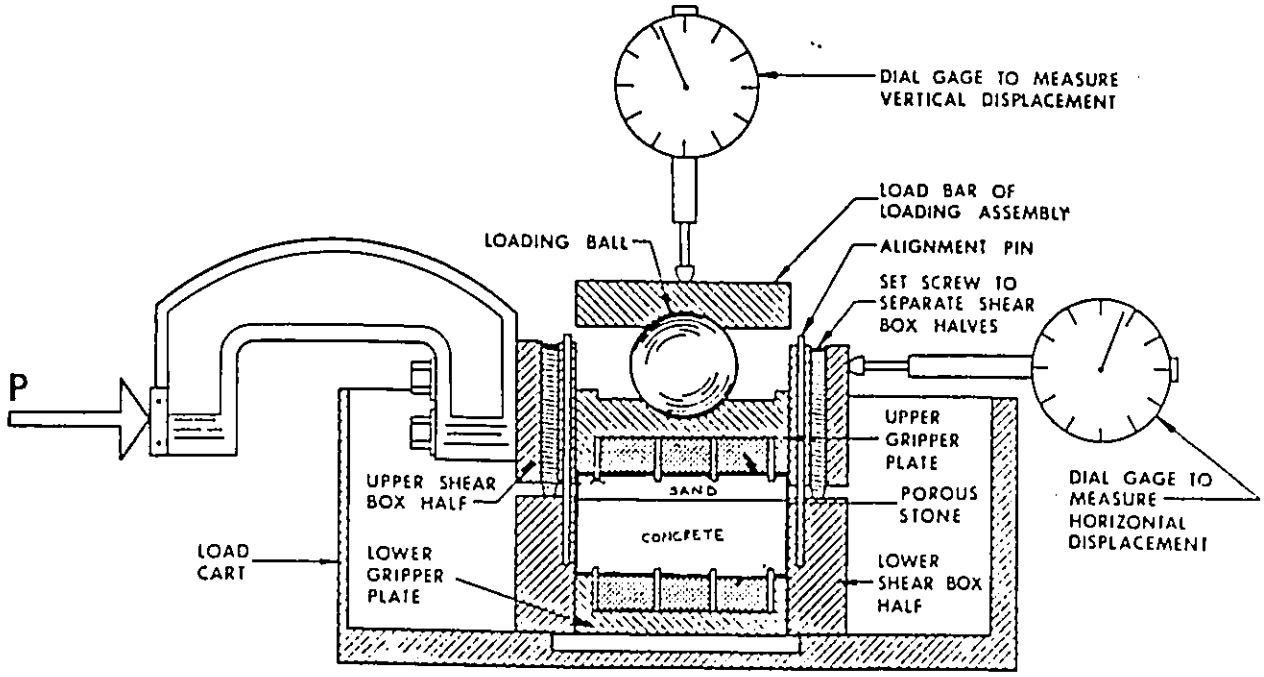

Figure 3.1: Direct shear test apparatus

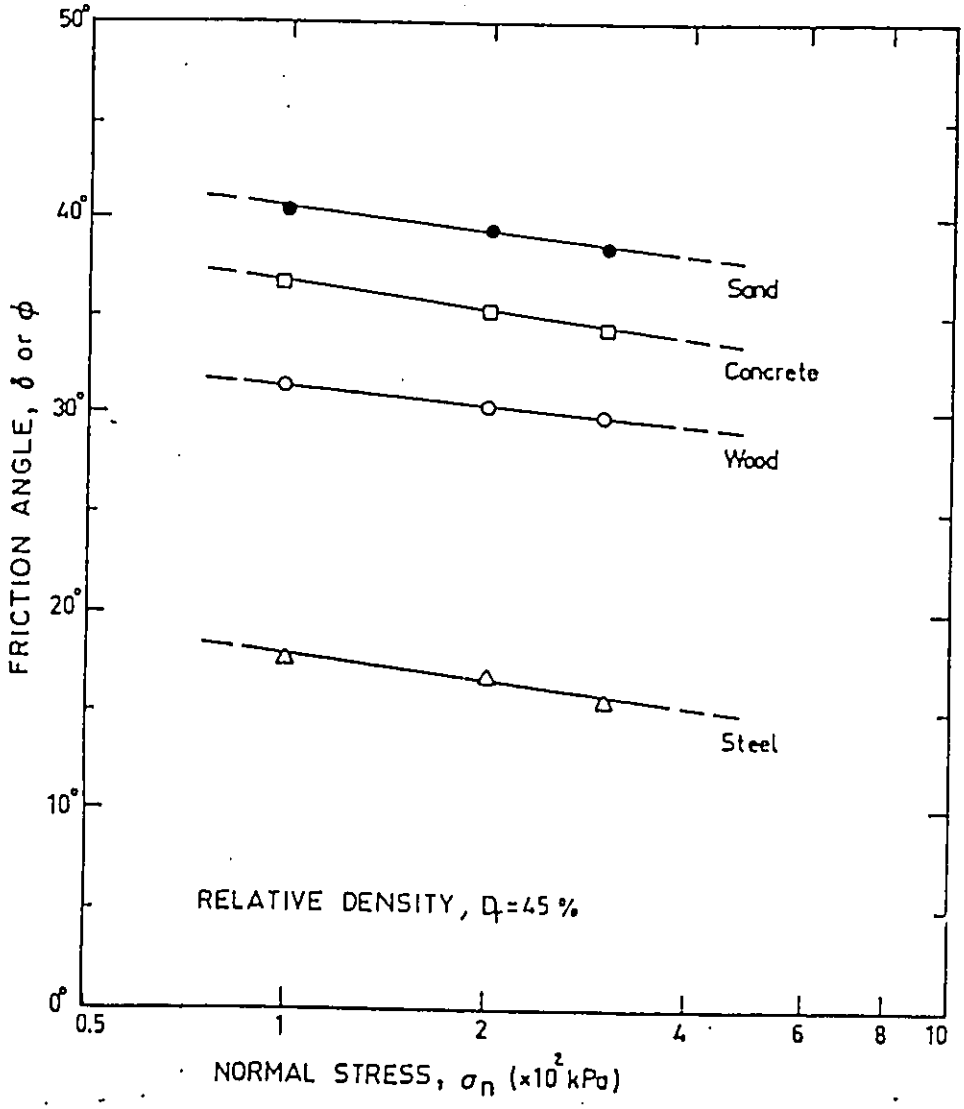

Figure 3.2: Variation of friction angle with normal stress (After Acar et al., 1982)

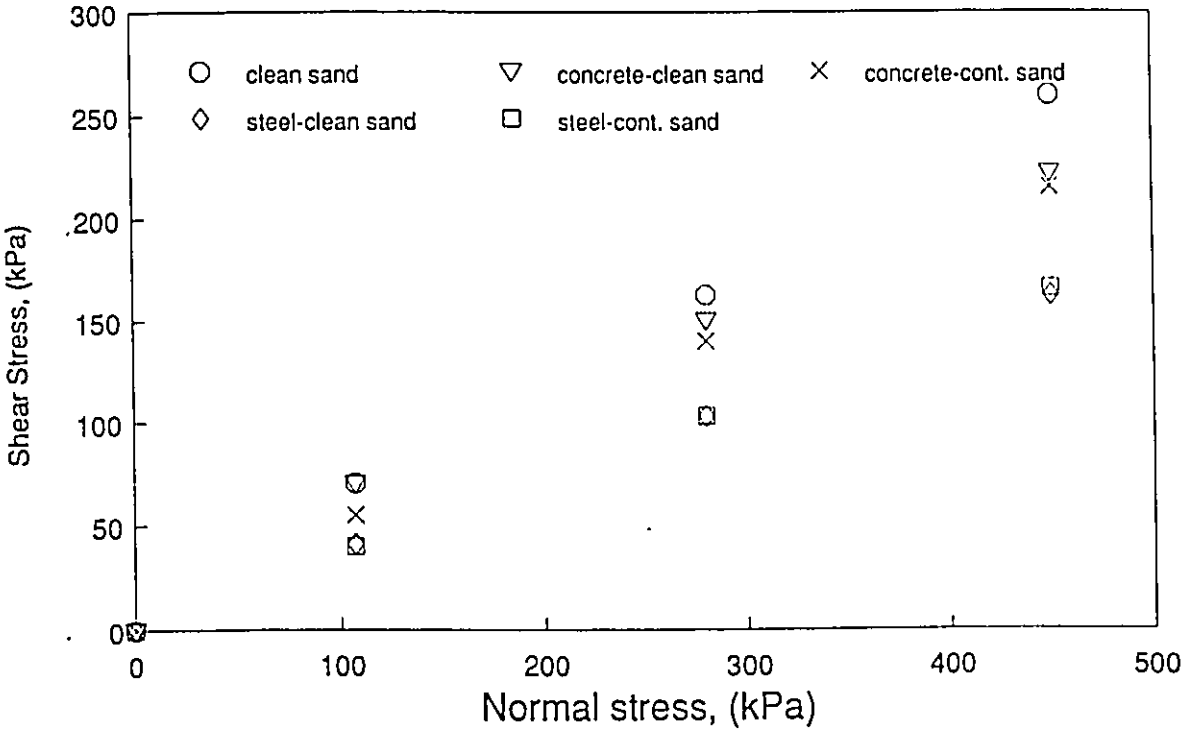

Figure 3.3: Results from direct shear and interface tests on loose crushed quartz sand.

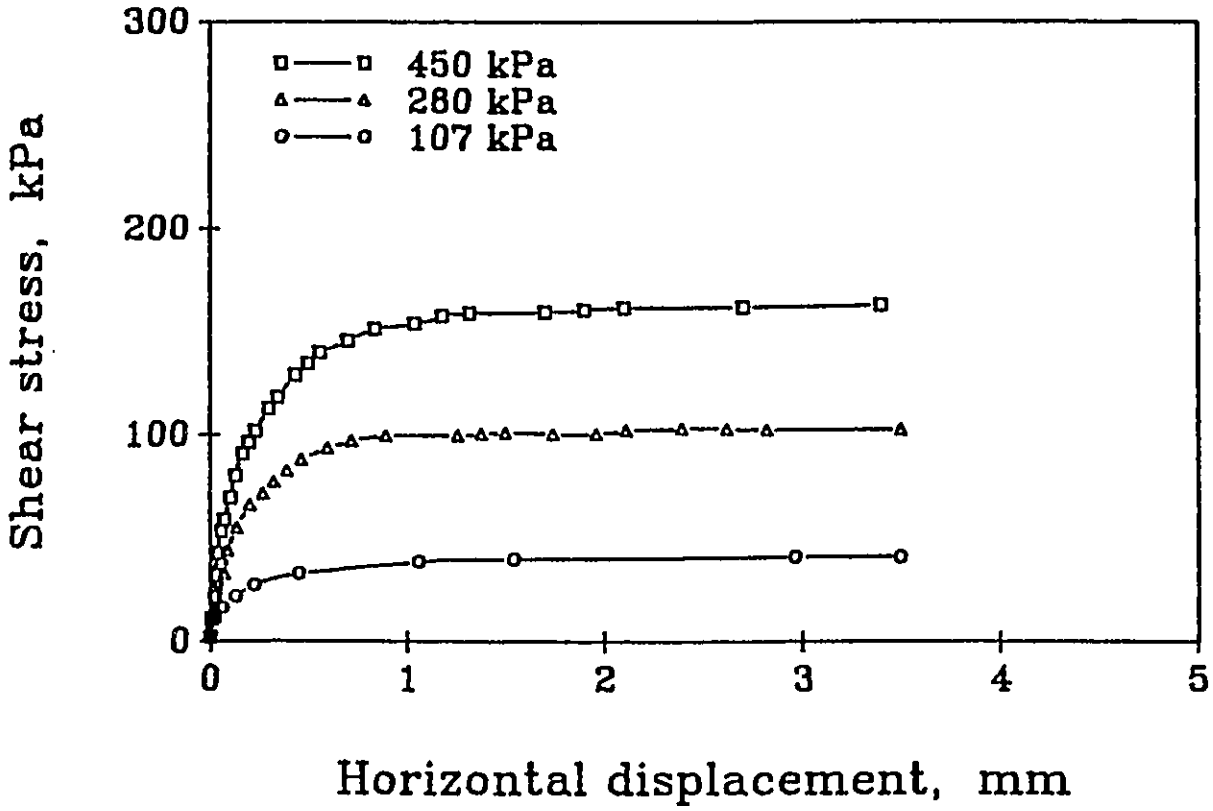

Figure 3.4: Results of tests on steel interface and clean loose crushed quartz sand.

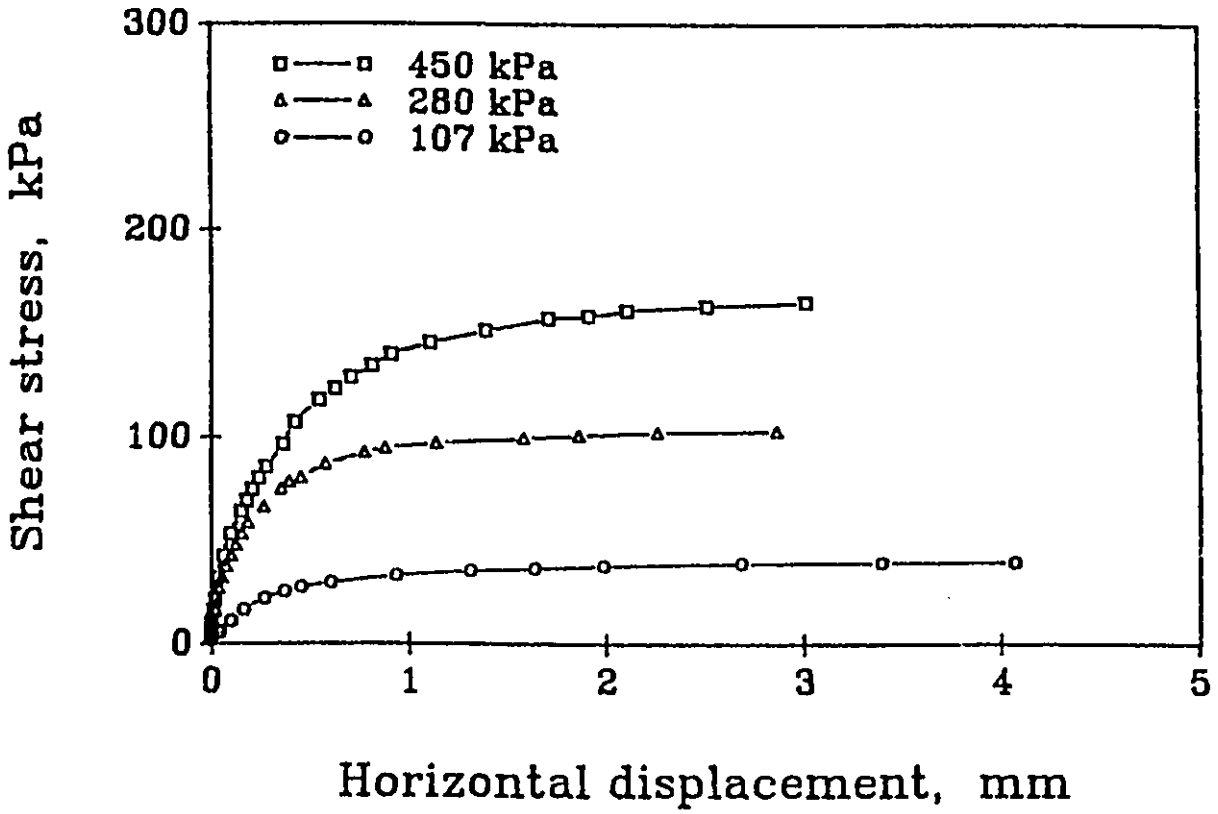

Figure 3.5: Results of steel interface and oil contaminated loose crushed quartz sand.

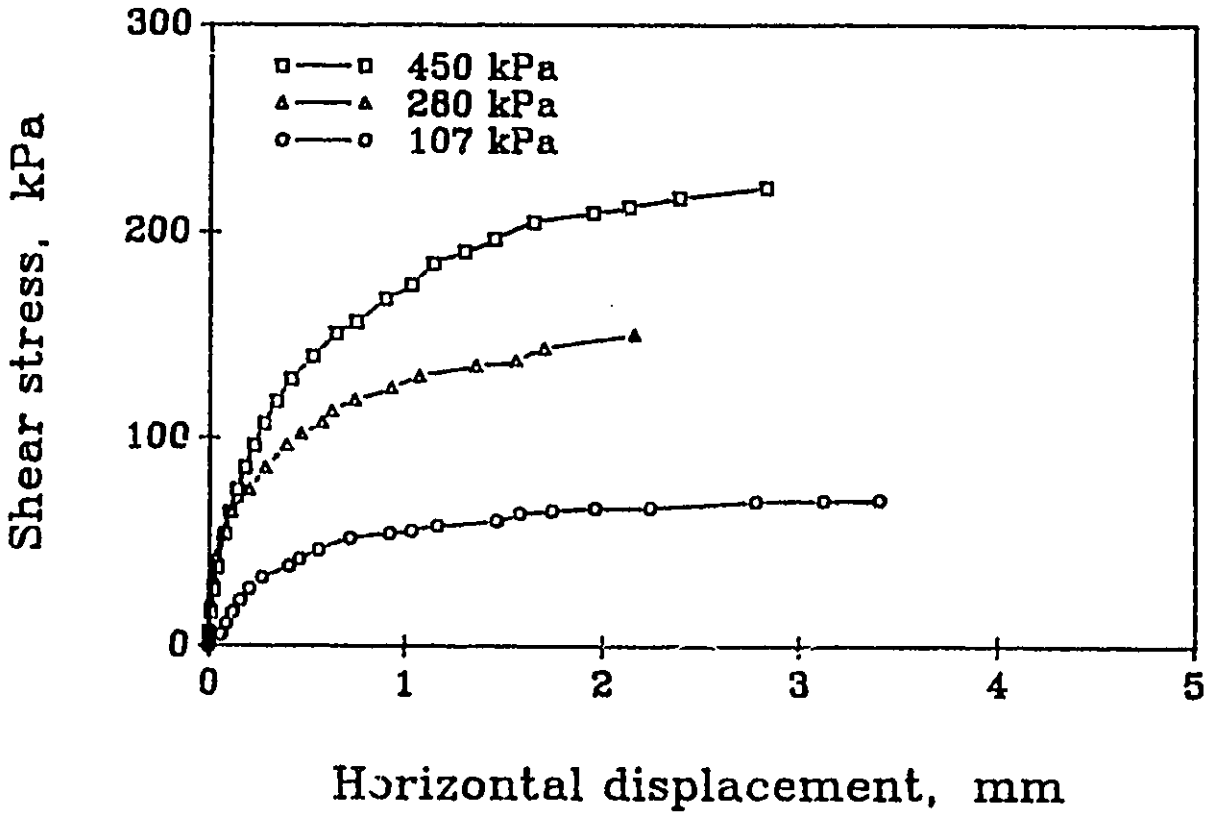

Figure 3.6: Results of tests on concrete interface and loose clean crushed quartz sand.

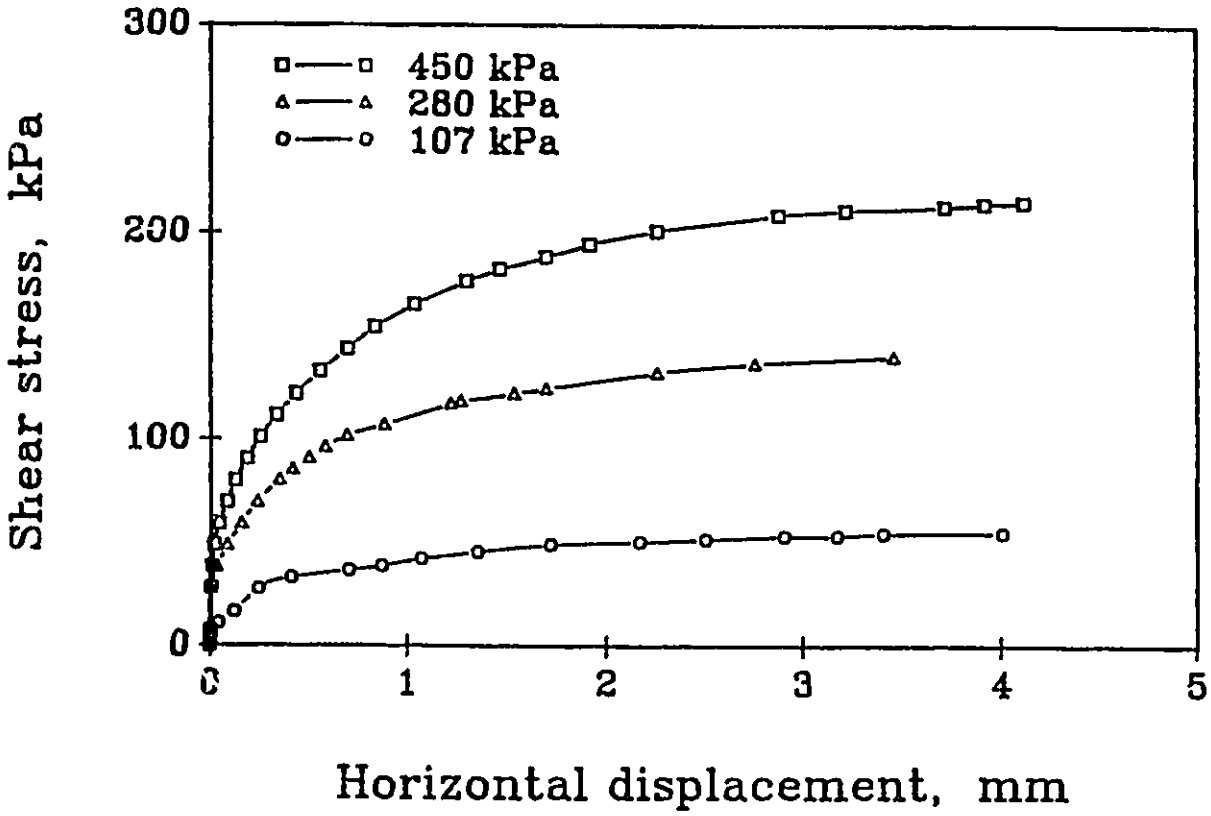

Figure 3.7: Results of tests on concrete interface and loose oil contaminated crushed quartz sand.

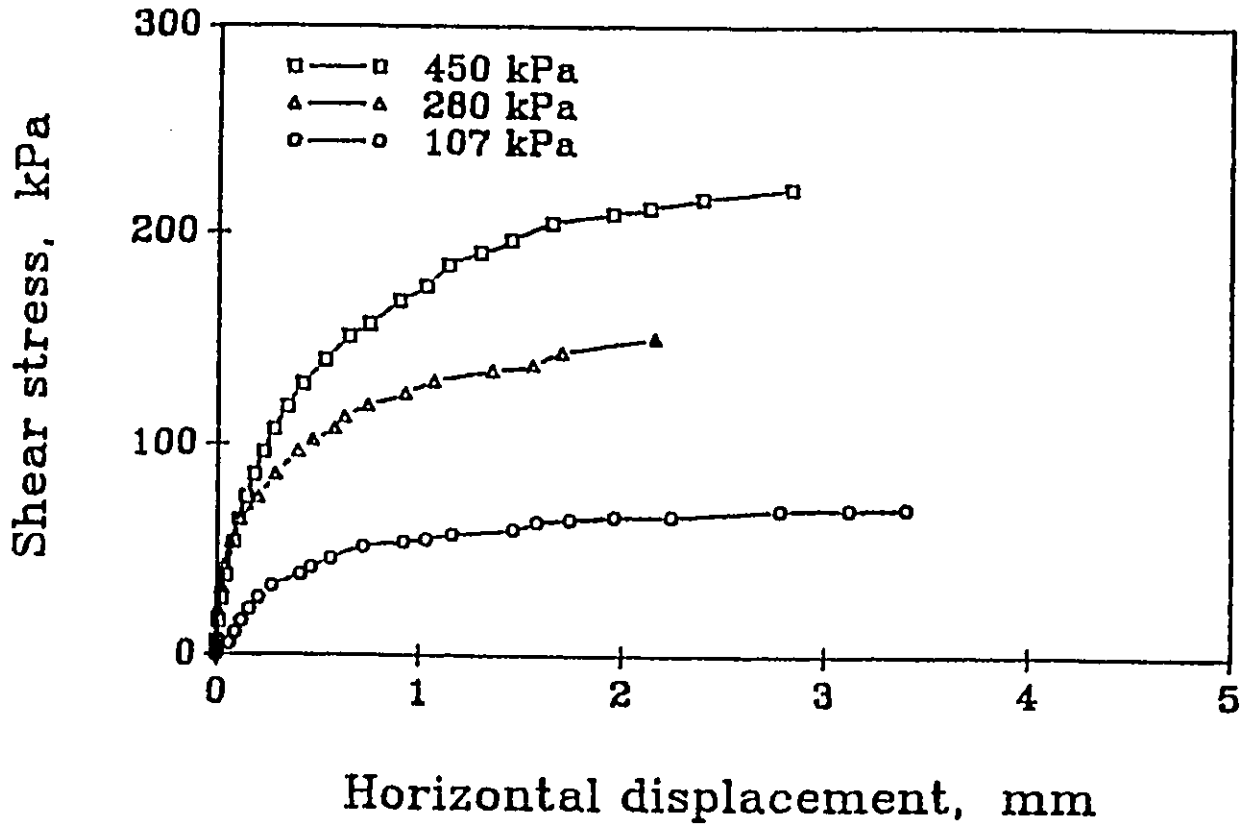

Figure 3.8: Results of direct shear tests on clean loose crushed quartz sand

Chapter 4

Practical Applications

This chapter is concerned with the application of the findings of the experimental work. The bearing capacity of shallow or deep foundations, stability of slopes and retaining walls, and the performance of pavements are all affected by the stress-strain behaviour of soil, the shear strength of soil, and the characteristics of interfaces. Some simple geotechnical problems are solved in this study to demonstrate how oil contamination might effect the stability of soil structures. Conventional methods of analysis are used.

4.1 Retaining Wall Problem

In this hypothetical problem, a road will cut into a granular soil requiring a 5 metre high cantilever retaining wall to be built along the side of the road, as indicated in Figure 4.1.

Given

The wall is made of concrete. Soil layers, soil parameters, and groundwater level

are all shown in Figure 4.1. It is assumed that the soil-concrete interface is rough along points C to D.

Required

1) Determine the factor of safety against sliding failure for

a) clean sand (B=2.0 m)

b) oil contaminated sand (B=2.0 m)

2) Determine the factor of safety against bearing capacity failure for

a) clean sand (B=6.0 m)

b) oil contaminated sand (B=6.0 m)

3) Compare the results to show the oil contamination effect.

Solution

1) **Factor of safety against sliding failure**

The solution given here follows the procedures described in the Canadian Foundation Engineering Manual (1985).

a) **Clean sand**

W : weight of soil in the area EFGD, it is assumed that the weight of the concrete is the same as soil.

S : distributed pressure due to surcharge acting between points F and G.

F_w : force resisting sliding $=(W + S \times FG)tan(32.2)$

K_a= active earth pressure coefficient =0.3

F_1 is the horizotal force acting on the wall due to the surcharge

F_1= (0.30)(10.0)(5.0) = 15.0 kN

F_2 is the lateral force due to soil

F_2= 1/2 $K_a\gamma h^2$= 0.5(0.3)(20.0)$(5.0)^2$ = 75 kN

F is the total lateral force which may cause sliding

F = $F_1 + F_2$ = 15.0 +75.0 = 90.0 kN

$W + S$= (5x20.0 + 10.0)x2.0 = 220.0 kN

F_w is the the force resisting sliding of the wall

$F_w = 220.0 tan 32.2 = 138.5$ kN

Factor of safety for clean sand = 138.5/90.0= 1.5

b) **Oil contaminated sand**

It is assumed that the oil contamination affecting the soil is between points C and D, and that the soil properties are similar to those obtained in Chapter 2. Therefore, oil contamination reduces the friction angle down to 26.2^0.

F_o : force resisting against sliding for the case where the sand is oil contaminated

F_o $=(W + SxFG)tan(26.2)$

K_a= active earth pressure coefficient=0.30

F_1= 0.30x10.0x 5.0 = 15.0 kPa

F_2= 1/2 $K_a \gamma h^2$ $= 0.5(0.30)(20.0)(5.0)^2$= 75 kPa

F :applied force = $F_1 + F_2$ = 15.0 + 75.0 = 90.0 kN

$W + S$= (5.0x20.0 + 10.0)x2.0 = 220.0 kN

F_o = 220.0 tan26.2 = 110.2 kN

Factor of safety for oil contaminated sand = 110.2/90.0 = 1.2

As the calculation given above show, the factor of safety against sliding reduces from 1.5 to 1.2 due to oil contamination at the base of the retaining wall.

2) **Factor of safety against bearing capacity failure**

The general equation of the ultimate bearing pressure may be calculated

using the following equation (CFEM, 1985):

$$q_u = s_c i_c c N_c + s_q i_q q' N_q + \frac{1}{2} s_{\gamma'} i_\gamma B' N_\gamma \tag{4.1}$$

where:

N_c, N_q, N_γ are the bearing capacity coefficients

$N_q = (\exp \pi tan\phi')(\frac{1+sin\phi'}{1-sin\phi'})$

$N_c = (N_q - 1)cot\phi'$

$N_\gamma = 1.5(N_q - 1)tan\phi'$

in which ϕ' is the effective internal friction angle

s_c, s_q, s_γ are the shape coefficients

$s_c = s_q = 1 + (B/L)(N_q/N_c)$

$s_\gamma = 1 - 0.4(B/L)$

i_c, i_q, i_γ are the inclination coefficients

$i_c = i_q = (1 - \delta/90^0)^2$

$i_\gamma = (1-\delta/\phi')^2$ where δ is the inclination of the resultant force on the footing

q' effective overburden pressure at the foundation level

B' effective width of the footing

γ' effective unit weight of soil below footing

For strip footings, $s_c = s_q = s_\gamma = 1.0$.

The cohesion, c, is zero since the soil is sand. In addition, because the soil may be excavated in the future for the placement of a storm sewer pipe, q' is assumed zero for the soil section in front of the retaining wall.

$$q_u = \frac{1}{2} i_\gamma \gamma' B' N_\gamma \tag{4.2}$$

The following numbers as substituted in Equation 4.2

$\phi' = 32.2^0$

γ'=20.0 kN/m^3

N_γ=21.5

B'=B-2e where e is the excentricity calculated = 2.6 m

B'=6.5-2(2.6)=1.3 m

$\delta = 22.2^0$

therefore i_γ=0.57

q_u=0.5(0.57)(21.5)(20.0)(1.3)=159.3 kPa

Applied pressure= $10.0 + 5.0 \times 20.0 = 110.0$ kPa

The factor of safety against bearing failure is F_s= 159.3/110.0=1.5

b) **Oil contaminated sand**

The same procedure as for the clean sand case is repeated with the only change being the angle of internal friction reduced to 26.2^0.

Equation 4.2 is used.

$\phi' = 26.2^0$

γ'=20.0 kN/m

N_γ=8.0

B'=B-2e where e is the excentricity calculated = 2.6m

B'=6.5-2(2.6)=1.3 m

$\delta = 7.8^0$

therefore i_γ=0.57

q_u=0.5(0.57)(8.0)(20.0)(1.3)=59.3 kPa

the factor of safety against bearing failure is F_s= 59.3/110.0=0.5

3) **Comparison**

In this specific problem, it has been demonstrated that oil contamination reduces the factor of safety of a retaining wall against sliding failure from 1.5 to 1.2, While, the factor of safety against bearing capacity failure is

reduced from 1.5 to 0.5.

4.2 Slope Stability Analysis

In order to determine the effect of oil contamination on the stability of a slope, the following analysis have been carried out. The slope shown in Figure 4.3 have been selected. The soil properties are shown on the Figure. The analysis have been carried out using a computer program PCSTABL4. Information about this slope stability program is given in the user manual (PCSTABLE4 user's manual, 1983).

PCSTABLE4 is a microcomputer version of the mainframe slope stability program, STABL4. The program is written in Fortran and calculates the factor of safety against failure using a two-dimensional limiting equilibrium method. The calculations of the factor of safety is performed using either the simplified Bishop method of slices, which is applicable to circular shaped failure surfaces, or the simplified Jambu method of slices which is applicable to failure surfaces of general shape.

Results indicate that prior to oil contamination, the factor of safety against slope instability was 1.04 which implies that the slope is stable. Upon oil contamination the factor of safety was reduced to 0.84. The factor of safety is less than 1.0, therefore, the slope is unstable and failure will occur along the slip surface shown in Figure 4.3. The input and output files of PCSTABL4 are presnted at the end of this chapter for the case where the soil is contaminated with oil.

Program Input

```
PROFIL
PCSTABL4 Example #1
5
5
20. 24. 58. 24. 1
58. 24. 80. 40. 1
80. 40. 140. 80. 1
140. 80. 167. 80. 1
167. 80. 200. 80. 1
SOIL
1
120. 125. 0. 32.2 0. 0. 1
WATER
1 62.4
4
20. 40.
80. 40.
124.0 54.
200. 54.
SURBIS
5
80. 40.
100. 46.
120. 57.
140. 76.
143. 80.
EXECUT
```

Program Output

```
                                        ** PCSTABL4 **

                                             by
                                        Purdue University

                                --Slope Stability Analysis--
                              Simplified Janbu Method of Slices
                                 or Simplified Bishop Method

                    Run Date:
                    Time of Run:
                    Run By:
                    Input Data Filename:       example1.in
                    Output Filename:           example1.out
                    Plotted Output Filename:   yes

                    PROBLEM DESCRIPTION   PCSTABL4 Example #1

                    BOUNDARY COORDINATES

                        5 Top   Boundaries
                        5 Total Boundaries

                    Boundary     X-Left      Y-Left      X-Right     Y-
Right               Soil Type
                       No.         (ft)        (ft)        (ft)
(ft)                Below Bnd

                        1         20.00       24.00       58.00
24.00                   1
                        2         58.00       24.00       80.00
40.00                   1
                        3         80.00       40.00      140.00
80.00                   1
                        4        140.00       80.00      167.00
80.00                   1
                        5        167.00       80.00      200.00
80.00                   1

                    ISOTROPIC SOIL PARAMETERS

                        1 Type(s) of Soil

Soil  Total  Saturated  Cohesion Friction   Pore   Pressure
Piez.
Type Unit Wt. Unit Wt. Intercept   Angle  Pressure Constant
Surface

No.   (pcf)     (pcf)      (psf)     (deg)   Param.     (psf)
No.

1    120.0     125.0        .0      32.2      .00         .0
1

                    PIEZOMETRIC SURFACE(S) HAVE BEEN SPECIFIED

                    Unit Weight of Water =  62.40

                    Piezometric Surface No.  1 Specified by  4 Coordinate Points

                        Point       X-Water     Y-Water
                         No.          (ft)        (ft)

                          1          20.00       40.00
                          2          80.00       40.00
                          3         124.00       54.00
                          4         200.00       54.00
```

Program Output

Trial Failure Surface Specified By 5 Coordinate Points

Point No.	X-Surf (ft)	Y-Surf (ft)
1	80.00	40.00
2	100.00	46.00
3	120.00	57.00
4	140.00	76.00
5	143.00	80.00

Circle Center At X = 60.4 ; Y = 141.7 and Radius, 103.6

Factor Of Safety For The Preceding Specified Surface = 1.043

WARNING - Factor Of Safety Is Calculated By The Modified Bishop Method. This Method Is Valid Only If The Failure Surface Approximates A Circle.

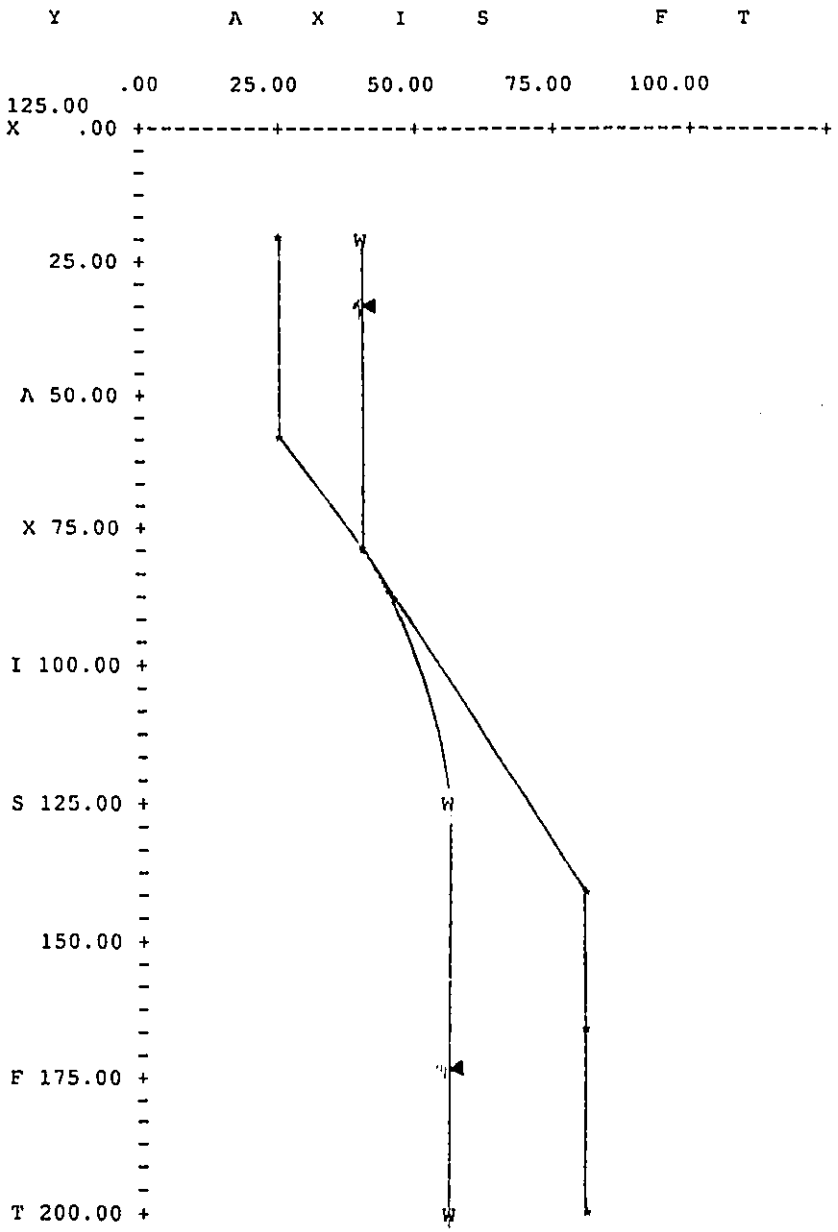

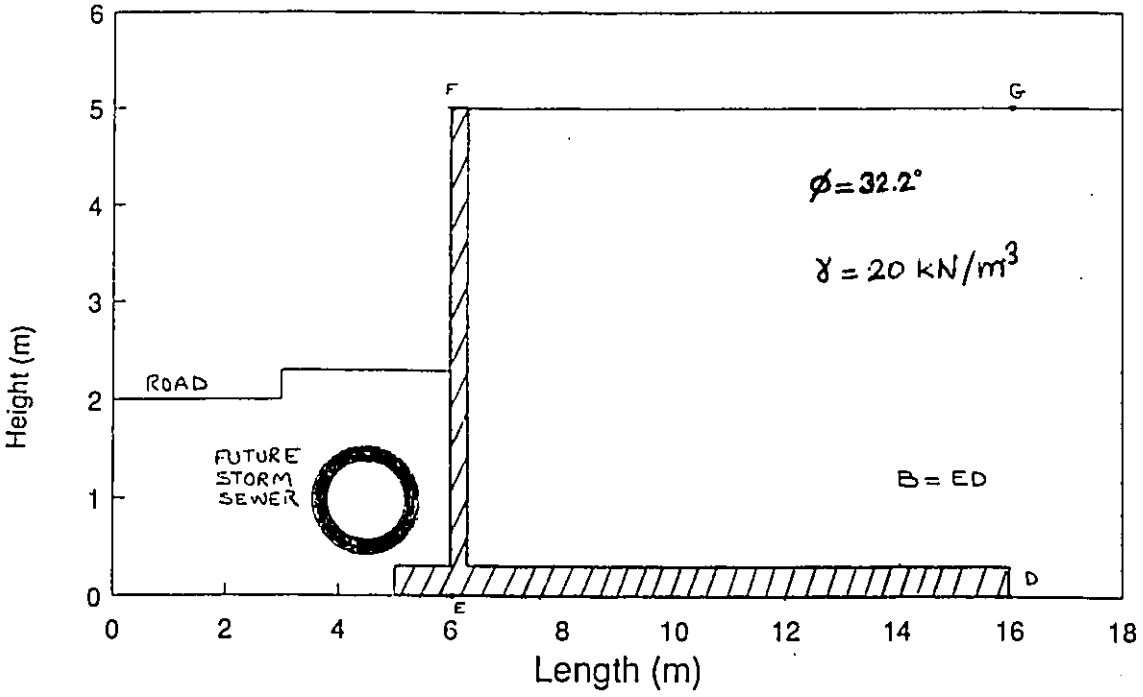

Figure 4.1: Retaining wall and soil parameters

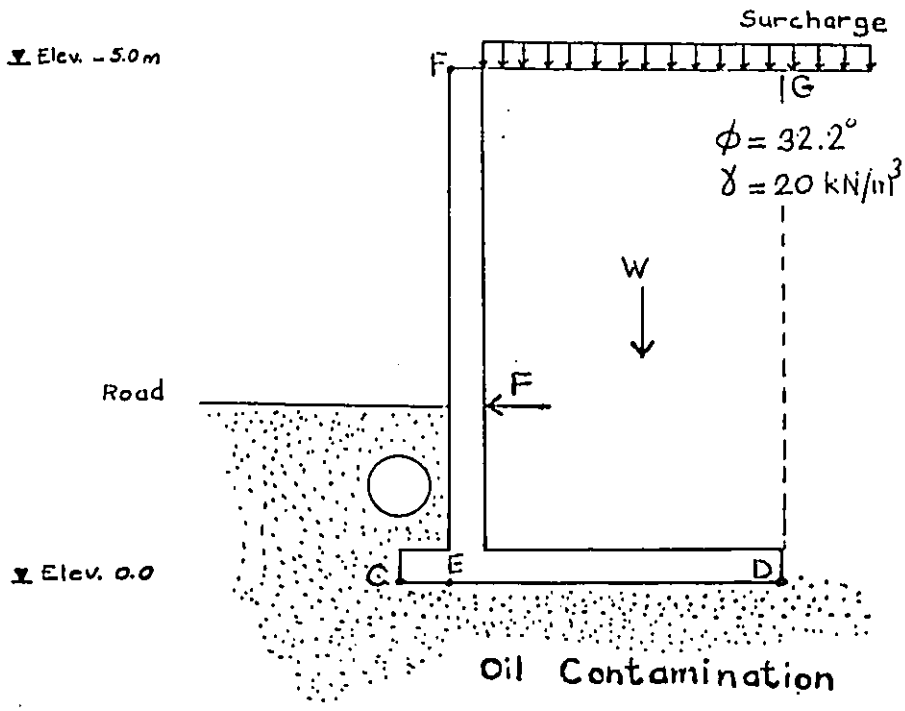

Figure 4.2: Forces applied on the retaining wall

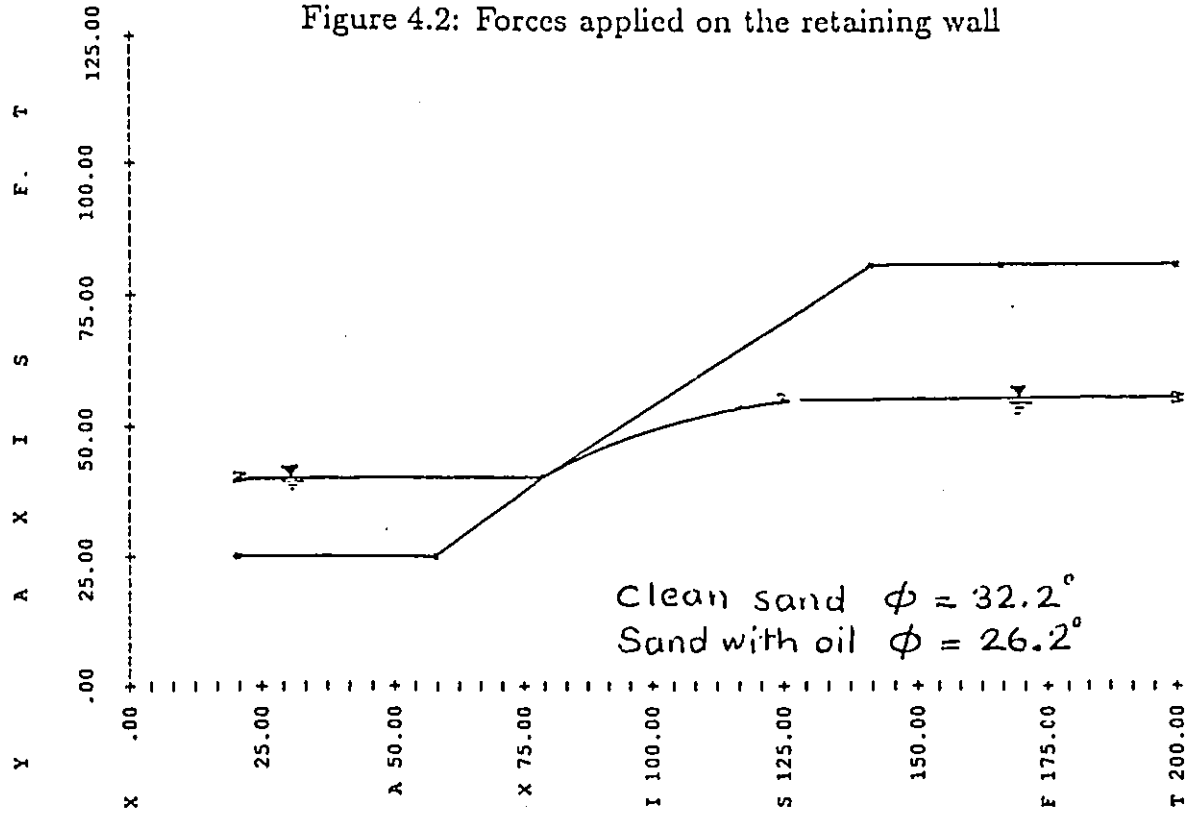

Figure 4.3: Analyzed Slope

Chapter 5

Mathematical Modelling

5.1 Intoduction

Lade (1975,1977) has developed two distinct elasto-plastic models for soils. These models totally differ from each other in the formulations of yield surfaces, flow rules, work hardening rules, and failure criteria. The first one, the work hardening model is a general three dimensional, elasto-plastic, work hardening stress-strain relationship for cohesionless soils. This model accounts for several important aspects of stress-strain and strength characteristics of cohesionless soils. The following aspects of the stress-strain behaviour of soil are modelled: nonlinearity, inelasticity, shear dilatancy, stress path dependency, influence of intermediate principal stress, and coincidence of strain increment and stress increment axes at low stress levels with transition to coincidence of strain increment and stress axes at high stress levels. This model has been developed on the bases of experimental results using Monterey No. 0 sand. The development of the model has been first presented in Lade's thesis (1972) and was subsequently published by

Lade and Duncan (1975). Additional developments and applications of the model have been published by Ozawa (1973) and Duncan et. al. (1977), Wong (1978) and Evgin and Einseintein (1980, 1985). This model does not account for strain softening behaviour and it is not designed to predict the behaviour of soil under cyclic loading conditions.

5.2 Work Hardening Model

During loading of a cohesionless soil, both elastic and plastic deformations occur from the begining of loading. The magnitude of the elastic strains are higher at the initial stage of loading. At higher stress levels plastic strains are dominant, therefore, it is assumed that the strain increments $\{d\epsilon_{ij}\}$ can be divided into an elastic part $\{d\epsilon^e_{ij}\}$ and a plastic part $\{d\epsilon^p_{ij}\}$.

$$\{d\epsilon_{ij}\} = \{d\epsilon^e_{ij}\} + \{d\epsilon^p_{ij}\} \tag{5.1}$$

These strain components are calculated separately. The elastic strains are obtained from the Hooke's law, using the unloading-reloading modulus defined by Duncan and Chang (1970). The plastic strains are calculated by using Lade's model. Figure 5.1 illustrates schematically the elastic and plastic components of the total strain in a triaxial compression test. The nature of each component and the methods of calculation for these components are discussed in the following.

5.2.1 Elastic Strains

The increments of elastic strains, which are recoverable upon unloading are determined using Hooke's law and the unloading-reloading modulus defined by Duncan

and Chang (1970)

$$E_{ur} = K_{ur} \cdot p_a \cdot (\frac{\sigma_3}{p_a})^n \tag{5.2}$$

The dimensionless, constant value of the modulus number K_{ur} and the exponent n are determined from the unloading reloading branches of triaxial compression tests performed at various confining pressures or from the results of an isotropic compression test. Details of the evaluation of elastic parameters are discussed in the next chapter.

5.2.2 Plastic Strains

The development of Lade's stress-strain relations, which are applicable to cohesionless soils under three dimensional stress conditions, are based on the concepts of plasticity theory. There are three basic requirements for a plastic stress-strain theory as stated by Lade and Duncan (1975).

1. There must exist a yield surface such that if the soil is subjected to changes in stress represented by points inside that surface, the soil will deform elastically, whereas if the changes in stress tend to cross the yield surface, it will simultaneously yield plastically and deform elastically. The yield surface expands as the soil is loaded to successively higher stress levels. And at failure the yield surface coincides with the failure surface.

2. A flow rule is also required. The flow rule is a law which relates the relative magnitudes of the strain increments to the stresses. The flow rule is derived from the requirement that the plastic strain increment direction should be normal to the plastic potential surface. There are an infinite number of such surfaces, and one passes through every point in stress space. In so-called perfect plasticity, the plastic potential surface is assumed to be the same

as the yield surface. This implies much higher rates of dilation than are observed in tests on real soils. When the plastic potential surface is assumed to differ from the yield surface, i.e. when the flow rule is non-associated, better agreement between model predictions and experimental results can be achieved.

3. A work-hardening law is needed, from which the magnitudes of the plastic strain increments caused by a given stress increment can be determined.

Failure and Yield Criteria

For most cohesionless soils the failure surface is curved. In the present model of Lade, a conical failure surface with the apex at the coordinate center of the principal stress space is used, as shown in Figure 5.2. The yield surface is expressed in terms of the first and third stress invariants as follows

$$f = \frac{I_1^3}{I_3} \tag{5.3}$$

where:

$$I_1 = \sigma_1 + \sigma_2 + \sigma_3$$

$$= \sigma_x + \sigma_y + \sigma_z$$

and

$$I_3 = \sigma_1.\sigma_2.\sigma_3$$

$$= \sigma_x\sigma_y\sigma_z + 2\tau_{xy}\tau_{yz}\tau_{zx} - (\sigma_x\tau_{xy}^2 + \sigma_y\tau_{zx}^2 + \sigma_z\tau_{xy}^2)$$

The failure is expressed as :

$$K_1 = \frac{I_1^3}{I_3} \tag{5.4}$$

where K_1 is a constant whose value depends on the density of the sand. The value of f varies between 27 for hydrostatic stress condition up to K_1 at failure.

Flow Rule

The yield criterion and the plastic potential function are usually assumed identical in the theory of plasticity. In the present model the plastic potential function is different from the yield function; for this reason the flow rule is said to be non-associative. The plastic potential function is expressed as:

$$g = I_1^3 - K_2.I_3 \tag{5.5}$$

where K_2 is constant for any given value of f and is calculated from

$$K_2 = Af + 27(1 - A) \tag{5.6}$$

where A is a model constant and it is evaluated from triaxial compression tests as it will be described in the following chapter. The plastic strain increments are related to the plastic potential function by the following expression:

$$d\epsilon_{ij}^p = \lambda.\frac{\delta g}{\delta \sigma_{ij}} \tag{5.7}$$

where λ is the proportionality constant and is determined by the work hardening rule.

Work Hardening Rule

The work hardening rule in this model is an experimentally determined relationship between the plastic work, W_p, and the stress level, f. Lade found experimentally that the plastic work starts after a certain stress level called threshold stress level, f_t. Therefore, the relation between W_p and $(f - f_t)$ as shown on Figure 5.3 is the following:

$$(f - f_t) = \frac{W_p}{a + b.W_p} \tag{5.8}$$

The initial slope of a curve representing the W_p versus $(f - f_t)$ relation is the reciprocal of the parameter a. The value of a increases with confining pressure, and this variation is expressed as

$$a = M.p_a(\frac{\sigma_3}{p_a})^l \tag{5.9}$$

where p_a is the atmospheric pressure and M and l are dimensionless numbers.

The parameter b in Equation 5.8 is the reciprocal of the ultimate value of $(f - f_t)$, which the hyperbola approaches asymptotically with increasing values of W_p. This relation is given by

$$b = \frac{1}{(f - f_t)_{ult}} \tag{5.10}$$

As the value of $(f - f_t)_{ult}$, determined by a curve-fitting procedure, was always larger than the value of $(f - f_t)$ at failure for finite values of W_p, a new parameter called r_f was introduced to relate the asymptotic value of $(f - f_t)$ to its value at failure, defined by

$$r_f = \frac{(K_1 - f_t)}{(f - f_t)_{ult}} \tag{5.11}$$

Plastic Strain Increments

In the theory of plasticity the relation between plastic strain increments and the plastic potential function is expressed by

$$d\epsilon_{ij}^p = \lambda \frac{\delta g}{\delta \sigma_{ij}} \tag{5.12}$$

The determination of the proportionality constant λ follows the development outlined by Hill (1950):

$$\lambda = \frac{dW_p}{3g} \tag{5.13}$$

in which the increments in plastic work for Lade's model is given by

$$dW_p = \frac{a.df}{[1 - r_f.\frac{(f-f_i)}{(K_1-f_i)}]^2} \tag{5.14}$$

The plastic strain increments, expressed in suffix notation in (4.12), become in matrix form:

$$\begin{Bmatrix} d\epsilon_x^p \\ d\epsilon_y^p \\ d\epsilon_z^p \\ d\epsilon_{xy}^p \\ d\epsilon_{yz}^p \\ d\epsilon_{zx}^p \end{Bmatrix} = \frac{a.df}{3g(1 - r_f.\frac{(f-f_i)}{(K_1-f_i)})^2} \begin{Bmatrix} 3I_1^2 - k_2(\sigma_y\sigma_z - \tau_{yz}^2) \\ 3I_1^2 - k_2(\sigma_z\sigma_x - \tau_{zx}^2) \\ 3I_1^2 - k_2(\sigma_x\sigma_y - \tau_{xy}^2) \\ K_2(\sigma_z\tau_{xy} - \tau_{yz}\tau_{zx}) \\ K_2(\sigma_x\tau_{yz} - \tau_{xy}\tau_{zx}) \\ K_2(\sigma_y\tau_{zx} - \tau_{yz}\tau_{xy}) \end{Bmatrix} \tag{5.15}$$

5.3 Modified Model

There are some limitation of Lade's work hardening model. One of these limitations is unsatisfactory modelling in proportional loading. Similarly, for all stress paths shown in Figure 5.4, the model predicts only recoverable strains which is in contradiction with observed soil behaviour. The cone shaped yield surface of the model which does not have a cap is shown in Figure 5.2a. In the calculations, any stress increment along a stress path remaining within that cone does not produce any plastic strains. In reality, however, plastic strains may take place for some stress paths in that zone. In order to overcome this limitation, the cap type yield surface formulated by Lade (1977) for his second model has been attached to the open end of the conical yield surface of the work hardening model. The second soil model of Lade accounts for additional features of soil behaviour such as the strain softening and the curvature in the failure envelope. Further, it differs entirely in its formulation, and appears to be more complete compared to the first model. These additional features may well be very important for the analysis of some

engineering problems. However, not in every geotechnical engineering project, the modelling of the strain softening and curvature of the failure envelope are essential. Usually, a better model brings its own complications. For example, adopting the second model requires additional parameters, and convergence becomes more difficult in the finite element analysis. With these considerations in mind, the first model of Lade has been complemented with a cap yield surface taken from his second model.

Plastic strains related to the cap yield surface are called collapse strains. Total plastic strain increments are calculated by adding the plastic strain increments given by Equation 5.15 to the plastic collapse strains as described in the following sections.

5.3.1 Plastic Collapse Strains

Contrary to the assumption made for metals in the classical theory of plasticity, soils behave in such a way that part of the strain increment due to hydrostatic compression is irrecoverable. Similarly, under proportional loading part of the strain increment is plastic in nature. It is believed that the plastic collapse strains are produced by re-arrangement of the grain structure and this results in a volumetric reduction. The development of the stress-strain relation is as follows.

Yield Criterion

The cap yield surface of Lade's second model was chosen without any change in its formulation as the desired cap for the work hardening model. The cap yield surface used by Lade (1977) is a sphere with the center in the origin of the principal

stress space as shown in Figure 5.5 and it is described by the function

$$f_c = I_1^2 + 2.I_2 \tag{5.16}$$

where I_1 and I_2 are the first and second stress invariants respectively. If a stress increment results in an increase in the value of the yield function f_c, i.e., $df_c > 0$, then the soil will undergo elastoplastic deformation while work hardening takes place. This type of yielding does not result in eventual failure. The type of yielding which causes the conical yield surface to expend is responsible for soil failure.

Flow Rule

An associated flow rule is used for the calculation of plastic collapse strain increments. Hence, the plastic potential function is identical to the yield function and it is expressed as:

$$g_c = I_1^2 + 2.I_2 \tag{5.17}$$

The relation between the plastic collapse strain increments and the plastic potential function is given as:

$$\Delta\epsilon_{ij}^p = \Delta\lambda_c . \frac{\delta f_c}{\delta \sigma_{ij}} \tag{5.18}$$

λ_c is the proportionality constant and its value is determined by the work hardening rule.

Work Hardening Rule

The work hardening rule required for the calculation of the magnitude of the plastic strain increments is expressed as an experimentally determined relation between the total plastic work, W_c due to collapse strain and the value of the

yield function f_c.

$$W_c = C.p_a.(\frac{f_c}{p_a^2})^p \tag{5.19}$$

where p_a is the atmospheric pressure, and C and p are constants which can be determined from a (W_c/p_a) versus (f_c/p_a^2) plot in $log - log$ scale. It is assumed that the work hardening relation is independent of the stress path.

The value of λ_c can be determined from the following expression.

$$\Delta\lambda_c = \frac{dW_c}{2.f_c} \tag{5.20}$$

where

$$dW_c = C.p.p_a.(\frac{p_a^2}{f_c})^{1-p}.d(f_c/p_a^2) \tag{5.21}$$

The derivation of Equation 5.21 is given by Lade (1977).

By substituting Equation. 5.20 into Equation 5.18 and calculating the partial derivatives of the plastic potential function, the final form of the stress-strain relation for the plastic collapse strains becomes

$$\Delta\epsilon_{ij}^c = \frac{dW_c}{2.f_c}.\frac{\delta f_c}{\delta\sigma_{ij}} \tag{5.22}$$

where dW_c is given by Equation 5.21.

5.3.2 Total Strain Increments

In the modified model, the total strain increments are calculated as the sum of elastic strains, plastic strains related to the expansion of the cone yield surface, and plastic collapse strains.

$$\{d\epsilon_{ij}\} = \{d\epsilon_{ij}^e\} + \{d\epsilon_{ij}^p\} + \{d\epsilon_{ij}^c\} \tag{5.23}$$

It is assumed that each part can be calculated separately and then superposed.

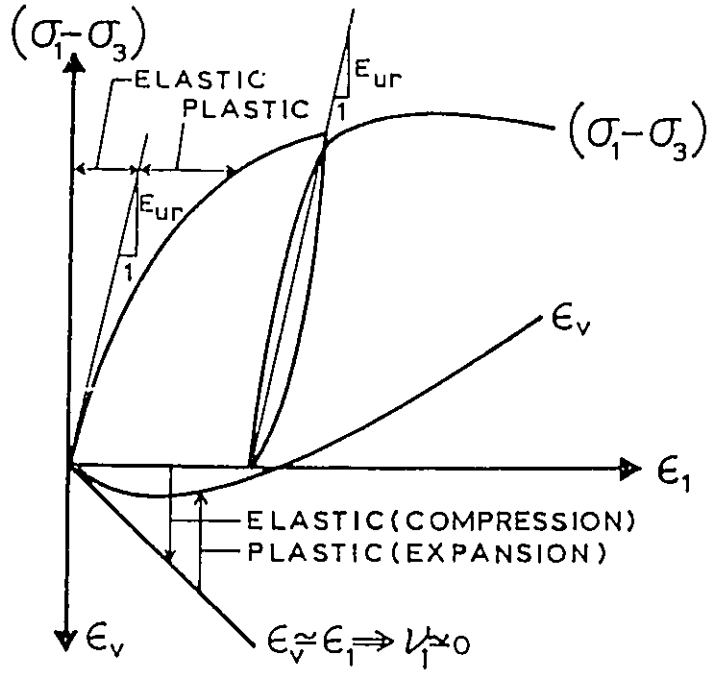

Figure 5.1: Elastic and plastic parts of strain in triaxial test (After Evgin, 1981)

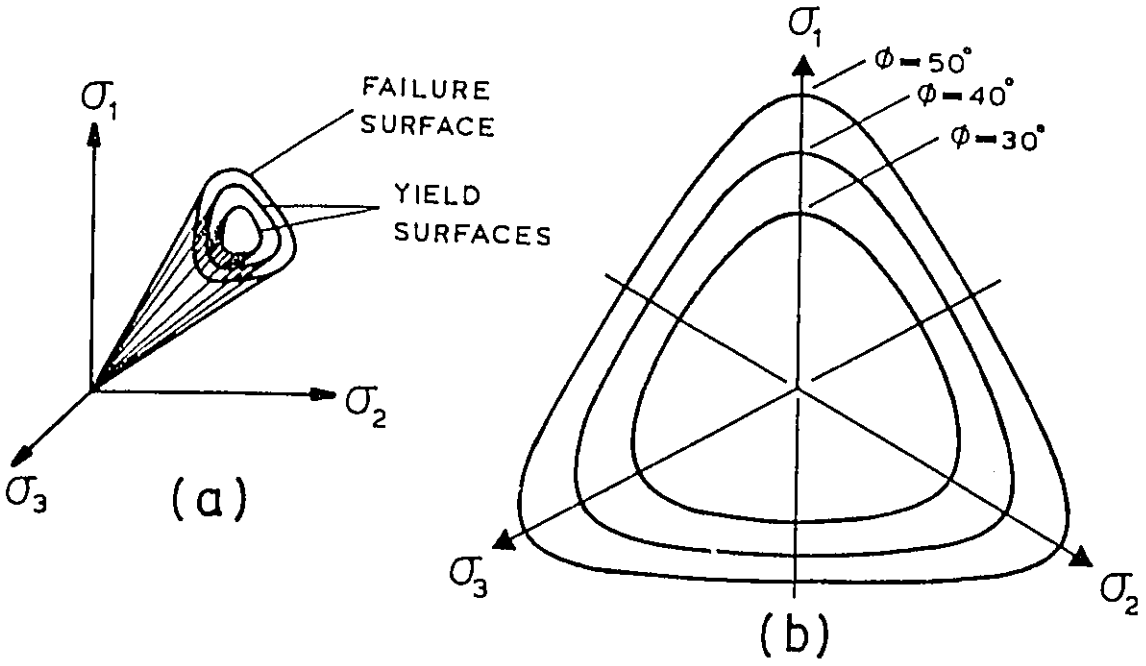

Figure 5.2: Yield and failure surfaces in (a) principal stress space (b) loci of surfaces on octahedral plane. (After Evgin, 1981)

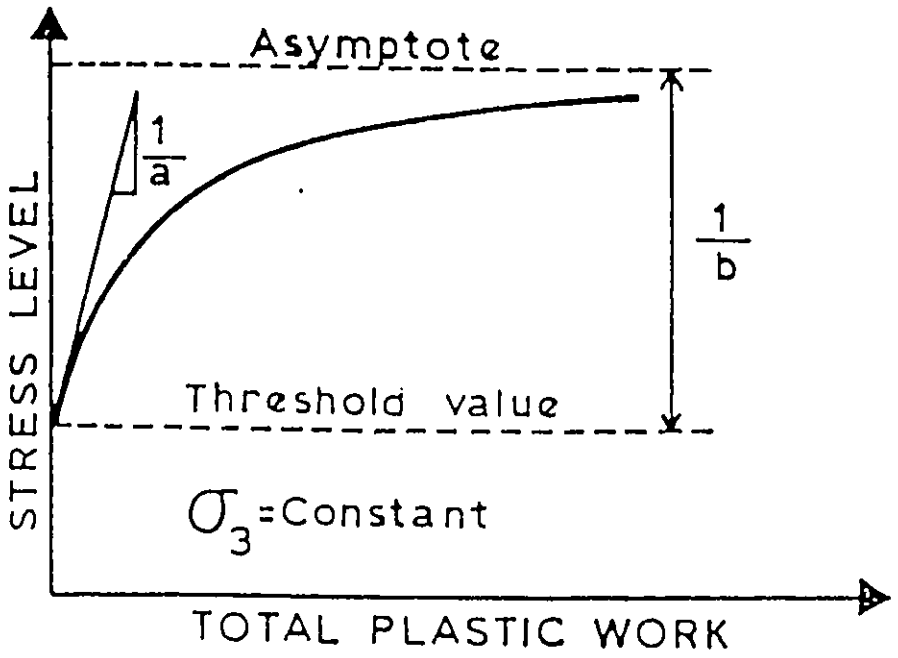

Figure 5.3: Relationship between plastic work and stress level. (After Evgin, 1981)

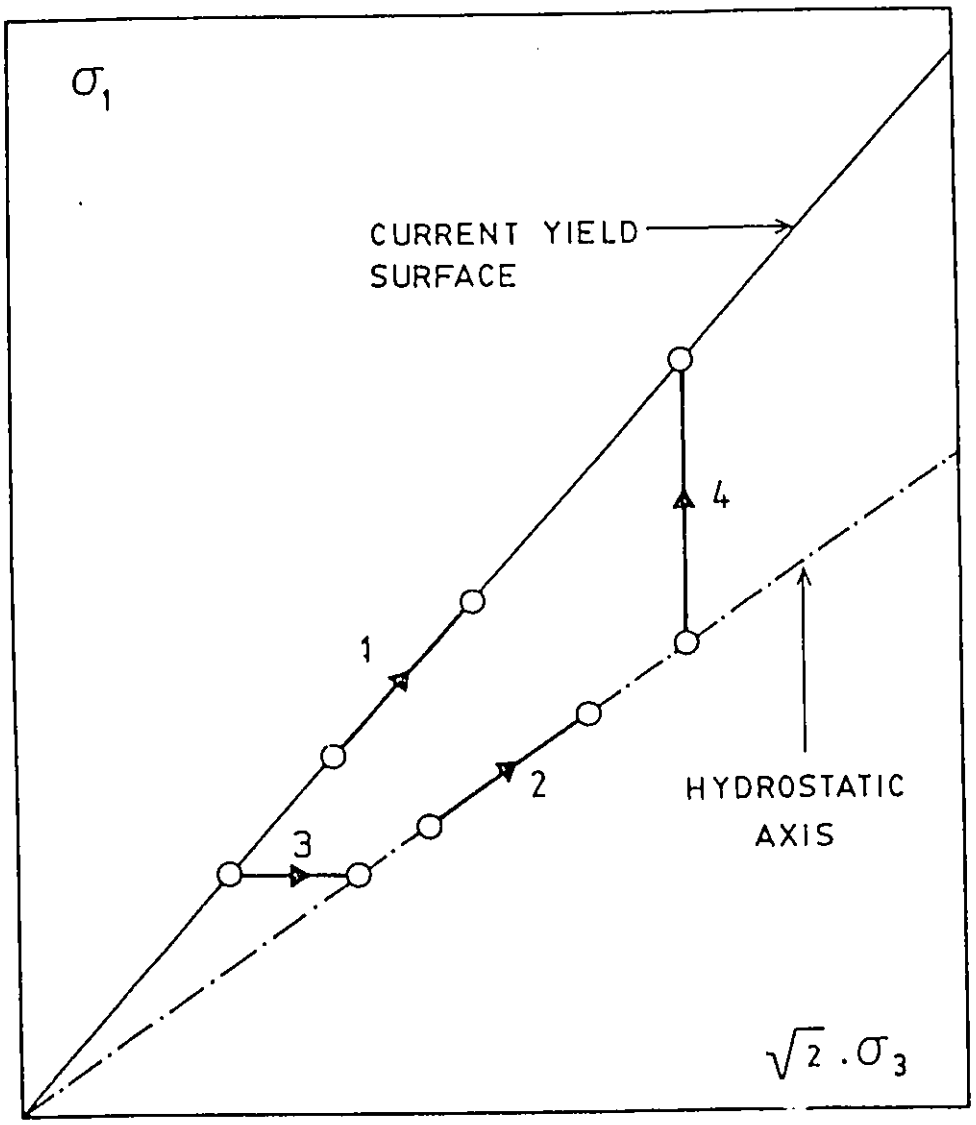

Figure 5.4: Example of stress paths where no plastic strain increments e and D are predicted by the work hardening model without a cap (After Evgin, 1981)

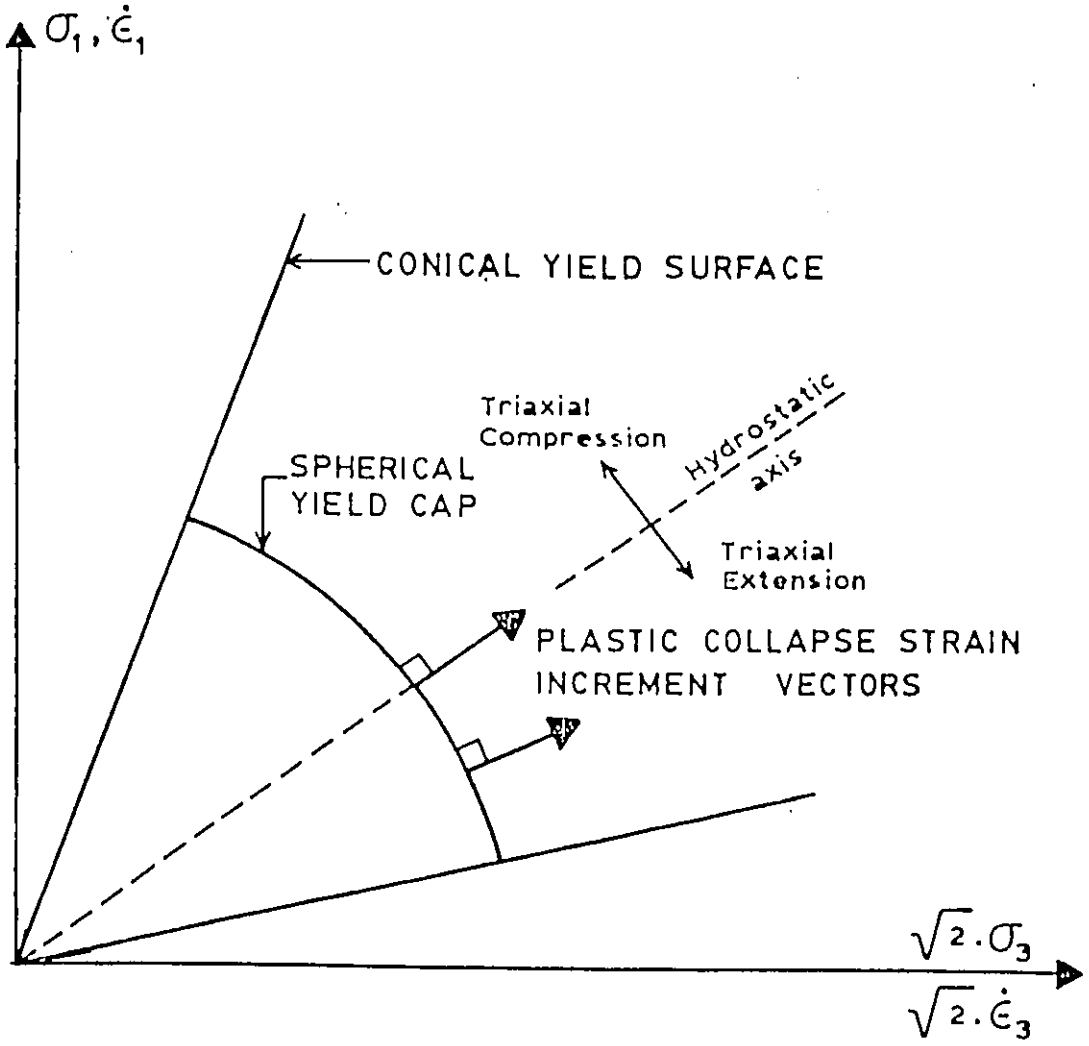

Figure 5.5: Location of yield cap relative to conical yield surface shown in triaxial plane (After Evgin, 1981)

Chapter 6

Model Parameters, Implementation and Simulations

6.1 Introduction

Lade's modified model has eleven elastic and plastic parameters. Two of these parameters are required by the work hardening rule of collapse strains. The remaining nine parameters belong to the work hardening model. The parameters related to the work hardening model can be obtained from the results of conventional triaxial tests while the parameters related to the collapse strains can be obtained from the results of isotropic compression test. The procedures to determine the parameters of the model are presented in this chapter.

Implementation of the model into a computer program was necessary in order to make simulations of soil behaviour within reasonable time. Model simulations of the behaviour of clean and oil contaminated sand are presented in the last section.

6.2 Model parameters

Nine parameters required for Lade's work hardening model are determined as follows.

1) Elastic parameters: K_{ur}, n and ν

ν is the Poisson's ratio, K_{ur} and n are modulus number and exponent.

First, E_{ur} for every σ_3 is determined from the unloading reloading branches of a stress-strain curve or from an isotropic compression test. Using a log-log scale as shown in Figure 6.1, the slope of the best fit line gives n. The ordinate of this line at $\frac{\sigma_3}{p_a} = 1$ gives the value of K_{ur}. The relation between E_{ur}, K_{ur}, n, and σ_3 is expressed in Equation 6.1.

$$E_{ur} = K_{ur} p_a (\frac{\sigma_3}{p_a})^n \tag{6.1}$$

Poisson's ratio, ν is determined from experiments as

$$\nu = -\frac{\Delta\epsilon_3}{\Delta\epsilon_1} \tag{6.2}$$

In Equation 6.2, the strain increments correspond to the unloading reloading portion of the stress strain curves. 2) Stress level at failure, K_1

It is calculated from

$$K_1 = \frac{I_1^3}{I_3} \tag{6.3}$$

where I_1 and I_3 are related to the state of stress at failure. 3) Threshold stress level, f_t

It is a value of f_p at which the plastic strains begin to take place. It is determined from the W_p versus f_p plot as shown in Figure 6.2.

4) Failure ratio, r_f

It is calculated from

$$r_f = \frac{K_1 - f_t}{(f - f_t)_{ult}} \tag{6.4}$$

5) Model parameter, A

Parameter A is used in the calculation of K_2 given by Equation 6.7. In order to

determine A from the experimental data, K_2 is found first from Equation 6.5. The derivation of Equation 6.5 is provided by Lade (1972).

$$K_2 = \frac{3I_1^2(1+\nu^p)}{\sigma_3(\sigma_1+\nu^p\sigma)} \tag{6.5}$$

where

$$-\nu^p = \frac{\Delta\epsilon_3^p}{\Delta\epsilon_1^p} \tag{6.6}$$

and

$$K_2 = Af + 27(1-A) \tag{6.7}$$

If the values of K_2 versus f are plotted as shown in Figure 6.3, the inclination of the straight line becomes the parameter A.

6) Dimensionless parameters, l and M

These parameters are related to the work hardening rule as explained in the following. The plastic work at each stage of the test is calculated as

$$W_p = \int \{\sigma_{ij}\}\{d\epsilon_{ij}^p\} \tag{6.8}$$

The reciprocal of the parameter, a, is the initial slope of the W_p versus $\frac{W_p}{(f-f_i)}$ relationship as shown in Figure 6.4. The value of a increases with confining pressure, and this variation is expressed as:

$$a = Mp_a(\frac{\sigma_3}{p_a})^l \tag{6.9}$$

In Equation 6.8, p_a is the atmospheric pressure expressed in the same units as a and σ_3. Both M and l are dimensionless numbers which may be determined by plotting the values of a versus the values of σ_3 on a log-log scale and fitting a straight line to the data as shown on Figure 6.5.

7) Collapse strain parameters C and p

Parameters C and p are used in the work hardening rule of a cap yield surface. The work due to collapse strains is calculated from

$$W_c = \int \{\sigma_{ij}\}\{d\epsilon_{ij}^c\} \tag{6.10}$$

The value of the yield function is calculated from

$$f_c = I_1^2 + 2I_2 \tag{6.11}$$

where

$$I_2 = -(\sigma_1\sigma_2 + \sigma_2\sigma_3 + \sigma_3\sigma_1) \tag{6.12}$$

When $\frac{f_c}{p_a^2}$ versus $\frac{W_c}{p_a}$ is plotted in a log-log scale, the slope of the straight line representative of the best fit curve is p and the ordinate of the point at $\frac{f_c}{p_a} = 1$ is C as shown in Figure 6.8.

A computer program, KPARA, was developed in order to obtain some of the parameters. The listing of KPARA can be found in Appendix A.

6.3 Model Implementation

A computer program, KLADE, was necessary to make simulations of the soil behaviour in laboratory experiments described in chapter 2. An explanation of the main considerations in the development of the program are provided in this section.

1. The program starts by reading all the model parameters and the initial stresses applied on the sample.

2. It is possible to have the following four cases of present state of stress, PRE, with respect to the current yield surfaces. In Figure 6.7, CURFC indicates the current cap yield surface, and CURFP denotes the current cone yield surface.

3. When a stress increment is applied, the stress state moves to a new location, which is indicated as PNEW in Figure 6.8. Only the old location of the yield

surfaces are shown in Figure 6.8. For each case shown above in Figure 6.7, PNEW can have values shown in Figure 6.8.

4. The plastic collapse strains are not added to the total strain increments if the cone yield surface is expanding at the same time as the cap. The only time plastic collapse strains are added to the total strain increments, is when the cap expands while the cone stays stationary.

5. It should be noted that for case(a)+case(3), case(a)+case(5), case(a)+case(7), case(a)+case(8), case(a)+case(9), case(a)+case(10), case(a)+case(11), case(a)+case(12) or case(a)+case(14), it is necessary to find the intersection between the stress path and the old yield surfaces. The stress path may intersect either one of the yield surfaces or both of them. This state of stress, which is called CEN, is found using an iteration technique.

6. If the stress increment causes an expansion of both yield surfaces, only the plastic strains caused by the expansion of the cone are calculated. At the end of the calculations, the CURFP will be updated using PNEW. It is assumed that when the cone expands the equations given for the plastic strain calculations take into account all plastic strains.

7. When PNEW goes beyond RLK1, the intersection between the stress path and RLK1=FP (FP is the value of the yield function at that stress level) has to be found and the calculation of strain increments are carried out using the stress increment from PRE to CEN.

8. Although the possibilities are many as shown in items 2 and 3, some of the cases disappear because of the reason given in item 6. Some of the cases which look like separate cases are not separate cases, and this reduces the

possibilities as well.

6.4 Results of Predictions

The computer program, KLADE, was used to obtain predictions for the behaviour of crushed quartz sand which was presented in Chapter 2. The computer program was verified prior to making predictions. Experimental data and model parameters for Monterey No. 0 sand provided by Lade (1975) were used to ensure that the model implementation was succesful. Figure 6.9 shows the experimental results and those predicted using KLADE.

The listing of KLADE and a sample of input and output are presented in Appendix A.

Loose clean sand

The model predictions for the loose clean sand are presented in Figures 6.10, 6.11, and 6.12. The parameters used to obtain these predictions were determined using the procedures described earlier and are listed in Table 6.1. The model predicts acceptable results in terms of shear stresses, however, it underestimates the volumetric strains.

Loose oil contaminated sand

The model predictions for the loose oil contaminated sand are presented in Figures 6.13, 6.14, and 6.15. The parameters used to obtain these predictions are listed in Table 6.2.

It is noted that all model paramaters change when oil contamination occurs, except for ν, which was assumed to stay at a constant value. As the prediction given above show, the model is able to simulate the behaviour of both clean and oil contaminated loose sand during shearing. The volumetric strain, however seems to be underestimated by the model.

Dense clean sand

As shown on Figures 6.16, 6.17, and 6.18, the model is also capable of predicting the most significant aspects of the behaviour for the clean dense sand. The model parameters used to obtain these predictions are presented in Table 6.3.

Dense oil contaminated sand

As shown on Figures 6.19, 6.20, and 6.21, the model is predicting the behaviour of the oil contaminated dense sand quite well. The model parameters used to obtain these predictions are given in Table 6.4.

Isotropic Compression

Figure 6.22 shows how much improvement, in predicting results of an isotropic compression, is brought to the model upon the addition of a cap type yield surface.

Isotropic compression causes the cap to expand while the cone remains stationary. The results of isotropic compression tests performed on clean sand and the predictions are shown in Figures 6.23 and 6.24. The model produces very good predictions for the results of isotropic compression tests on clean crushed quartz sand. The predictions for the isotropic compression tests on oil contaminated sand are presented in Figures 6.25 and 6.26. The predictions are again very close to the measured values. The parameters C and p are given in Table 6.5.

Table 6.1: Model parameters for loose clean sand (e=1.13)

K_{ur}	280.0
n	0.61
ν	0.30
K_1	45.7
f_t	33.0
r_f	0.93
l	1.217
M	0.00258
A	0.35

Table 6.2: Model parameters for loose oil contaminated sand (e=1.13)

K_{ur}	130.0
n	1.2
ν	0.30
K_1	37.0
f_t	28.0
r_f	0.82
l	0.83
M	0.00523
A	0.30

Table 6.3: Model parameters for dense clean sand (e=0.42)

K_{ur}	456.0
n	0.79
ν	0.30
K_1	65.6
f_t	30
r_f	0.92
l	2.89
M	0.0000414
A	0.38

Table 6.4: Model parameters for oil contaminated sand (e=0.42)

K_{ur}	456.0
n	0.76
ν	0.30
K_1	48.4
f_t	33
r_f	0.97
l	3.36
M	0.0000414
A	0.45

Table 6.5: Model parameters C and p

Desciption	C	p
Dense, clean sand	0.000138	0.41
Dense oil contaminated sand	0.000147	0.57
Loose, clean sand	0.000152	0.59
Loose oil contaminated sand	0.000174	0.63

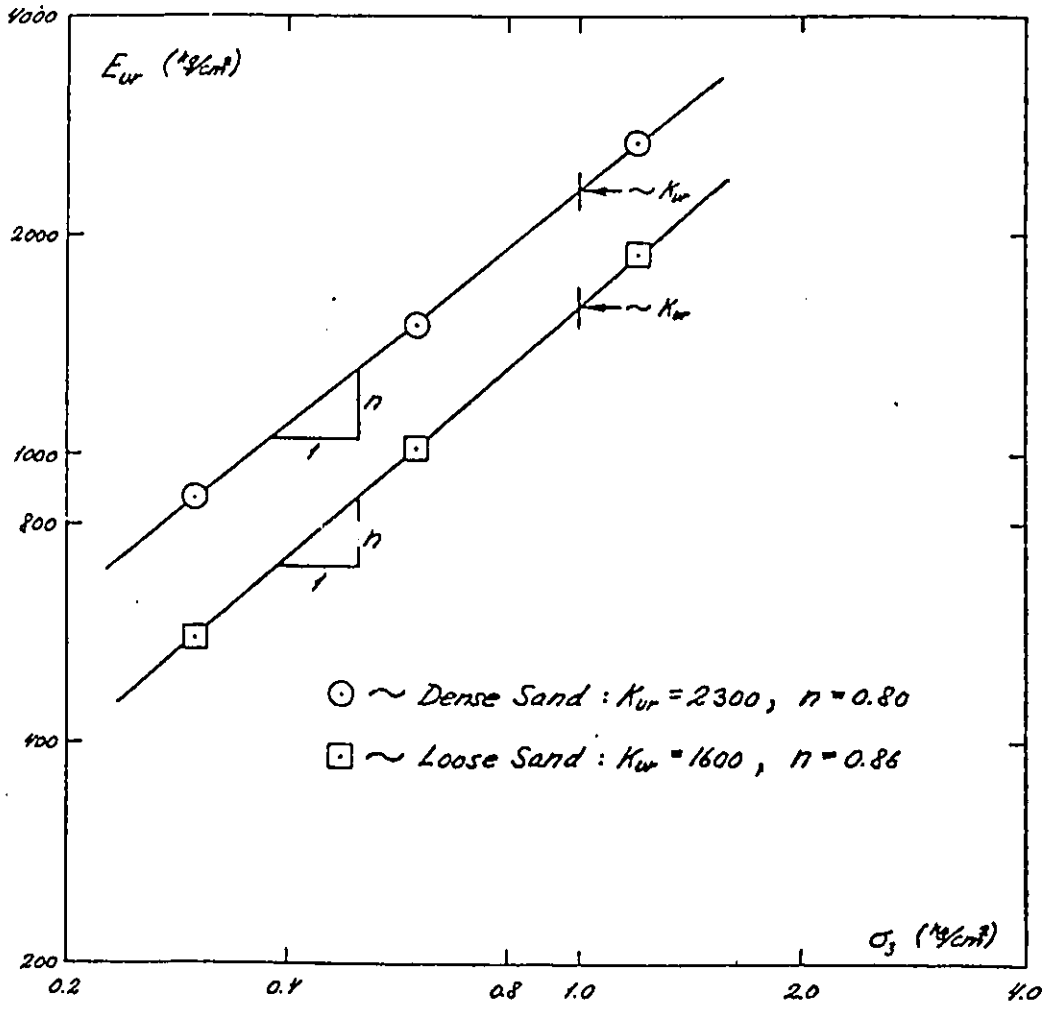

Figure 6.1: Derivation of elastic strain parameters (After Lade, 1972)

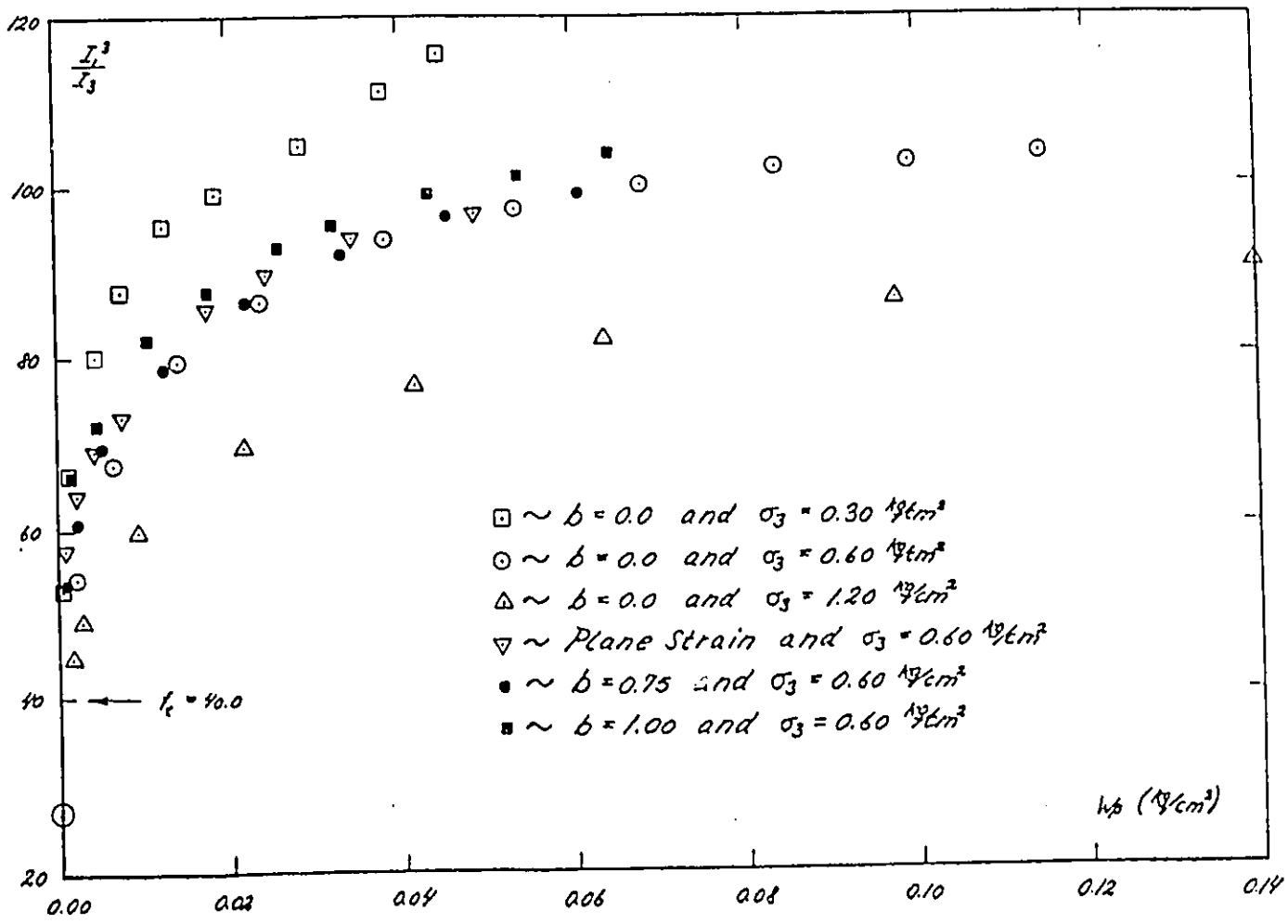

Figure 6.2: Variation of plastic work for dense Monterey No. 0 sand (After Lade, 1972)

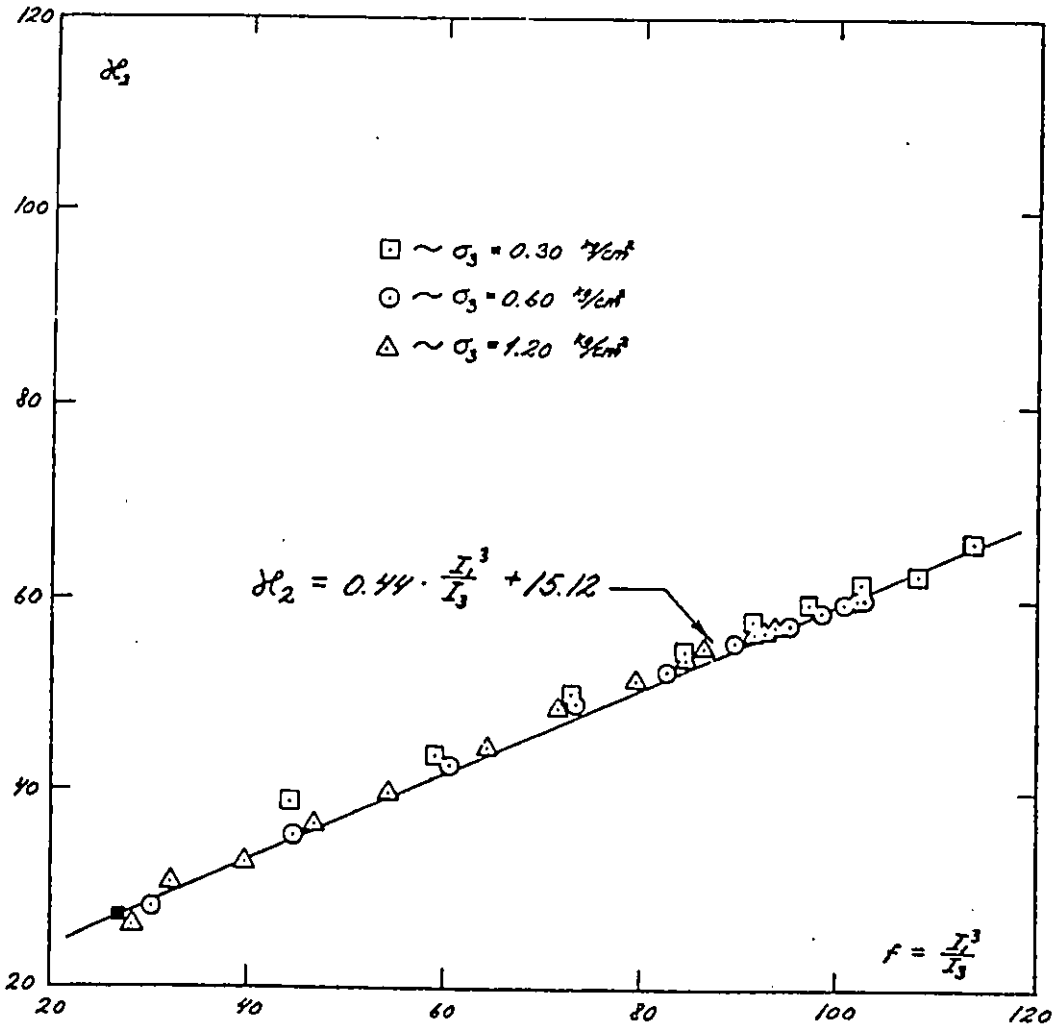

Figure 6.3: Variation of K_2 with stress level for dense Monterey No. 0 sand (After Lade, 1972)

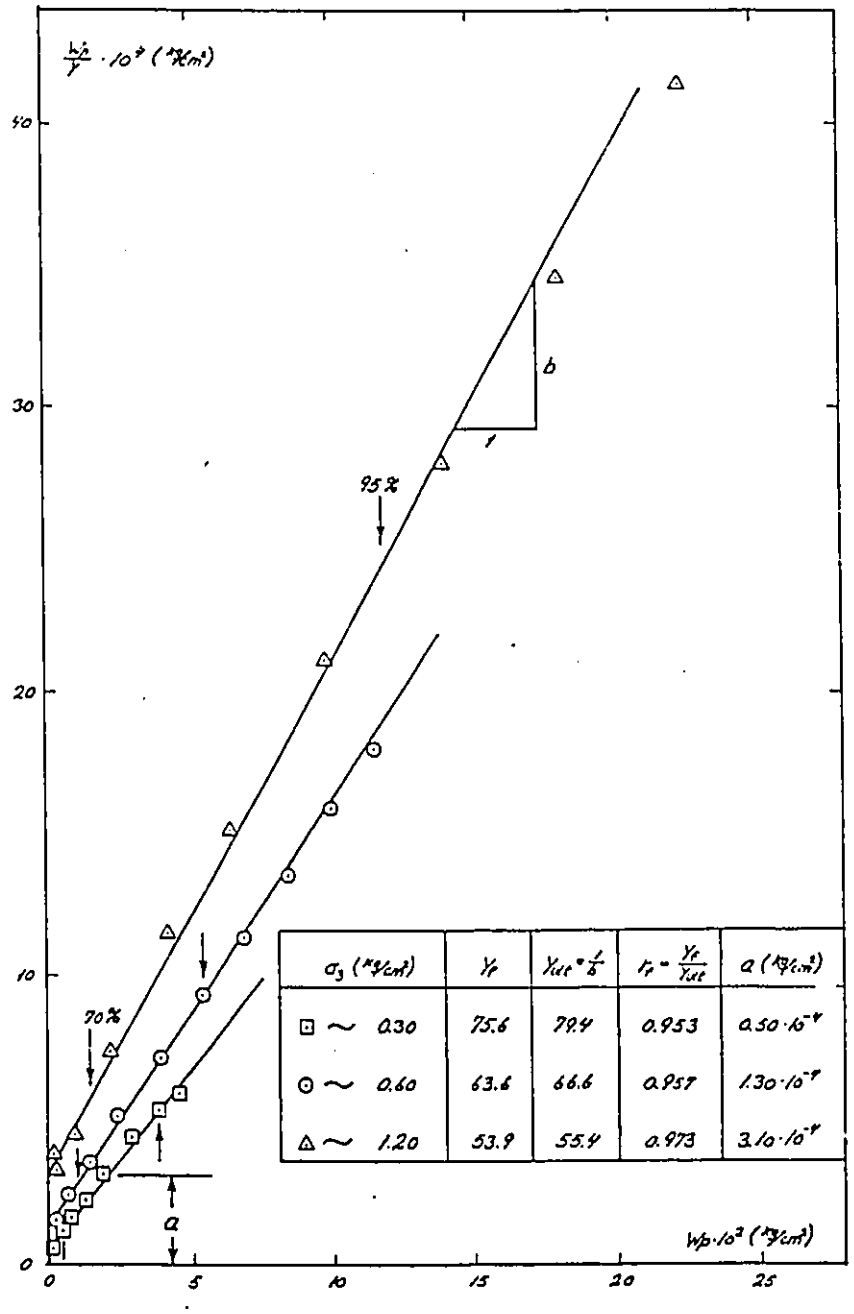

Figure 6.4: Transformed plastic work curves for dense Monterey No. 0 sand (After Lade, 1972)

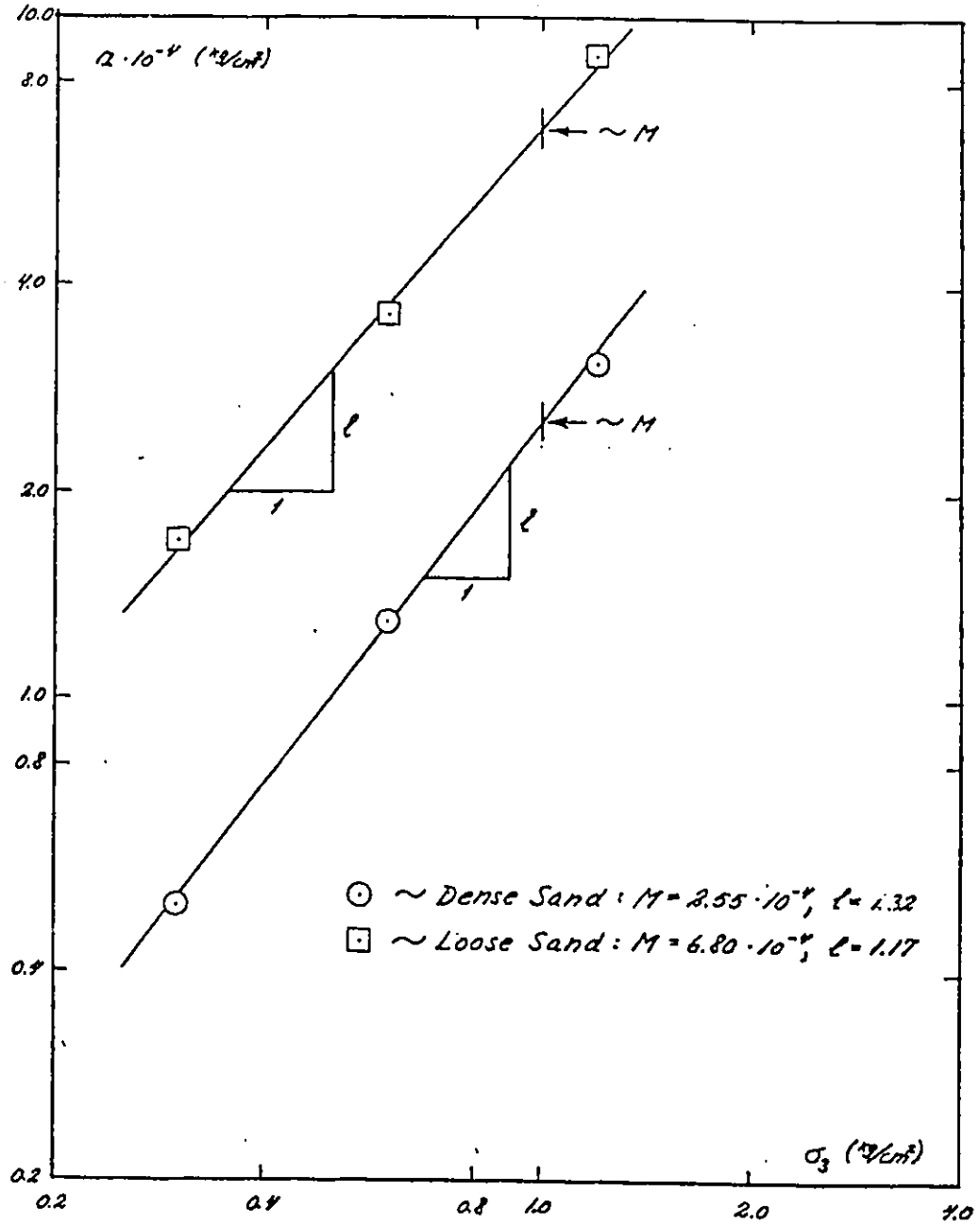

Figure 6.5: Variation if initial slope of plastic curves with confining pressure for dense Monterey No. 0 sand (After Lade, 1972)

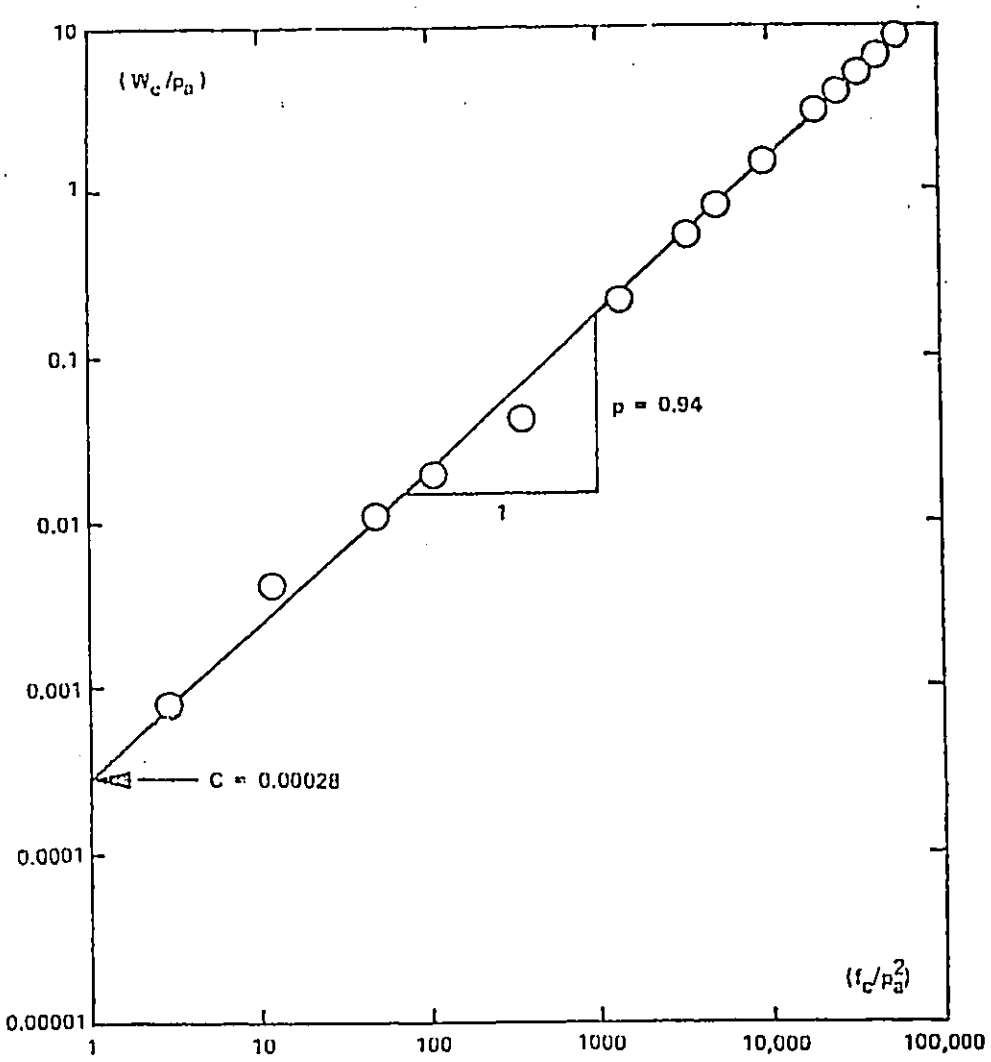

Figure 6.6: Determination of plastic collapse strains parameters (After Lade, 1977)

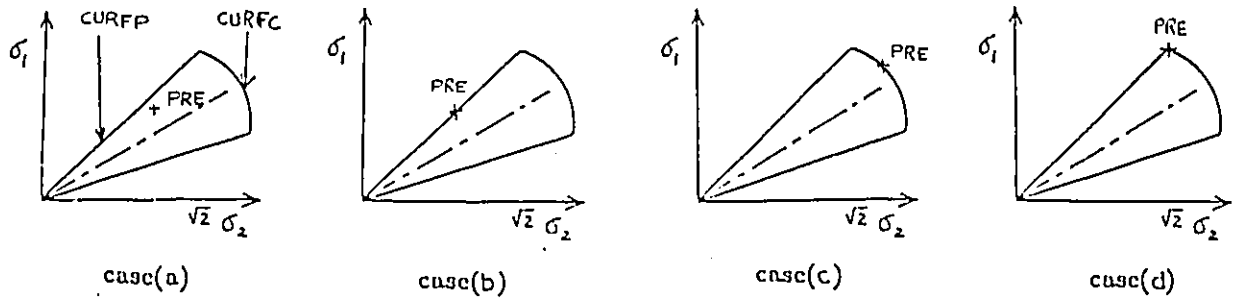

Figure 6.7: Location of new state of stress, PNEW, in the triaxial plane

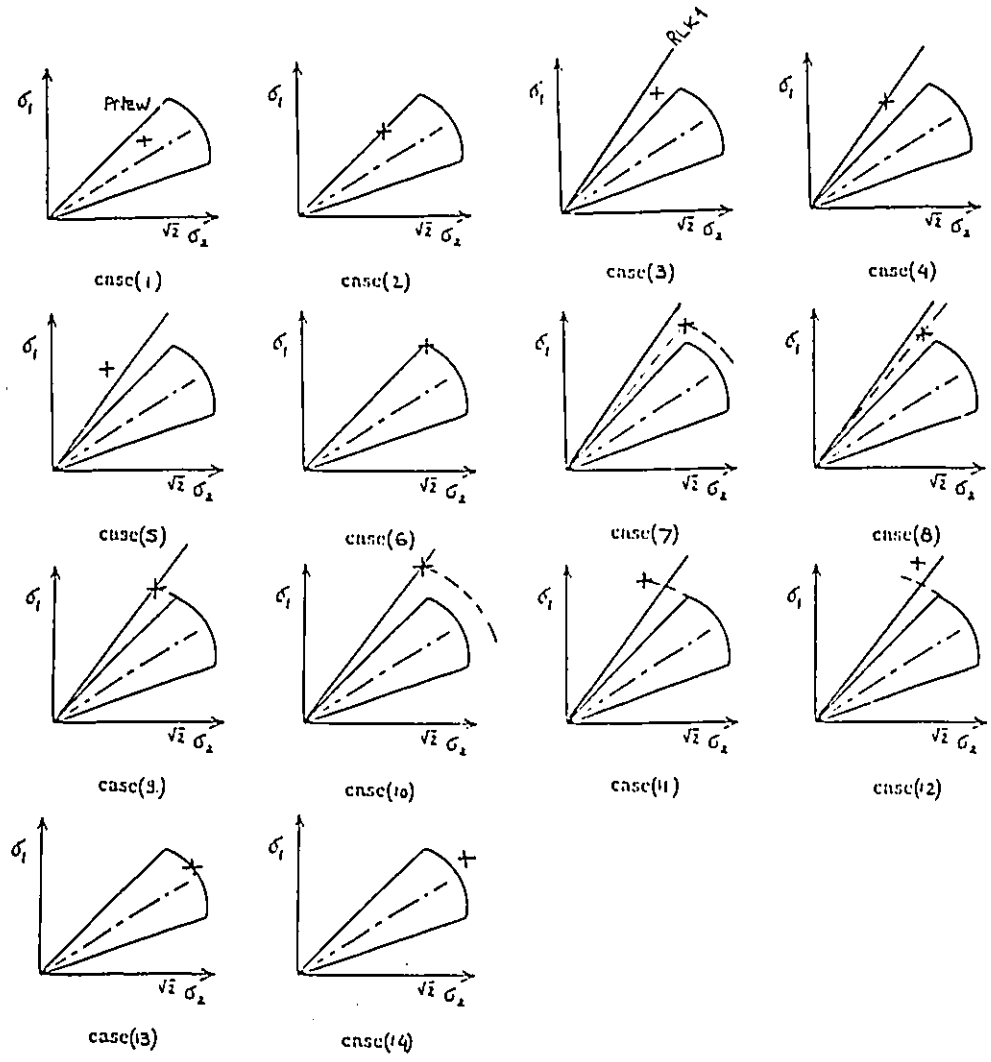

Figure 6.8: Present state of stress and location of current yield surfaces

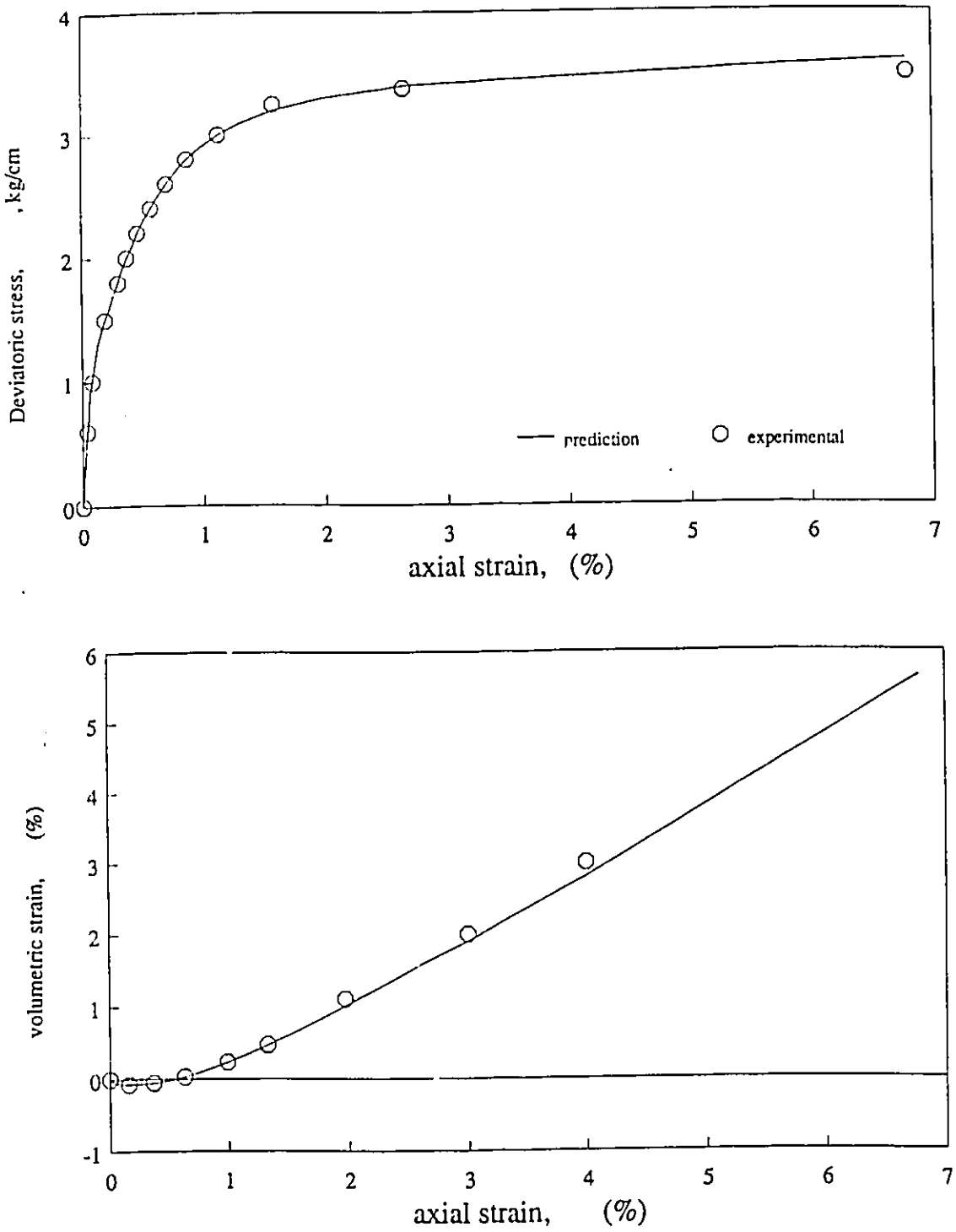

Figure 6.9: Measured and predicted triaxial test results on dense Monterey No. 0 sand

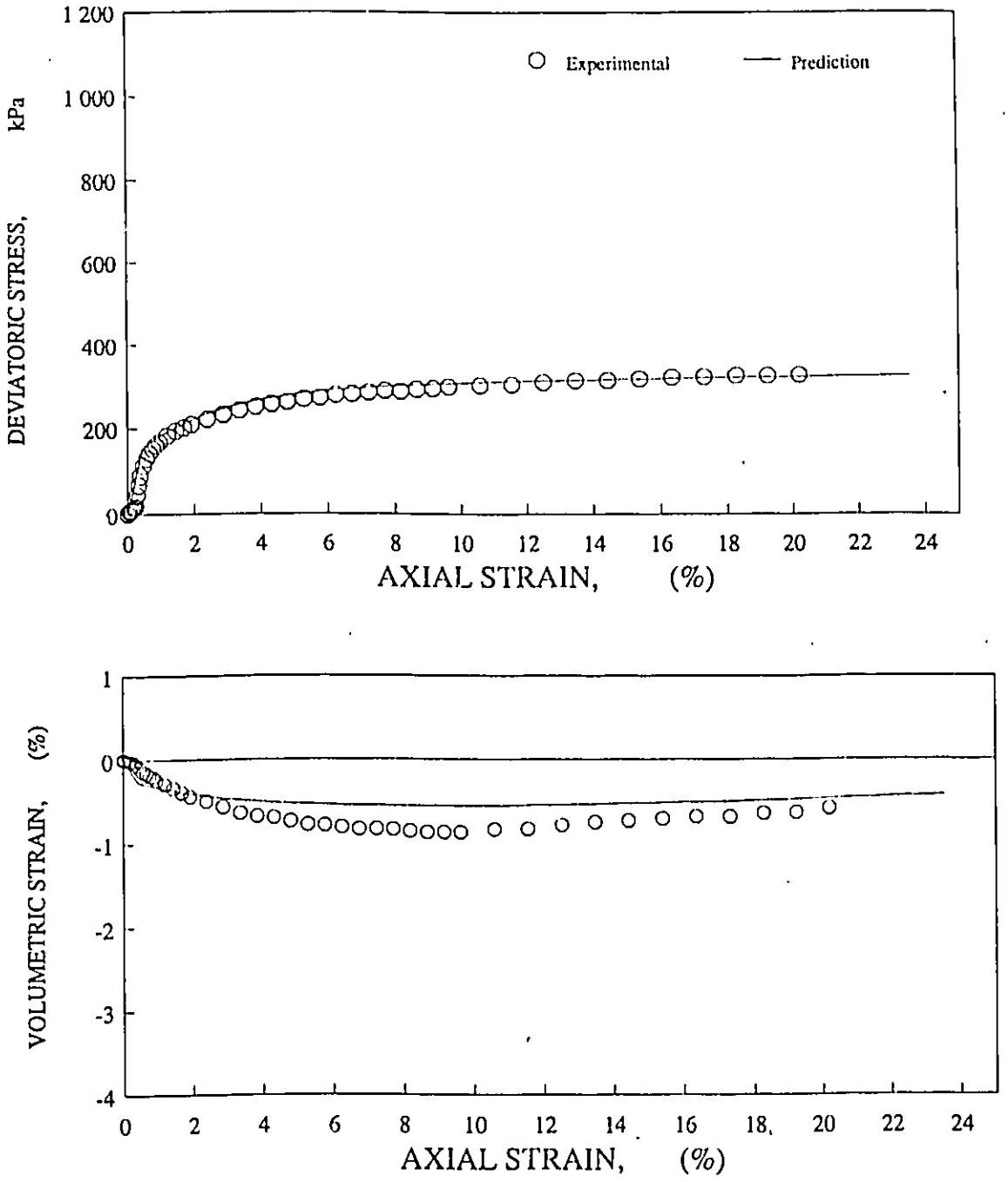

Figure 6.10: Measured and predicted triaxial test results on loose clean crushed quartz sand, σ_3=138 kPa

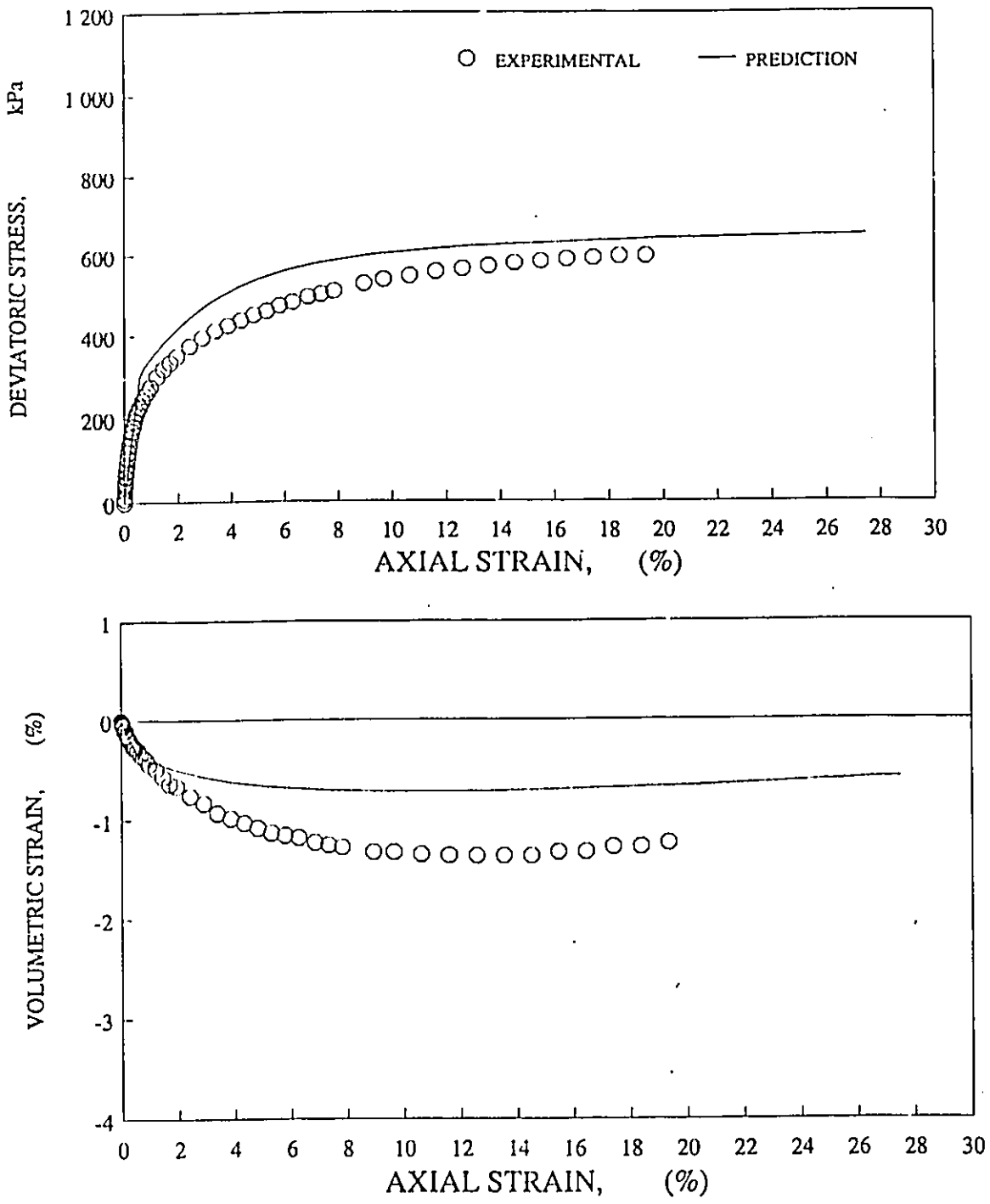

Figure 6.11: Measured and predicted triaxial test results on loose clean crushed quartz sand, σ_3=276 kPa

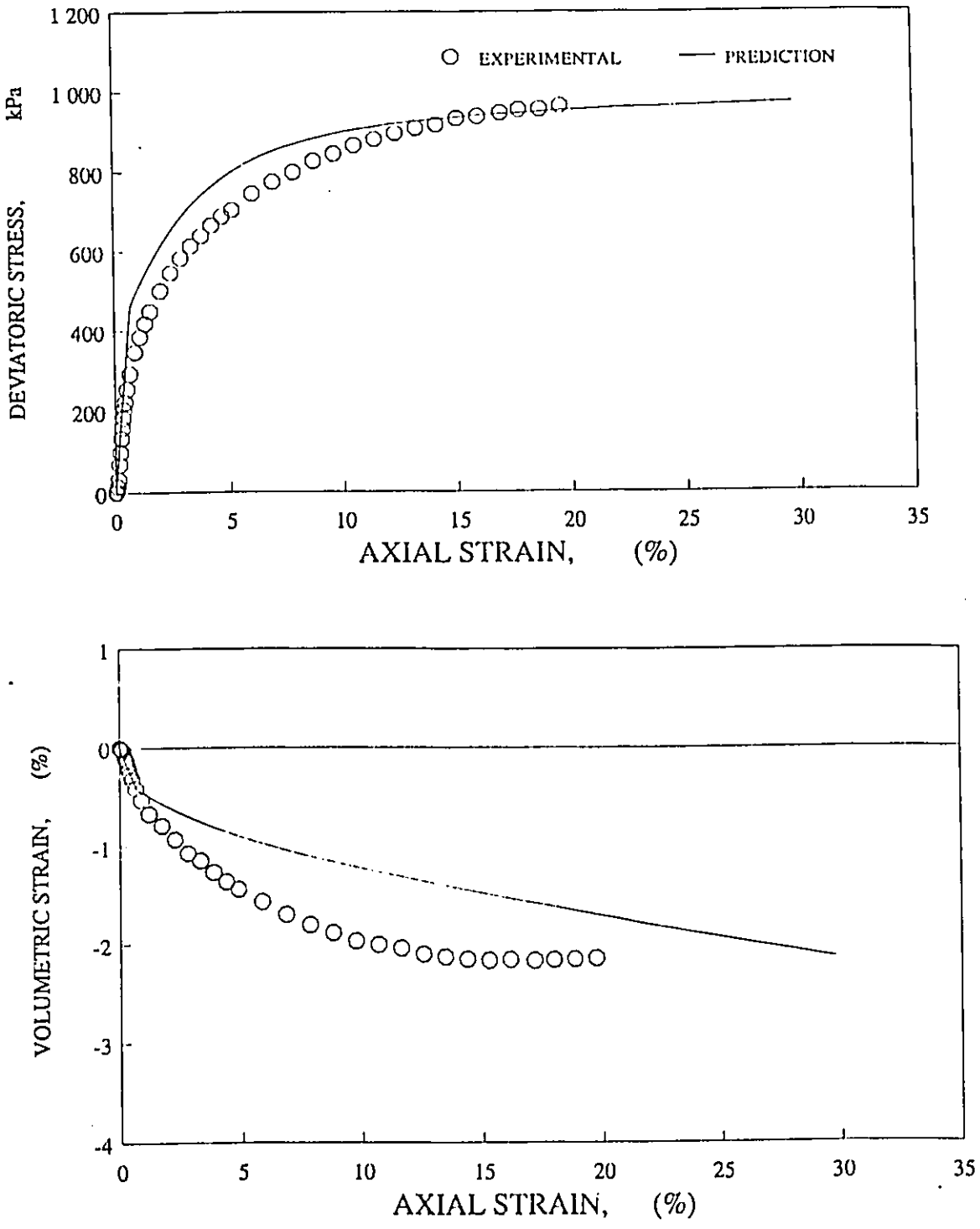

Figure 6.12: Measured and predicted triaxial test results on loose clean crushed quartz sand, σ_3=414 kPa

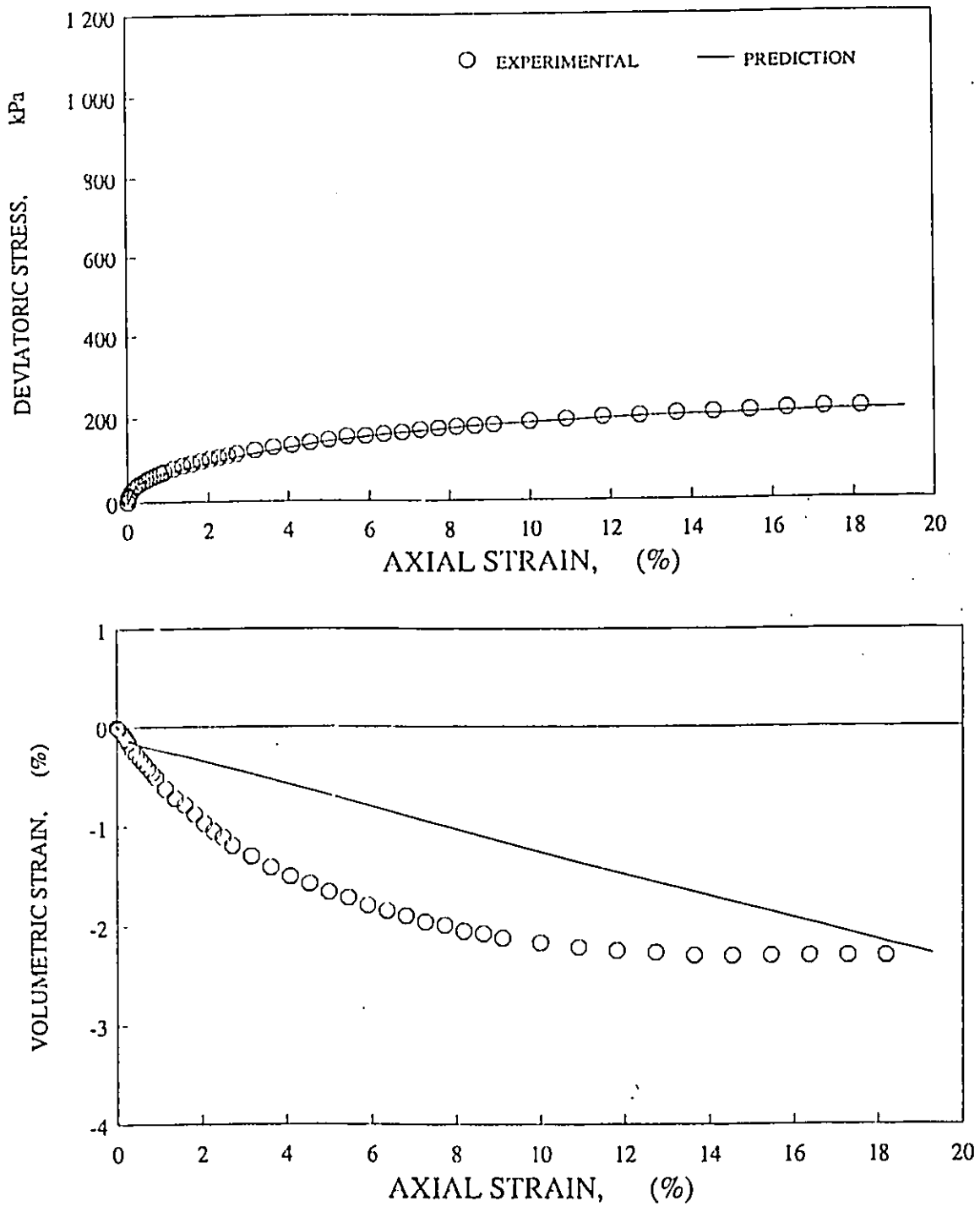

Figure 6.13: Measured and predicted triaxial test results on loose oil contaminated crushed quartz sand, σ_3=138 kPa

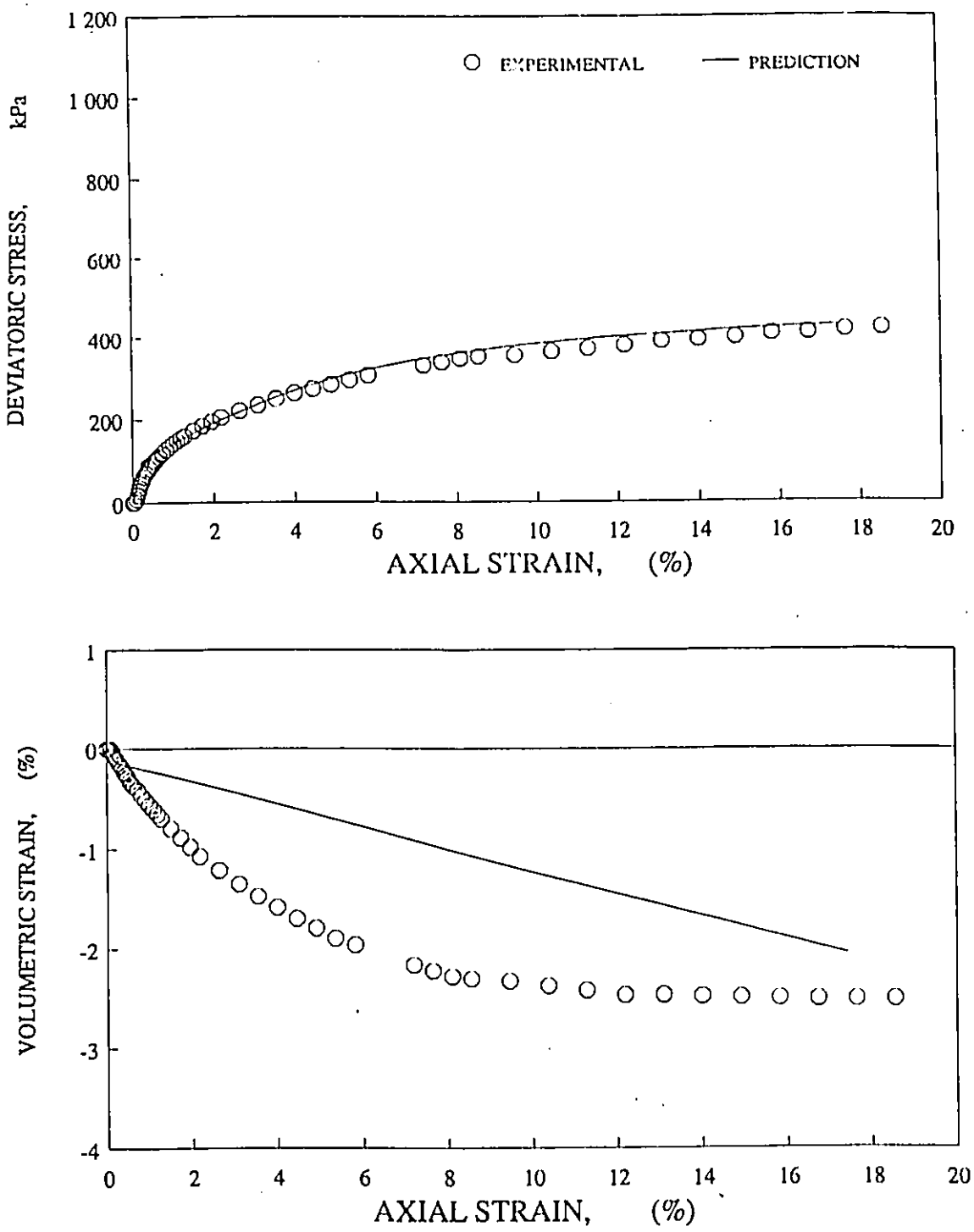

Figure 6.14: Measured and predicted triaxial test results on loose oil contaminated crushed quartz sand, σ_3=276 kPa

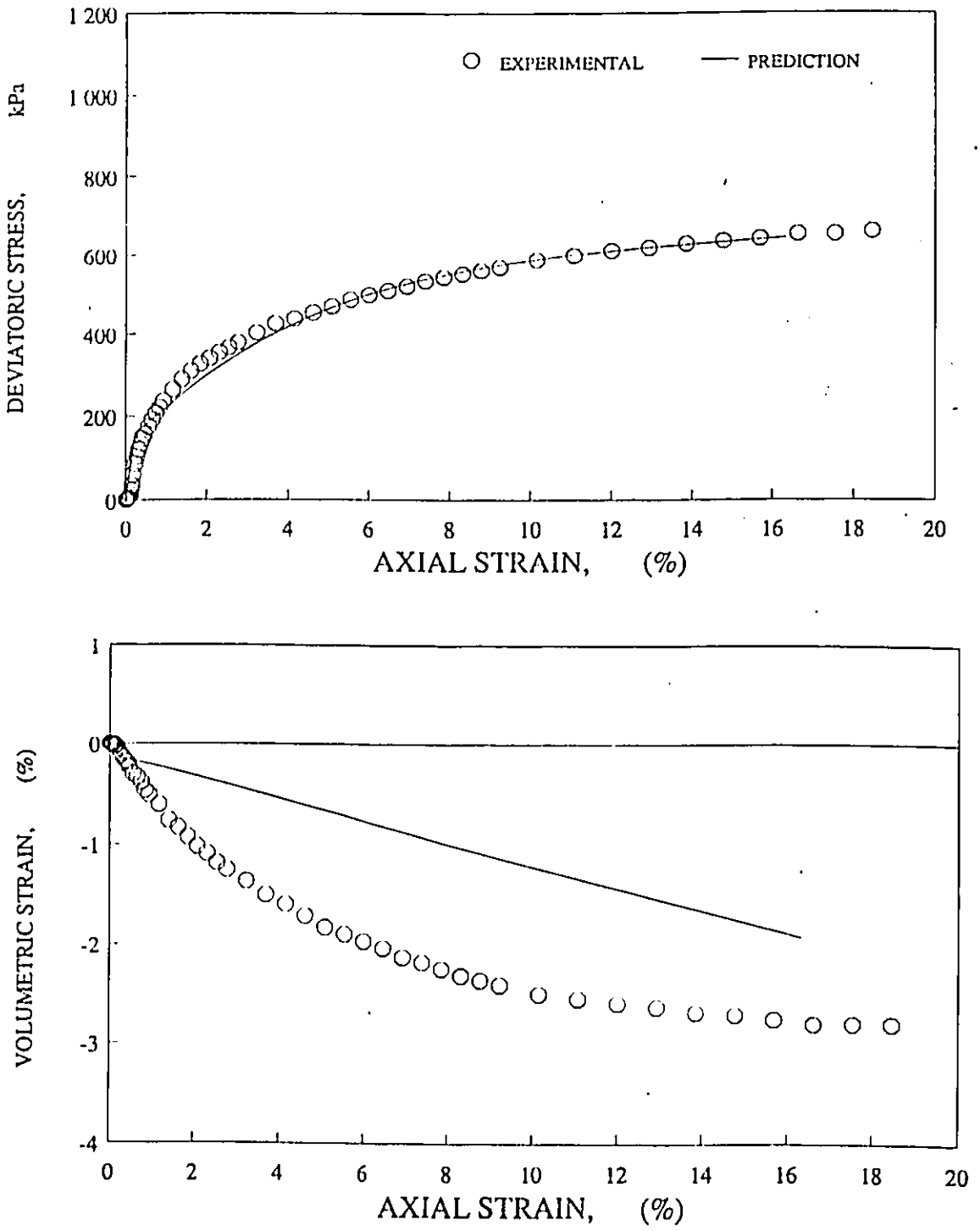

Figure 6.15: Measured and predicted triaxial test results on loose oil contaminated crushed quartz sand, σ_3=414 kPa

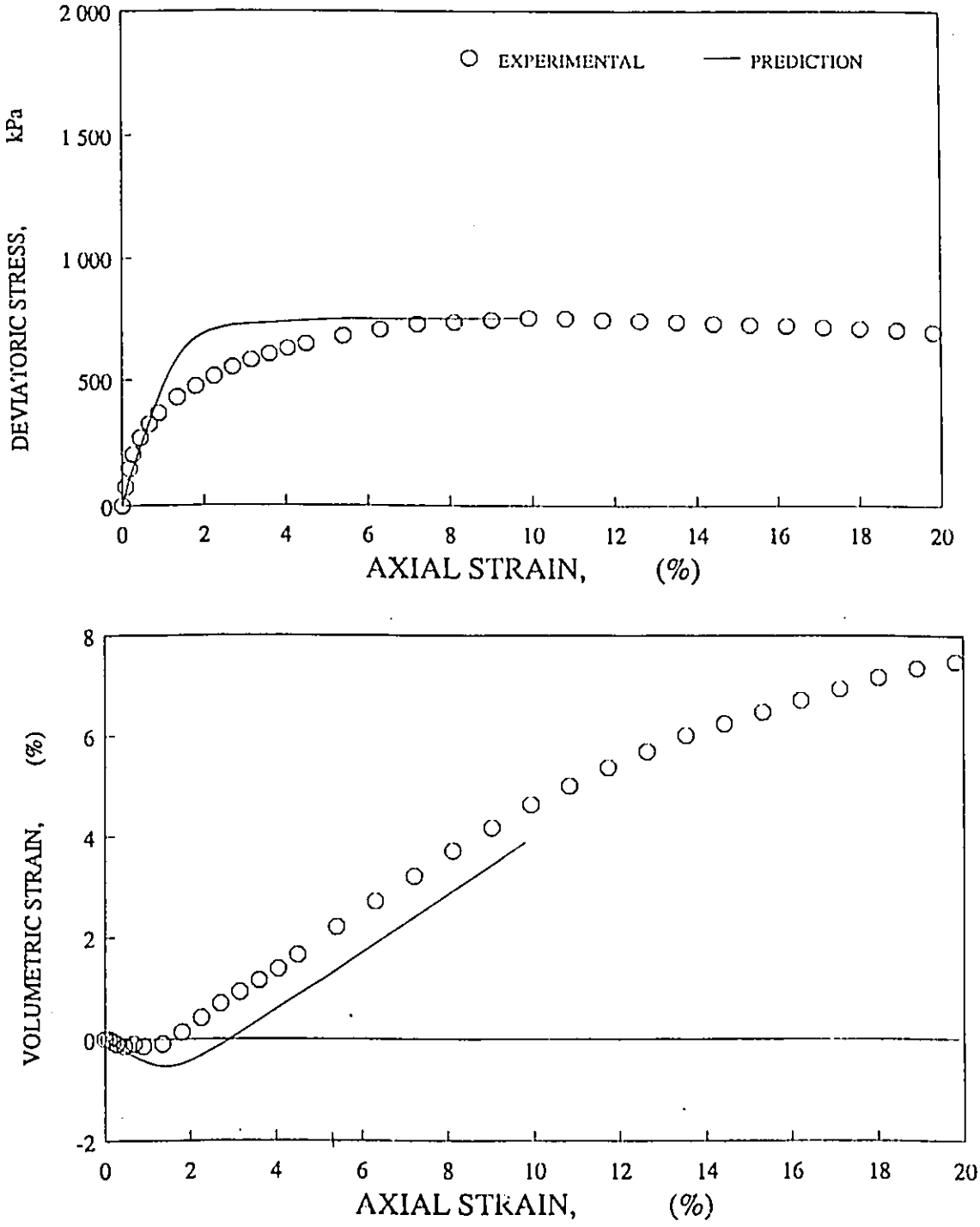

Figure 6.16: Measured and predicted triaxial test results on dense clean crushed quartz sand, σ_3=138 kPa

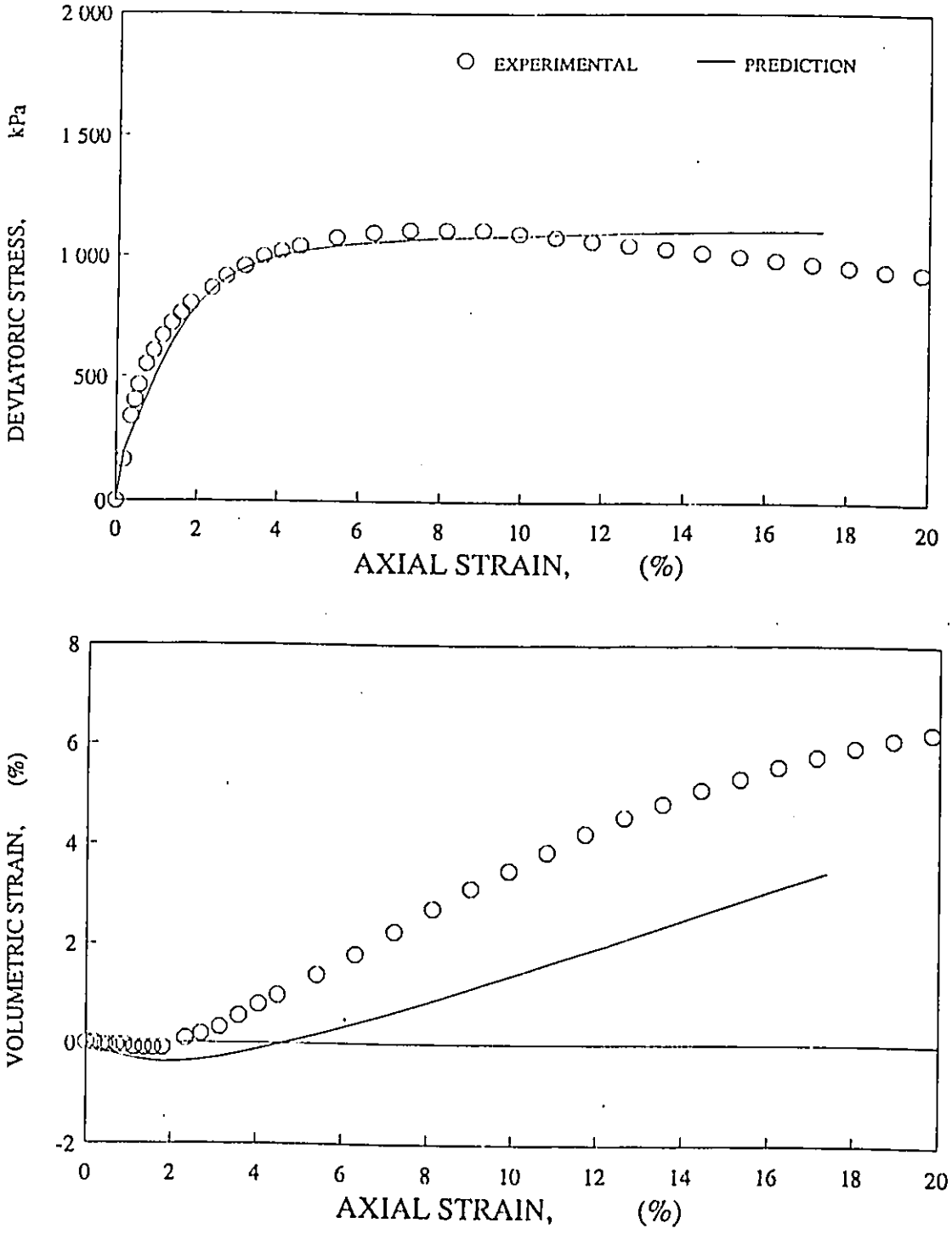

Figure 6.17: Measured and predicted triaxial test results on dense clean crushed quartz sand, σ_3=276 kPa

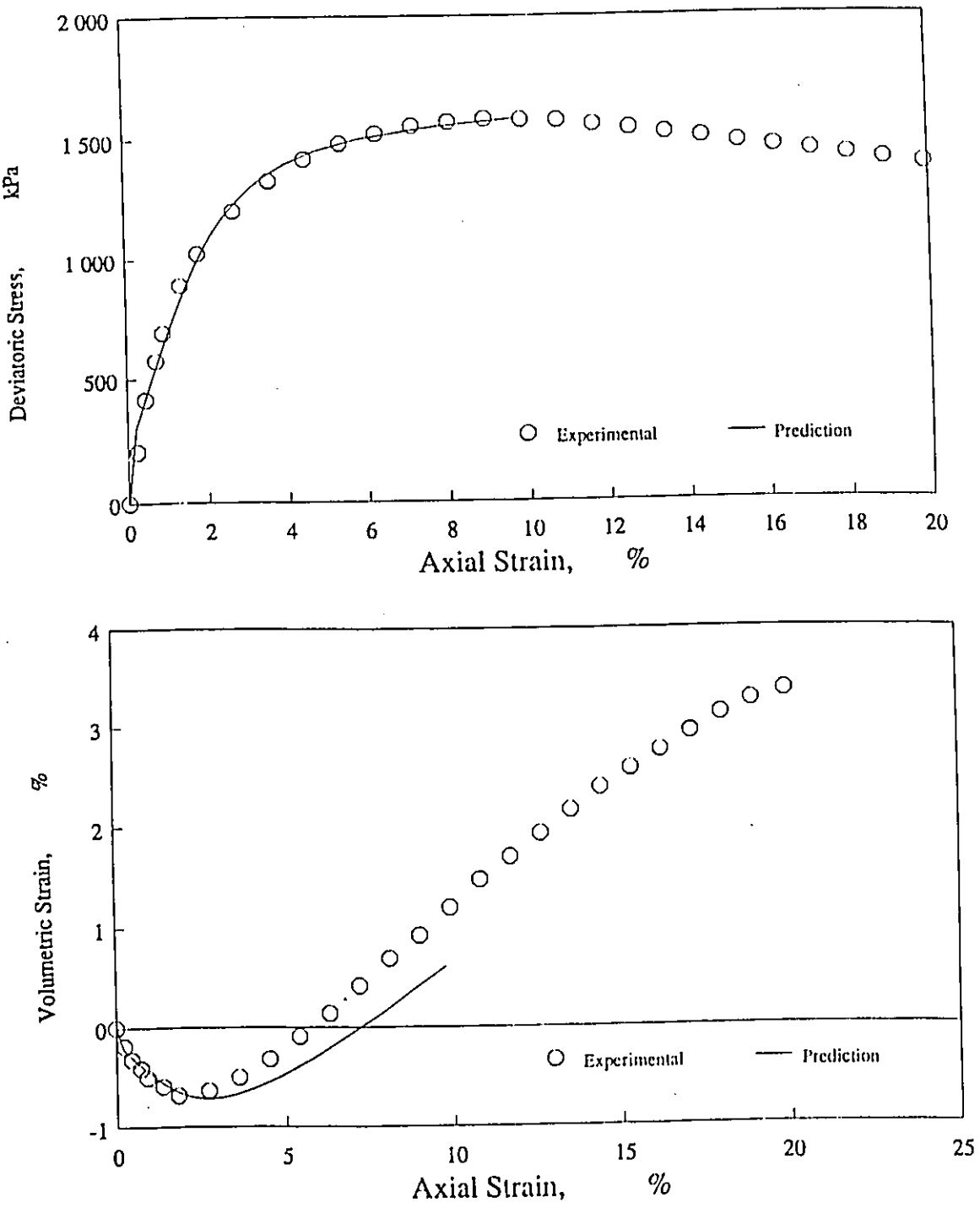

Figure 6.18: Measured and predicted triaxial test results on dense clean crushed quartz sand, σ_3=414 kPa

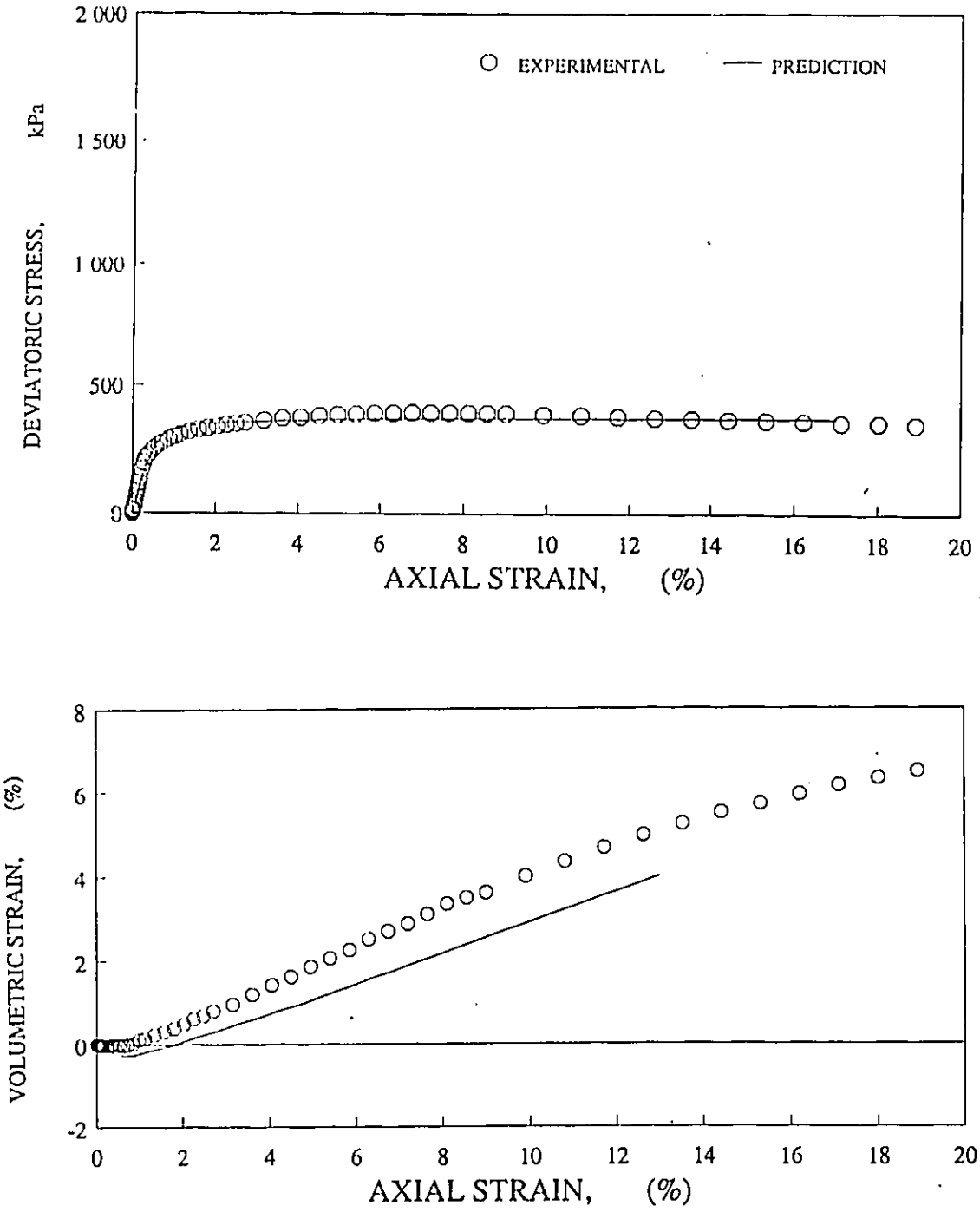

Figure 6.19: Measured and predicted triaxial test results on dense oil contaminated crushed quartz sand, σ_3=138 kPa

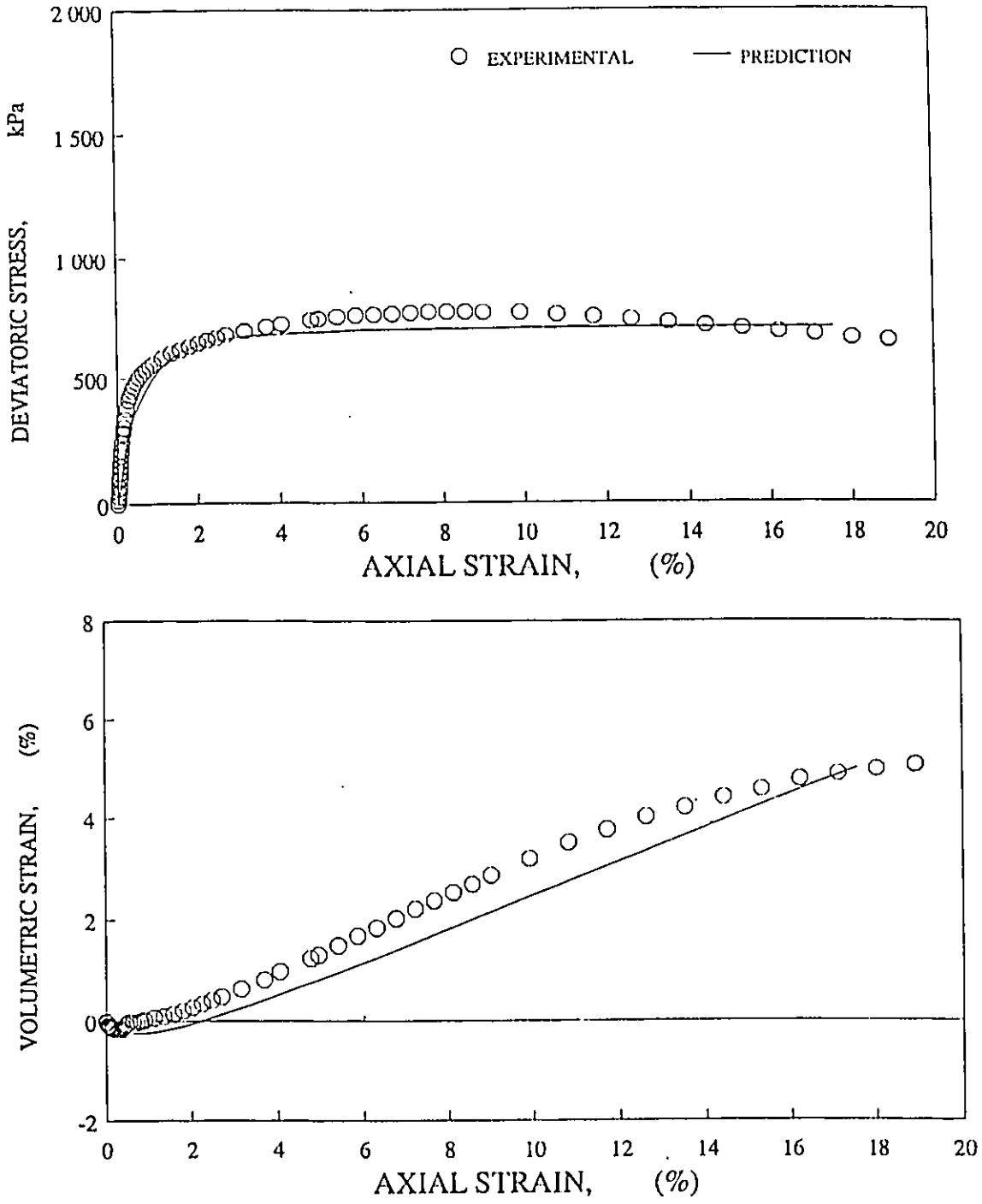

Figure 6.20: Measured and predicted triaxial test results on dense oil contaminated crushed quartz sand, σ_3=276 kPa

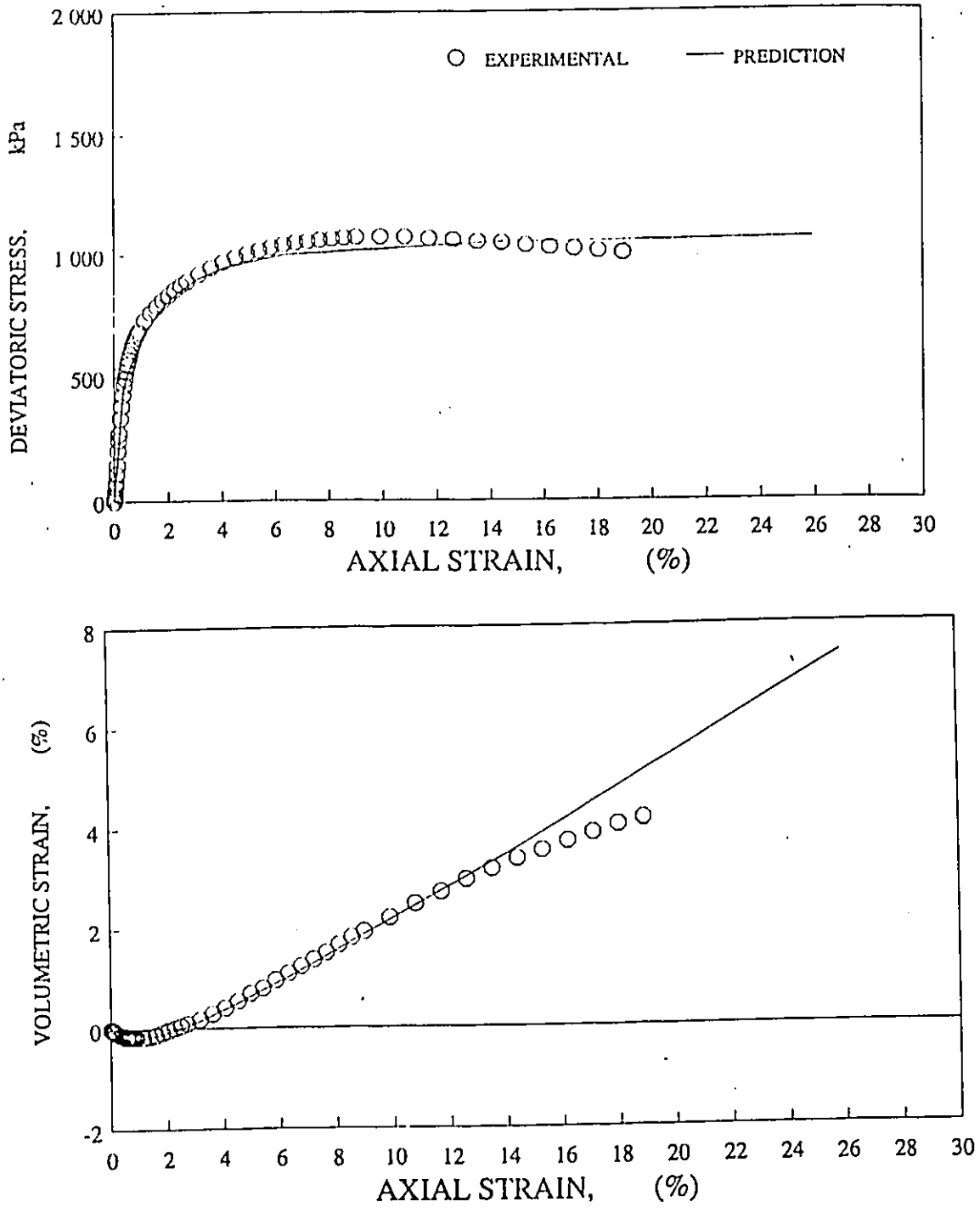

Figure 6.21: Measured and predicted triaxial test results on dense oil contaminated crushed quartz sand, σ_3=414 kPa

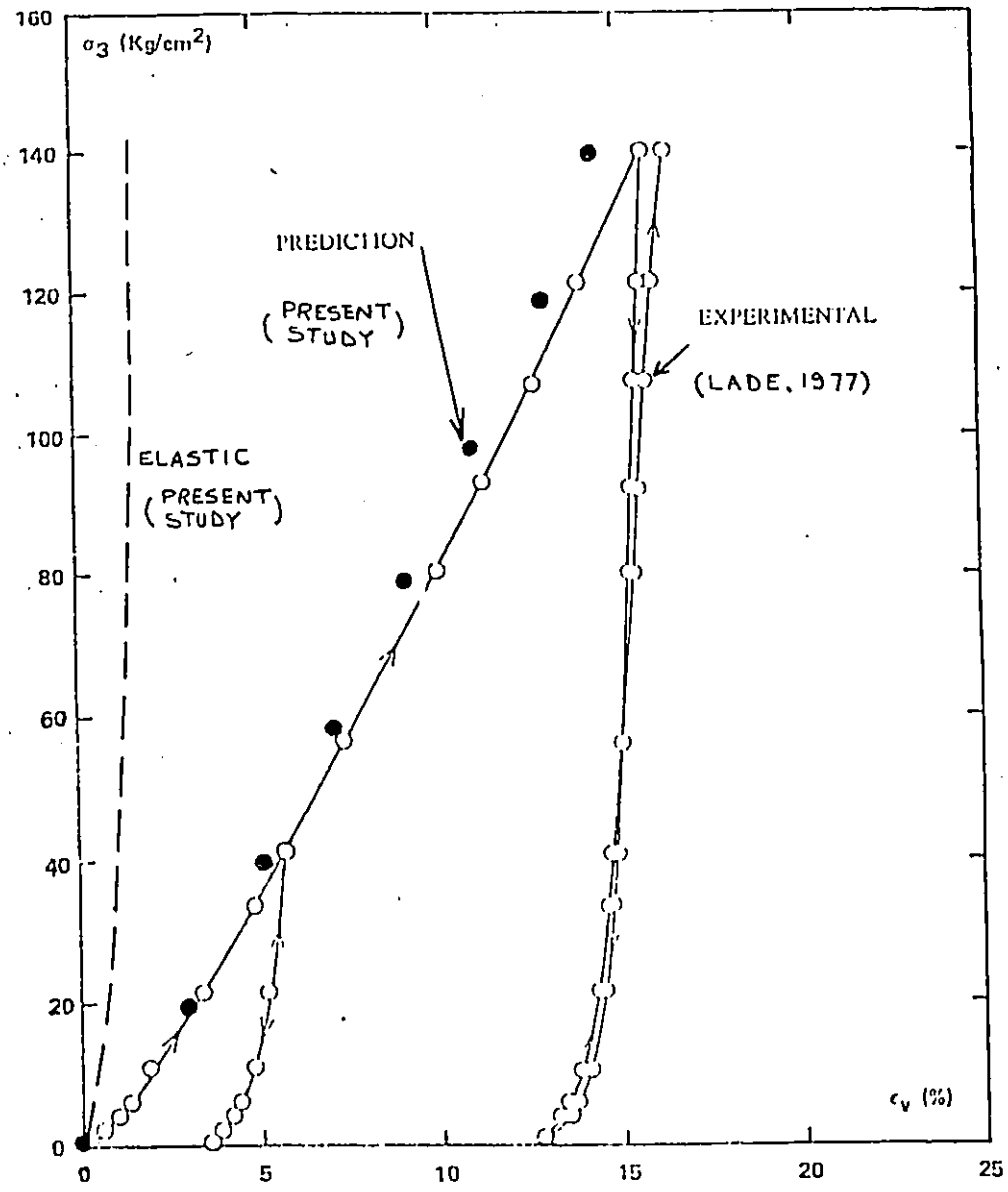

Figure 6.22: Comparisons of measured and predicted hydrostatic pressure versus volume change for loose Sacramento river sand (After Lade, 1979)

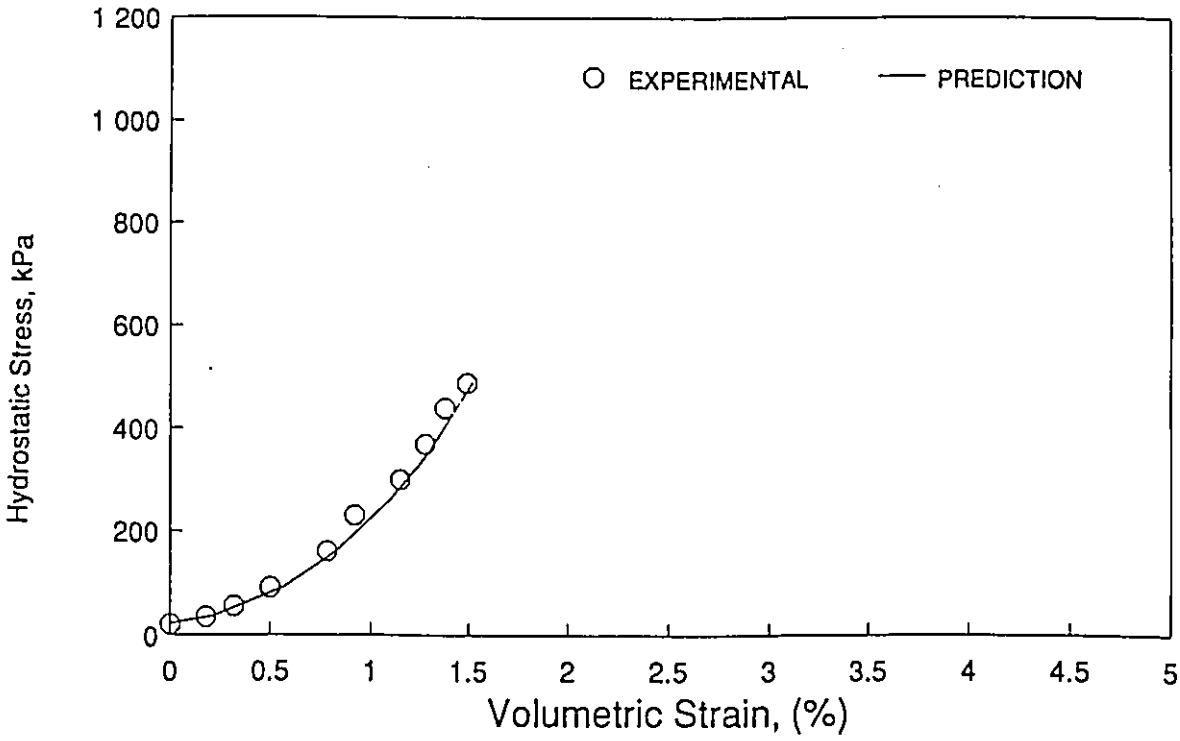

Figure 6.23: Comparisons of measured and predicted hydrostatic pressure versus volume change for loose clean crushed quartz sand

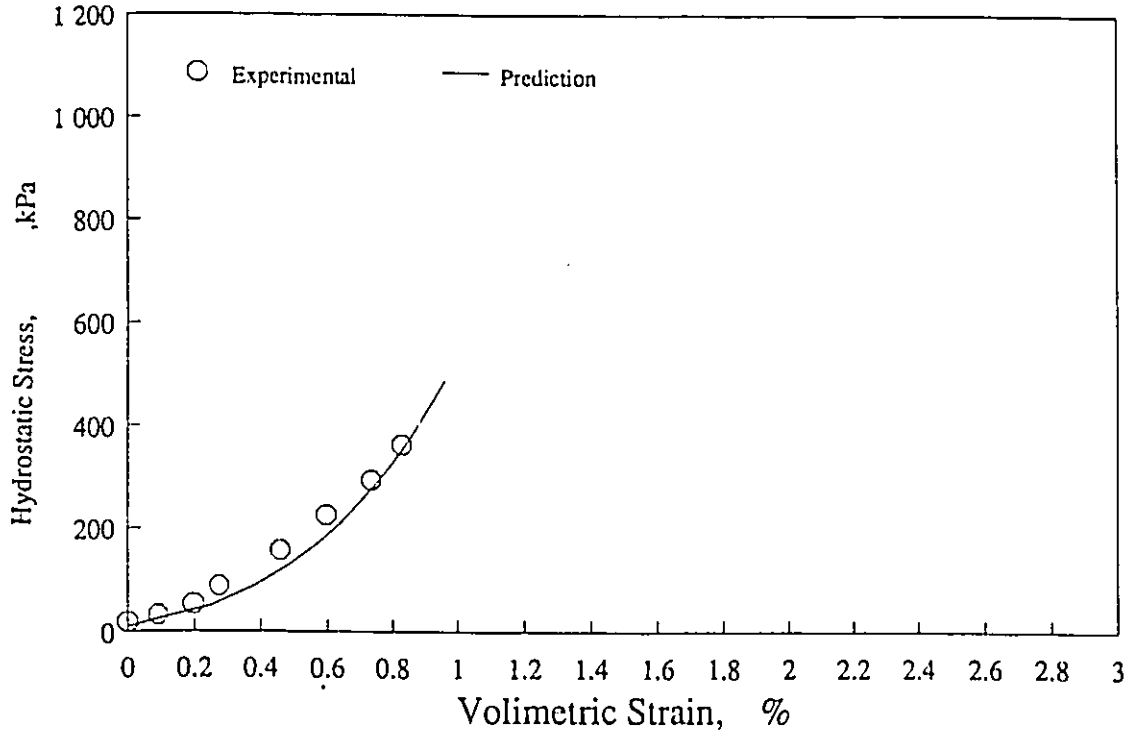

Figure 6.24: Comparisons of measured and predicted hydrostatic versus volume change for dense clean crushed quartz sand

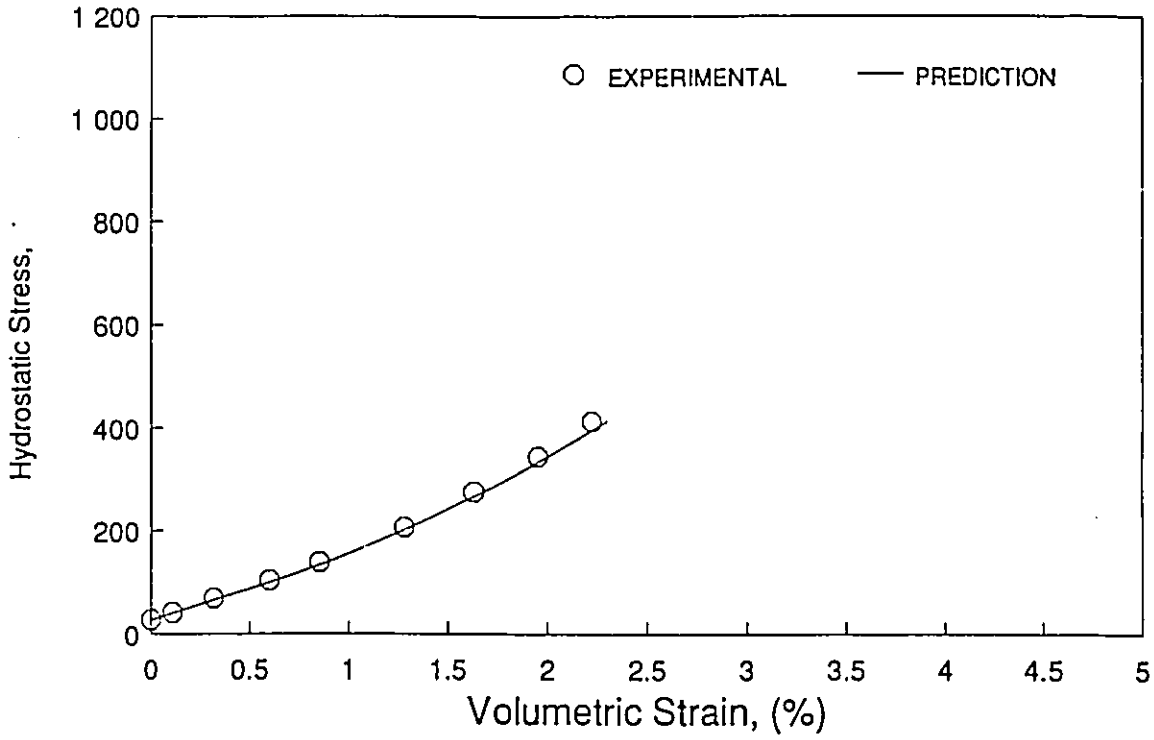

Figure 6.25: Comparisons of measured and predicted hydrostatic pressure versus volume change for loose oil contaminated crushed quartz sand

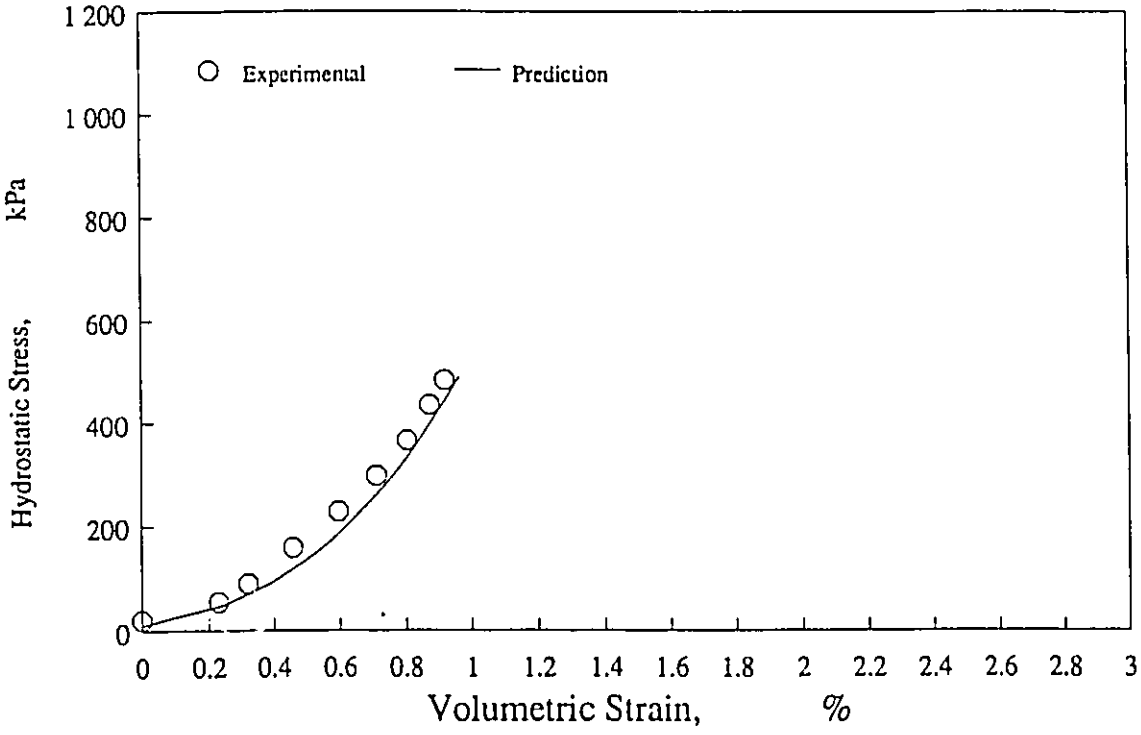

Figure 6.26: Comparisons of measured and predicted hydrostatic pressure versus volume change for dense oil contaminated crushed quartz sand

Chapter 7

Conclusions and Recommendations

Based on the experimental data obtained and on the results of the modified model predictions, the following conclusions have been reached.

1- Oil contamination reduces the angle of internal friction significantly. The reduction is about 6° for both loose and dense sands.

2- The initial tangent modulus calculated from the deviatoric stress versus axial strain data was reduced for loose sand due to oil contamination. Depending on the confining pressure, the reduction was in the range of 1.7 to 3.2 times. For the dense sand, however, the initial tangent modulus increased when it was saturated with oil.

3- In the case of volumetric strains, the effect of oil contamination was large only for loose sand but very minor for the dense sand. For this reason, the pore pressures developed in the clean and oil contaminated dense sands were similar in undrained tests. For the loose sand, the oil contamination caused a significant increase in the pore pressure.

4- Oil contamination does not have much effect on the interface behaviour on smooth surface, however on a rough surface the interface friction angle is reduced by 1 to 2 degrees.

5- The work hardening model of Lade is able to predict the triaxial test results on oil contaminated samples.

6- The addition of a cap type yield surface to Lade's work hardening model improves the predictions in the cases of isotropic compression.

The recommendations for future research are:

1- Further research may be done by changing the variables involved in the experimental work, such as; soil type (different gradations), temperature and viscosity of the oil, percentage of saturation of the soil and rate of shearing.

2- Finite element programs where elasto-plastic models are incorporated may be used to determine the effect of oil contamination on the performance of full scale structures.

3- More tests should be done for example consolidation and undrained triaxial compression tests.

Bibliography

[1] ACAR B. Y.et al., 1982. Interface Properties of Sand. Journal of Soil Mechanics and Foundation Division, ASCE, Vol. 108, No.GT4 pp. 648-653.

[2] AMERICAN PETROLIUM INSTITUTE, 1985. Oil Spill Conference, American Petrolium Institute, Washington, DC, and previous proceedings in 1983 and 1981.

[3] ATKINSON, J. H., and BRANSBY, P. L., 1977. The mechanics of soils, An introduction to the critical state soil mechanics. McGraw Hill, London.

[4] BISHOP, A. W., 1966. The strength of soils as engineering materials, Geotechnique, Vol. 16, No.2, pp. 91-130.

[5] BISHOP, A. W. and HENKEL, D. J., 1962. The measurement of soil properties in the triaxial test. A. Edward publishers, London.

[6] BRUMUND, W.F and G.A. LEONARDS, 1973. Experimental Study of Static and Dynamic Friction Between Sand and Typical Construction Materials, J. Test. Eval., 1(2):162-165.

[7] CHANG, C-Y. and DUNCAN, J. M., 1970. Analysis of soil movement around a deep excavation. Journal of the Soil Mechanics and Foundation Division, ASCE, Vol. 96, No. SM5, pp. 1655-1681.

[8] CHEN, W. F., and BALADY, G. Y., 1985. Soil plasticity, theory and implementation. Elsevier Science Publishing Company Inc.

[9] CHEN, W. F., and SALEEB, A. F., 1982. Constitutive equations for engineering materials, Vol. 1., elasticity and modelling. John Wiley & Sons, Inc.

[10] CLEMENCE, S.P., 1973. Development of Instrumentation and Model testing for the Load Distribution in a Drilled Pier. Ph.D. Thesis, Ga. Inst. Tech. bibitemr:11 CLOUGH, G.W., 1969. Finite Element Analyses of Soil-Structure Interaction in U-Frame Locks. Ph.D., Thesis U. Calif., Berkeley.

[11] CONFORTH, D. H., 1964. Some experiments on the influence of strain conditions on the strength of sand. Geotechnique, Vol. XIV, No. 2, pp. 143-167.

[12] DERRADJI-AOUAT, A. 1988. Evaluation of Prevost's elastoplastic models. M.A.Sc. thesis, University of Ottawa, Ottawa, Ontario.

[13] DESAI, C. S., and SIRIWARDANE, H. J., 1984. Constitutive laws for engineering materials with emphasis on geologic materials. Prentice-Hall. Inc.

[14] DUNCAN, J. M., BYRNE, P., WONG, K. S. and MABRY, P., 1978. Strength, stress-strain and bulk modulus parameters for finite element analyses of stresses and movements in soil masses. Report No. UCB/GT/78-02, University of california, Berkeley.

[15] DUNCAN, J. M., and CHANG, C. Y., 1970. Nonlinear analysis of stress and strain in soils. ASCE journal of the Soil Mechanics and Foundations Division, Vol. 96, SM5, pp. 1629-1653.

[16] DUNCAN, J. M., OZAWA, Y. LADE, P. V. and BROOKER, J. R., 1977. An elasto-plastic stress strain relationship for cohesionless soil.

Ninth International Conference on Soil Mechanics and Foundation Engineering, Specialty Session No. 9, Tokyo, Japan, pp. 45-50.

[17] EVGIN, E., 1981. Evaluation of an elasto-plastic model. Ph. D. thesis, University of Alberta, Alberta, Canada.

[18] EVGIN, E. and EISENSTEIN, Z., 1980. Re-evaluation of work hardening model. Application of plasticity and generalized stress-strain in geotechnical engineering. Proceedings, Symposium on Limit Equilibrium, Plasticity and generalized stress-strain application in geotechnical engineering, ASCE. Edited by R. N. Yong and E. T. Selig., pp. 226-239.

[19] EVGIN, E. and EISENSTEIN, Z., 1985. Performance of an elasto-plastic model. Canadian Geotechnical Journal, Vol. 22, pp. 177-185.

[20] FEENSTRA, S. and CHERRY, J. A., 1988. Subsurface contamination by dense non-aqueous phase liquid (DNAPL) chemicals. Proceedings, International Groundwater Symposium, Halifax, Nova Scotia.

[21] GOODMAN, R.E., R.L. TAYLOR and T.L. BREKKE, 1968. Model for the Mechanics of Jointed Rock, J. Soil Mech. Foundation Division., ASCE, 94(SM3):637-659.

[22] HILL, R. 1950. The mathematical theory of plasticity. Oxford University press, London, England.

[23] KULHAWY, H. F. and PETERSON, M. S., 1975. Behavior of sand-concrete interfaces. Canadian Geotechnical Journal, Vol. ,pp. 225-236.

[24] KONDNER, R. L., 1963. Hyperbolic stress-strain response: cohesive soils. Journal of the Soil Mechanics and Foundation Division, ASCE, Vol. 89, No. SM1, pp. 115-143.

[25] LADE, P. V. and DUNCAN, J. M., 1975. Elastoplastic stress strain theory for cohesionless soil. American Society for Civil Engineers, ASCE

Journal of the Geotechnical Engineering Division, Vol. 101, GT 10, pp. 1037-1053.

[26] LADE, P. V. and DUNCAN, J. M., 1976. Stress-path dependant behavior of cohesionless Soil. Journal of the Geotechnical Engineering Division, Vol. 102, No. GT1, pp. 51-68.

[27] LADE, P. V., 1972. The stress-strain and strength characteristics of cohesionless soils. Ph. D. thesis, University of California, Berkeley, CA, U.S.A.

[28] LADE, P. V., 1978. Prediction of undrained behavior of sand. Journal of the Geotechnical Engineering Division, ASCE, Vol. 104, N0. GT6, pp. 721-735.

[29] LADE, P. V., 1977. Elasto-plastic stress-strain theory for cohesionless soil with curved yield surface. Int. Journal of Solids and Structures, Pergamon Press, Inc. New York, N. Y., Vol. 13, Nov., pp. 1019-1035.

[30] LEE, K. L., 1970. Comparison of plain strain and triaxial tests on sand. Journal of Soil Mechanics and Foundation Division, ASCE, Vol. 96, No. SM3, pp. 901-923.

[31] LEE, K. L., and SEED, H. B., 1967. Drained strength characteristics of sands. Journal of the Soil Mechanics and Foundation Division, ASCE, Vol. 93, No. SM6, pp. 117-141.

[32] MENDELSON, A., 1968. Plasticity: theory and applications, MacMillan Publishing Company, Amsterdam.

[33] KACHANOV, L. M., 1971. Foundations of theory of plasticity. North-Holland Publishing Company, Amsterdam.

[34] OZAWA, Y. and DUNCAN, J. M., 1976. Elasto-plastic finite element analyses of sand deformation. Proceedings of the 2nd International Conference on Numerical Methods in Geomechanics, Blacksburg. Virginia,

pp. 243-263.

[35] POTYONDY, J.G., 1961. Skin Friction Between Various Soils and Construction Materials. Geotechnique, 11(4):339-353.

[36] SEED, H. B. and LEE, K. L., 1966. Liquefaction of saturated sands during cyclic loading. Journal of the Soil Mechanics and Foundation Division, ASCE, Vol. 92, No. SM6, pp. 105-134.

[37] SEED, H. B. and LEE, K. L., 1967. Undrained strength characteristics of cohesionless soils, Journal of the Soil Mechanics and Foundation Division, ASCE, Vol. 93, No. SM6, pp. 333-360.

[38] SLATER, R. A. C., 1979. Engineering plasticity and applications to metal forming. Halsted Press, New York 1979.

[39] U.S. ARMY ENG. SW Div., 1962. Results of Tests in Foundation Materials, Lock and Dam No. 4, Arkansas River Navigation Project. SWDGL Rpts. 7920 and 7932, Dallas.

[40] WONG, K. S., 1978. Elasto-plastic finite element analyses of passive earth pressure tests. Ph. D. thesis, University of California, Berkeley, CA, U.S.A.

[41] WU, T.H., 1976. Soil Mech. Boston, Allyn and Bacon.

[42] ZIENKIEWICZ, O. C., 1971. The finite element method in engineering science. London: McGraw-Hill Book Company.

Appendix A

Program Listing

```
C*************************************************************
C
C                          KLADE
C                   (DATE: JUNE 20, 1988)
C
C    THIS PROGAM FINDS THE AXIAL AND VOLUMETRIC STRAINS FOR GIVEN
C    STRESSES USING LADE'S FIRST MODEL WITH A CAP ADDED TO THE
C    OPEN END OF THE CONE.
C    PRE(1)=SIGMAX                PRE(8)=FP
C    PRE(2)=SIGMAY                PRE(9)=FC
C    PRE(3)=SIGMAZ                PRE(10)=SIGMA1
C    PRE(4)=TAUXY                 PRE(11)=SIGMA2
C    PRE(5)=TAUYZ                 PRE(12)=SIGMA3
C    PRE(6)=TAUZX                 PRE(13)=I1
C    PRE(7)=E                     PRE(14)=I2
C                                 PRE(15)=I3
ccccccccccccccccccccccccccccccccccccccccccccccccccccccc
C    CURFP= CURRENT FP;           CURFC= CURRENT FC
C    MEAN STRESS=(SIGMAX+SIGMAY+SIGMAZ)/3.0
C*************************************************************
      IMPLICIT REAL*8(A-H,O-Z)
C
C     REAL E,CE11,CE44,ULT1,ULT2,EPSVOL
C
      COMMON /TRY / CURFP,CURFC,GP,RK2,DWP,DWC
C
      COMMON/TRU/RLKUR,RLM,RLA,RLFT,RLK1,RF,RLL,RLN,RLC,
     *RLP,PR,PA C
      COMMON /MAXI / PRE(15),PNEW(15),AVG(15),CEN(15)
C
      DIMENSION DEPE(6),DEPP(6),DEPC(6),DEPT(6),DSGA(6),EPS(15)
C     *EPS(15)
C
      OPEN(UNIT=5,FILE='INPUT1')
      OPEN(UNIT=6,FILE='OUTPUT')
      WRITE(*,*)'BEGIN EXECUTION .....'
C
      READ(5,*)  RLKUR,RLM,RLA,RLK1,RF,RLL,RLN,RLFT,RLC,RLP,PR,PA
      WRITE(6,2044)RLKUR,RLM,RLA,RLK1,RF,RLL,RLN,RLFT,PR,
     *RLC,RLP,PA
2044   FORMAT(//,'PARAMETERS(IN METRICUNITS):',//,'RLKUR=',F8.2,/
     1'RLM  =',F10.6,/,'RLA  =',F8.4,/,'RLK1 =',F8.2,/,'RF   =',
     2F8.4,/,'RLL  =',F8.4,/,'RLN  =',F8.4,/,'RLFT =',F8.2,/,
     3'PR   =',F8.4,/,'RLC  =',F8.4,/,'RLP  =',F8.4,/,'PA   =',
     4F8.2,//)
      WRITE(6,2000)
      WRITE(6,2100)
      WRITE(6,2000)
C
```

```
C  INITIALIZE ALL VECTORS
C
      DO 50 I=1,15
      PRE(I)=0.0
      PNEW(I)=0.0
      AVG(I)=0.0
      CEN(I)=0.0
   50 EPS(I)=0.0
      EPSVOL=0.0
C
C  READ INITIAL STATE OF STRESSES
C
      READ(5,*) (PRE(I), I=1,6)
      CALL PRINCP(PRE,RLKUR,RLN,PA)
      DEV=PRE(10)-PRE(12)
      AXIAL=0.0
      VOL=0.0
      SMEAN=(PRE(1)+PRE(2)+PRE(3))/3.0
      WRITE(6,2200) DEV,SMEAN,AXIAL,VOL,PRE(8),PRE(9)
      CURFP=RLFT
      CURFC=PRE(9)
      IF (PRE(8).GT.RLK1) GO TO 1999
      READ(5,*) XLOAD
 99   PNEW(1)=PRE(1)+XLOAD
      IF(PNEW(3).GT.16.0) STOP
      PNEW(3)=PRE(3)+XLOAD
      PNEW(2)=PRE(2)+XLOAD
      DO 49 I=4,6
 49   PNEW(I)=PRE(I)
      CALL PRINCP(PNEW,RLKUR,RLN,PA)
      DO 700 I=1,6
      DEPE(I)=0.0
      DEPP(I)=0.0
 700  DEPC(I)=0.0
      IF(PNEW(8).LE.RLK1) GO TO 210
      CALL PLAST3
      DO 76 I=1,15
 76   PNEW(I)=CEN(I)
      PNEW(8)=RLK1
 210  DO 55 I=1,6
  55  AVG(I)=(PRE(I)+PNEW(I))/2.0
      CALL PRINCP(AVG,RLKUR,RLN,PA)
      DO 61 I=1,6
   61 DSGA(I)=PNEW(I)-PRE(I)
C
C*****************************************************************
C     CALCULATION OF COMPONENTS OF ELASTIC STRAIN INCREMENT.
C*****************************************************************
C
```

```
 211    E=AVG(7)
        CE11=1.0/E
        CE44=2.0*CE11
        DEPE(1)=CE11*(DSGA(1)-PR*(DSGA(2)+DSGA(3)))
        DEPE(2)=CE11*(DSGA(2)-PR*(DSGA(1)+DSGA(3)))
        DEPE(3)=CE11*(DSGA(3)-PR*(DSGA(1)+DSGA(2)))
        DEPE(4)=CE44*DSGA(4)
        DEPE(5)=CE44*DSGA(5)
        DEPE(6)=CE44*DSGA(6)
C
C*****************************************************************
C      MAKE SURE THAT CURFP DOES NOT GO BELOW RLFT.
C*****************************************************************
C
 209    IF(PNEW(8).LE.CURFP) GO TO 200
        IF(PRE(8).LT.CURFP) GO TO 206
        CALL PLAST2
        GO TO 204
 206    CALL PLAST1
        GO TO 204
 200    IF(PNEW(9).LE.CURFC) GO TO 202
        IF(PRE(9).LT.CURFC) GO TO 219
        CALL COLAP1
        GO TO 207
 219    CALL COLAP2
        GO TO 207
 212    GO TO 202
C
C*****************************************************************
C  NOW I CAN CALCULATE THE PLASTIC EXPANSIVE STRAIN
C  INCREMENTS.
C*****************************************************************
C
 204    ULT1=DWP/(3*GP)
        DEPP(1)=ULT1*(3*AVG(13)**2-RK2*(AVG(2)*AVG(3)-AVG(4)**2))
        DEPP(2)=ULT1*(3*AVG(13)**2-RK2*(AVG(3)*AVG(1)-AVG(4)**2))
        DEPP(3)=ULT1*(3*AVG(13)**2-RK2*(AVG(1)*AVG(2)-AVG(4)**2))
        DEPP(4)=ULT1*(RK2*(AVG(3)*AVG(4)-AVG(4)*AVG(4)))
        DEPP(5)=ULT1*(RK2*(AVG(3)*AVG(4)-AVG(4)*AVG(4)))
        DEPP(6)=ULT1*(RK2*(AVG(3)*AVG(4)-AVG(4)*AVG(4)))
        GO TO 202
C*****************************************************************
C  NOW I CALCULATE THE PLASTIC COLLAPSE INCREMENT OF STRAIN
C*****************************************************************
C
 207    ULT2=DWC/AVG(9)
        DEPC(1)=ULT2*AVG(1)
        DEPC(2)=ULT2*AVG(2)
        DEPC(3)=ULT2*AVG(3)
```

```
      DEPC(4)=ULT2*(2*AVG(4))
      DEPC(5)=ULT2*(2*AVG(5))
      DEPC(6)=ULT2*(2*AVG(6))
C
 202  DO 65 I=1,6
      DEPT(I)=DEPE(I)+DEPP(I)+DEPC(I)
  65  EPS(I)=EPS(I)+DEPT(I)
      EPSVOL=EPS(1)+EPS(2)+EPS(3)
      IF(PNEW(8).GT.CURFP) CURFP=PNEW(8)
      IF(PNEW(9).GT.CURFC) CURFC=PNEW(9)
      DO 75 I=1,15
  75  PRE(I)=PNEW(I)
      DEV=(PNEW(10)-PNEW(12))
      AXIAL=EPS(1)*100
      VOL=EPSVOL*100
      SMEAN=(PNEW(1)+PNEW(2)+PNEW(3))/3.0
      WRITE(6,2200) DEV,SMEAN,AXIAL,VOL,PNEW(8),PNEW(9)
      IF(CURFP.GE.RLK1) GO TO 1997
      GO TO 99
1999  WRITE(6,*) 'INITIAL STRESS LEVEL, (PRE(8)), EXCEEDS K1'
      GO TO 1997
1998  GO TO 99
2000  FORMAT(1X,70('-'))
2100  FORMAT(1X,'DEVIATORIC',5X,'MEAN',5X,'AXIAL',5X,'VOL',10X,
     *'FP',15X,'FC',/
     *,3X,'STRESS',6X,'STRESS',4X,'STRAIN',3X,'STRAIN',/
     *,2X,' kPa',10X,' kPa',7X,'%', 7X,'%')
2200 FORMAT(1X,1F8.1,3X,1F8.1,2X,1F8.2,1F10.5,5X,1F8.2,5X,1E14.7)
1997  WRITE(*,*) 'END OF EXECUTION ........'
      WRITE(6,2000)
      CLOSE(UNIT=5)
      CLOSE(UNIT=6)
      STOP
      END
C
C
C*************************************************************
C
                SUBROUTINE PLAST1
C
C   THIS SUBROUTINE CALCULATE THE INCREMENTS OF PLASTIC WORK
C
C
C*************************************************************
C
      IMPLICIT REAL*8(A-H,O-Z)
      COMMON /TRY / CURFP,CURFC,GP,RK2,DWP,DWC
      COMMON/TRU/RLKUR,RLM,RLA,RLFT,RLK1,RF,RLL,RLN,RLC,RLP,PR,PA
      COMMON /MAXI/ PRE(15),PNEW(15),AVG(15),CEN(15)
```

```
      DIMENSION TOP(15),BOT(15)
C
      DO 55 I=1,6
      BOT(I)=PRE(I)
   55 TOP(I)=PNEW(I)
      IY=0
  502 IF (IY.GT.30) STOP
      IY=IY+1
      DO 60 I=1,6
   60 CEN(I)=(BOT(I)+TOP(I))/2.0
      CALL PRINCP(CEN,RLKUR,RLN,PA)
      IF(DABS(CEN(8)-CURFP).LE.0.005) GO TO 199
      IF((CEN(8)-CURFP).GT.0.0) GO TO 110
      DO 507 I=1,13
  507 BOT(I)=CEN(I)
      GO TO 502
  110 DO 508 I=1,15
  508 TOP(I)=CEN(I)
      GO TO 502
  199 DO 510 I=1,6
  510 AVG(I)=(PNEW(I)+CEN(I))/2.0
      CALL PRINCP(AVG,RLKUR,RLN,PA)
      RK2=RLA*AVG(8)+27.0*(1.0-RLA)
      GP=AVG(13)**3-RK2*AVG(15)
      SMOLA=RLM*PA*(AVG(12)/PA)**RLL
      DFP=PNEW(8)-CURFP
      D=RF/(RLK1-RLFT)
      DWP=SMOLA*DFP/(1.0-D*(AVG(8)-RLFT))**2
      RETURN
      END
C
C*****************************************************************
C
            SUBROUTINE PLAST2
C
C*****************************************************************
C
      IMPLICIT REAL*8(A-H,O-Z)
      COMMON /TRY/ CURFP,CURFC,GP,RK2,DWP,DWC
      COMMON/TRU/RLKUR,RLM,RLA,RLFT,RLK1,RF,RLL,RLN,RLC,RLP,PR,PA
      COMMON /MAXI / PRE(15),PNEW(15),AVG(15),CEN(15)
      DIMENSION TOP(15),BOT(15)
C
      RK2=RLA*AVG(8)+27.0*(1.0-RLA)
      GP=AVG(13)**3-RK2*AVG(15)
      SMOLA=RLM*PA*(AVG(12)/PA)**RLL
      DFP=PNEW(8)-PRE(8)
      D=RF/(RLK1-RLFT)
      DWP=SMOLA*DFP/(1.0-D*(AVG(8)-RLFT))**2
```

```
      RETURN
      END
C*****************************************************************
C
                SUBROUTINE PLAST3
C
C   THIS SUBROUTINE CALCULATE THE INCREMENTS OF PLASTIC WORK
C
C*****************************************************************
C
      IMPLICIT REAL*8(A-H,O-Z)
      COMMON /TRY / CURFP,CURFC,GP,RK2,DWP,DWC
      COMMON/TRU/RLKUR,RLM,RLA,RLFT,RLK1,RF,RLL,RLN,RLC,RLP,PR,PA
      COMMON /MAXI/ PRE(15),PNEW(15),AVG(15),CEN(15)
      DIMENSION TOP(15),BOT(15)
C
      DO 55 I=1,6
      BOT(I)=PRE(I)
   55 TOP(I)=PNEW(I)
      IY=0
  502 IF (IY.GT.30) STOP
      IY=IY+1
      DO 60 I=1,6
   60 CEN(I)=(BOT(I)+TOP(I))/2.0
      CALL PRINCP(CEN,RLKUR,RLN,PA)
      IF(DABS(CEN(8)-RLK1).LE.0.005) GO TO 199
      IF((CEN(8)-RLK1).GT.0.0) GO TO 110
      DO 507 I=1,13
  507 BOT(I)=CEN(I)
      GO TO 502
  110 DO 508 I=1,15
  508 TOP(I)=CEN(I)
      GO TO 502
  199 DO 510 I=1,6
  510 AVG(I)=(PRE(I)+CEN(I))/2.0
      CALL PRINCP(AVG,RLKUR,RLN,PA)
      RK2=RLA*AVG(8)+27.0*(1.0-RLA)
      GP=AVG(13)**3-RK2*AVG(15)
      SMOLA=RLM*PA*(AVG(12)/PA)**RLL
      DFP=RLK1-PRE(8)
C*****************************************************************
C     IN THE FOLLOWING STATEMENT DFP WILL BE ASSIGNED A VALUE
C
C*****************************************************************
      IF(DFP.LE.0.0) DFP=5.0
      D=RF/(RLK1-RLFT)
      DWP=SMOLA*DFP/(1.0-D*(AVG(8)-RLFT))**2
      RETURN
      END
```

```
C
C*************************************************************
C
          SUBROUTINE COLAP2
C
C*************************************************************
C
      IMPLICIT REAL*8(A-H,O-Z)
      COMMON /TRY / CURFP,CURFC,GP,RK2,DWP,DWC
                              C    O    M    M    O    N          /
TRU/RLKUR,RLM,RLA,RLFT,RLK1,RF,RLL,RLN,RLC,RLP,PR,PA       COMMON
/MAXI/ PRE(15),PNEW(15),AVG(15),CEN(15)
      DIMENSION RIGHT(15),LEFT(15)
C
      DO 55 I=1,6
      LEFT(I)=PRE(I)
   55 RIGHT(I)=PNEW(I)
      IY=0
  502 IF (IY.GT.30) STOP
      IY=IY+1
      DO 60 I=1,6
   60 CEN(I)=(LEFT(I)+RIGHT(I))/2.0
      CALL PRINCP(CEN,RLKUR,RLN,PA)
      IF(DABS(CEN(8)-CURFC).LE.0.005) GO TO 199
      IF((CEN(8)-CURFC).GT.0.0) GO TO 110
      DO 507 I=1,13
  507 LEFT(I)=CEN(I)
      GO TO 502
  110 DO 508 I=1,15
  508 RIGHT(I)=CEN(I)
      GO TO 502
  199 DO 510 I=1,6
  510 AVG(I)=(PNEW(I)+CEN(I))/2.0
      CALL PRINCP(AVG,RLKUR,RLN,PA)
      DFC=PNEW(9)-CURFC
      DWC=RLC*RLP*PA*(PA**2/AVG(9))**(1.0-RLP)*(DFC/PA**2)
C
      RETURN
      END
C




C*************************************************************
C
          SUBROUTINE COLAP1
C
```

```
C*****************************************************************
C
      IMPLICIT REAL*8(A-H,O-Z)
      REAL DFC
      COMMON /TRY / CURFP,CURFC,GP,RK2,DWP,DWC
                              C    O    M    M    O    N            /
TRU/RLKUR,RLM,RLA,RLFT,RLK1,RF,RLL,RLN,RLC,RLP,PR,PA        COMMON
/MAXI/ PRE(15),PNEW(15),AVG(15),CEN(15)
      DIMENSION RIGHT(15),LEFT(15)
C
      DFC=PNEW(9)-PRE(9)
      DWC=RLC*RLP*PA*(PA**2/AVG(9))**(1-RLP)*(DFC/PA**2)
C
      RETURN
      END
C
C*****************************************************************
C
            SUBROUTINE PRINCP(WW,RLKUR,RLN,PA)
C
C     THIS SUBROUTINE FINDS THE PRINCIPAL STRESSES AND
C     CALCULATES THE STRESS INVARIANTS.
C
C*****************************************************************
C
      IMPLICIT REAL*8(A-H,O-Z)
      DIMENSION WW(15)
      A=WW(1)
      B=WW(2)
      C=WW(3)
      SMAX=A
      IF(B.GT.SMAX) SMAX=B
      IF(C.GT.SMAX) SMAX=C
      IF(A.EQ.SMAX) GO TO 51
      IF(B.EQ.SMAX) GO TO 52
      WW(10)=C
      IF(A.LE.B) GO TO 53
      WW(12)=B
      WW(11)=A
      GO TO 19
  53  WW(12)=A
      WW(11)=B
      GO TO 19
  52  WW(10)=B
      IF(A.LE.C) GO TO 54
      WW(12)=C
      WW(11)=A
      GO TO 19
  54  WW(12)=A
```

```
      WW(11)=C
      GO TO 19
51    WW(10)=A
      IF(B.LE.C) GO TO 55
      WW(12)=C
      WW(11)=B
      GO TO 19
55    WW(12)=B
      WW(11)=C
19    WW(13)=WW(10)+WW(11)+WW(12)
      WW(14)=-1*(WW(10)*WW(11)+WW(11)*WW(12)+WW(12)*WW(10))
      WW(15)=WW(10)*WW(11)*WW(12)
      WW(7)=RLKUR*PA*(WW(12)/PA)**RLN
      WW(8)=WW(13)**3/WW(15)
      WW(9)=WW(13)**2+2*WW(14)
      RETURN
      END
```

Appendix B

Triaxial Compression Test Results

Table B.1: Drained triaxial compression on dense oil contaminated sand σ_3=138 kPa

Date of Testing.....:July 29,1988
Tested by.....:Faouzi B. Amor
Type of Sample.....:Dense Sand
Type of test.....:Drained
Confining pressure.....:20 psi
Density.....:1.40 g/cc
Void ratio.....:

Disp reading	Load reading	P.w.P reading	V. chng reading	Dev(kPa) calcul	axStrn %	pwp(kPa) calcul	Volumetri Strain
0	2		12.48	0.000	0.000		0
1	10		12.48	5.732	0.009		0
2	18		12.49	11.463	0.018		-0.00492
3	24		12.49	15.760	0.027		-0.00492
5	39		12.5	26.501	0.045		-0.00985
7	50		12.5	34.373	0.063		-0.00985
9	69		12.51	47.971	0.081		-0.01477
11	95		12.52	66.574	0.099		-0.01969
13	120		12.52	84.455	0.117		-0.01969
15	142		12.53	100.183	0.135		-0.02462
17	166		12.54	117.336	0.153		-0.02954
20	195		12.54	138.047	0.180		-0.02954
25	239		12.55	169.442	0.225		-0.03447
30	275		12.54	195.092	0.270		-0.02954
35	302		12.53	214.290	0.315		-0.02462
40	312		12.52	221.333	0.360		-0.01969
45	326		12.51	231.224	0.405		-0.01477
55	348		12.5	246.701	0.495		-0.00985
60	360		12.53	255.142	0.541		-0.02462
70	377		12.55	267.016	0.631		-0.03447
80	391		12.5	276.733	0.721		-0.00985
95	409		12.45	289.144	0.856		0.014771
110	423		12.25	298.682	0.991		0.113245
125	435		12.2	306.777	1.126		0.137863
150	451		12	317.388	1.351		0.236337
175	464		11.85	325.832	1.577		0.310192
200	475		11.7	332.826	1.802		0.384047
225	484		11.5	338.381	2.027		0.482521
250	493		11.25	343.907	2.252		0.605613
275	500		11.1	348.006	2.477		0.679468
300	508		10.85	352.780	2.703		0.80256
350	524		10.55	362.250	3.153		0.950271
400	537		10.05	369.545	3.604		1.196455
450	548		9.6	375.381	4.054		1.418021
500	558		9.2	380.461	4.505		1.614968
550	568		8.7	385.477	4.955		1.861152
600	574		8.3	387.717	5.405		2.058099
650	580		7.9	389.919	5.856		2.255047
700	586		7.4	392.081	6.306		2.501231
750	591		7	393.537	6.757		2.698178
800	594		6.65	393.631	7.207		2.870507
900	598		5.7	392.443	8.108		3.338257
950	601		5.4	392.485	8.559		3.485968
1000	601		5.15	390.551	9.009		3.60906
1100	601		4.35	386.685	9.910		4.002954
1200	603		3.65	384.096	10.811		4.347612
1300	602		3	379.583	11.712		4.667651
1400	599		2.4	373.832	12.613		4.963072
1500	600		1.85	370.597	13.514		5.233875
1600	602		1.3	367.964	14.414		5.504677
1700	605		0.9	365.911	15.315		5.701625
1800	604		0.45	361.418	16.216		5.923191
1900	602		0	356.344	17.117		6.144756
2000	606		-0.35	354.820	18.018		6.317085
2100	605		-0.7	350.340	18.919		6.489414
2200	606		-1.05	347.022	19.820		6.661743

Table B.2: Drained triaxial compression on dense oil contaminated sand σ_3=276 kPa

Date of Testing.....:August 2, 1988
Tested by.....:Faouzi B. Amor
Type of Sample.....:Dense Sand
Type of test.....:Drained
Confining pressure.....:40 psi
Density.....:
Void ratio.....:

Disp reading	Load reading	P.w.P reading	V. chng reading	Dev(kPa) calcul	axStrn %	pwp(kPa) calcul	Volumetri Strain
0	6		14.95	0	0		0
1	26		14.97	15.18708	0.009009		-0.00917
2	45		14.98	29.61214	0.018018		-0.01376
3	64		15	44.03459	0.027027		-0.02294
4	92		15.1	65.28679	0.036036		-0.06881
5	135		15.1	97.92136	0.045045		-0.06881
6	170		15.1	124.478	0.054054		-0.06881
7	200		15.1	147.235	0.063063		-0.06881
8	229		15.13	169.2291	0.072072		-0.08257
9	259		15.15	191.9781	0.081081		-0.09174
10	285		15.17	211.688	0.09009		-0.10092
12	322		15.2	239.718	0.108108		-0.11468
15	375		15.22	279.8482	0.135135		-0.12385
17	405		15.25	302.5455	0.153153		-0.13761
20	446		15.27	333.5438	0.18018		-0.14679
25	504		15.3	377.3406	0.225225		-0.16055
30	551		15.3	412.7666	0.27027		-0.16055
35	574		15.3	429.9918	0.315315		-0.16055
40	602		15.31	450.9847	0.36036		-0.16514
45	624		15.2	467.4204	0.405405		-0.11468
52	649		15.1	486.021	0.468468		-0.06881
60	674		15	504.552	0.540541		-0.02294
70	696		15	520.6969	0.630631		-0.02294
80	717		15	536.0578	0.720721		-0.02294
90	734		14.95	548.3769	0.810811		0
100	749		14.9	559.1675	0.900901		0.022936
125	783		14.8	583.4263	1.126126		0.068807
150	810		14.75	602.3246	1.351351		0.091743
175	831		14.65	616.6459	1.576577		0.137615
200	852		14.5	630.8953	1.801802		0.206422
225	872		14.35	644.3289	2.027027		0.275229
250	890		14.2	656.2094	2.252252		0.344037
275	906		14.05	666.5471	2.477477		0.412844
300	924		13.9	678.3079	2.702703		0.481651
350	951		13.55	695.0254	3.153153		0.642202
410	982		13.15	713.8187	3.693694		0.825688
450	1000		12.8	724.2632	4.054054		0.986239
530	1031		12.25	741.2407	4.774775		1.238532
550	1040		12.1	746.3343	4.954955		1.307339
600	1057		11.7	755.0095	5.405405		1.490826
650	1070		11.3	760.7086	5.855856		1.674312
700	1080		10.95	764.1842	6.306306		1.834862
750	1089		10.55	766.8832	6.756757		2.018349
800	1100		10.15	770.93	7.207207		2.201835
850	1111		9.8	774.9016	7.657658		2.362385
900	1117		9.45	775.3087	8.108108		2.522936
950	1123		9.1	775.6747	8.558559		2.683486
1000	1126		8.7	773.9267	9.009009		2.866972
1100	1136		8	773.1057	9.90991		3.188073
1200	1137		7.3	766.0519	10.81081		3.509174
1300	1133		6.75	755.6321	11.71171		3.761468
1400	1127		6.2	743.9398	12.61261		4.013761
1500	1118		5.8	730.3591	13.51351		4.197248
1600	1111		5.35	718.2015	14.41441		4.40367
1700	1103		5	705.4966	15.31532		4.56422
1800	1093		4.55	691.6286	16.21622		4.770642
1900	1085		4.3	679.1562	17.11712		4.885321
2000	1073		4.1	664.303	18.01802		4.977064
2100	1068		3.9	653.9243	18.91892		5.068807

Table B.3: Drained triaxial compression on dense oil contaminated sand σ_3=414 kPa

Date of Testing.....:August 3, 1988
Tested by.....:Faouzi B. Amor
Type of Sample.....:Dense Sand
Type of test.....:Drained
Confining pressure.....:60 psi
Density.....:
Void ratio.....:

Disp reading	Load reading	P.w.P reading	V. chng reading	Dev(kPa) calcul	axStrn %	pwp(kPa) calcul	Volumetri Strain
0	5		14.23	0	0		0
1	21		14.23	12.14966	0.009009		0
2	36		14.24	23.53785	0.018018		-0.00459
3	55		14.25	37.96086	0.027027		-0.00917
5	81		14.27	57.6901	0.045045		-0.01835
7	102		14.3	73.61752	0.063063		-0.03211
10	150		14.3	110.017	0.09009		-0.03211
12	197		14.31	145.6515	0.108108		-0.0367
15	272		14.32	202.4918	0.135135		-0.04128
18	330		14.35	246.412	0.162162		-0.05505
20	364		14.4	272.1414	0.18018		-0.07798
25	445		14.42	333.3933	0.225225		-0.08716
30	509		14.45	381.7144	0.27027		-0.10092
35	571		14.5	428.4777	0.315315		-0.12385
40	624		14.51	468.3885	0.36036		-0.12844
45	661		14.51	496.1614	0.405405		-0.12844
50	698		14.52	523.9091	0.45045		-0.13303
55	733		14.55	550.1201	0.495495		-0.14679
60	762		14.6	571.7753	0.540541		-0.16972
65	791		14.6	593.4106	0.585586		-0.16972
70	815		14.6	611.2529	0.630631		-0.16972
75	838		14.6	628.3245	0.675676		-0.16972
80	855		14.6	640.8567	0.720721		-0.16972
85	875		14.6	655.8361	0.765766		-0.16972
90	890		14.6	666.6394	0.810811		-0.16972
95	904		14.6	676.8776	0.855856		-0.16972
100	918		14.6	687.1062	0.900901		-0.16972
125	980		14.6	732.0986	1.126126		-0.16972
150	1024		14.55	763.394	1.351351		-0.14679
175	1062		14.5	790.0541	1.576577		-0.12385
200	1099		14.4	815.8386	1.801802		-0.07798
225	1131		14.3	837.7763	2.027027		-0.03211
250	1162		14.2	858.8623	2.252252		0.013761
275	1190		14.11	877.6203	2.477477		0.055046
300	1212		14.02	891.8492	2.702703		0.09633
350	1258		13.85	921.5522	3.153153		0.174312
400	1299		13.6	947.2802	3.603604		0.288991
450	1336		13.35	969.8132	4.054054		0.40367
500	1370		13.05	989.9174	4.504505		0.541284
550	1398		12.72	1005.458	4.954955		0.692661
600	1422		12.5	1017.934	5.405405		0.793578
700	1469		11.85	1041.681	6.306306		1.091743
750	1488		11.55	1050.127	6.756757		1.229358
800	1503		11.25	1055.624	7.207207		1.366972
850	1519		10.95	1061.72	7.657658		1.504587
900	1533		10.61	1066.311	8.108108		1.66055
950	1546		10.3	1070.112	8.558559		1.802752
1000	1557		10.05	1072.441	9.009009		1.917431
1100	1576		9.45	1074.822	9.90991		2.192661
1200	1589		8.85	1072.879	10.81081		2.46789
1300	1596		8.35	1066.735	11.71171		2.697248
1400	1604		7.8	1061.159	12.61261		2.949541
1500	1609		7.35	1053.504	13.51351		3.155963
1600	1618		6.9	1048.379	14.41441		3.362385
1700	1620		6.55	1038.63	15.31532		3.522936
1800	1622		6.15	1028.853	16.21622		3.706422
1900	1628		5.8	1021.567	17.11712		3.866972
2000	1632		5.45	1012.953	18.01802		4.027523
2100	1636		5.2	1004.285	18.91892		4.142202

Table B.4: Drained triaxial compression on loose oil contaminated sand σ_3=138 kPa

Date of Testing.....:july 6, 1988
Tested by.....:Faouzi B. Amor
Type of Sample.....:Loose Sand
Type of test.....:Drained
Confining pressure.....:20 psi
Density.....:1.38 g/cc
Void ratio.....:

Disp reading	Load reading	P.w.P reading	V. chng reading	Dev(kPa) calcul	axStrn %	pwp(kPa) calcul	Volumetri Strain
0	39		18.5	0	0		0
1	42		18.51	2.224583	0.009091		-0.00461
2	51		18.52	8.897524	0.018182		-0.00922
3	57		18.54	13.34507	0.027273		-0.01844
5	63		18.55	17.79019	0.045455		-0.02305
10	74		18.6	25.93224	0.090909		-0.0461
15	81		18.65	31.10453	0.136364		-0.06915
20	87		18.7	35.53185	0.181818		-0.0922
25	92		18.77	39.21522	0.227273		-0.12448
30	96		18.85	42.15564	0.272727		-0.16136
40	103		19	47.2895	0.363636		-0.23051
50	110		19.1	52.41393	0.454545		-0.27661
60	116		19.2	56.79136	0.545455		-0.32271
70	121		19.3	60.42383	0.636364		-0.36882
80	126		19.4	64.04956	0.727273		-0.41492
90	131		19.5	67.66854	0.818182		-0.46102
100	136		19.6	71.28078	0.909091		-0.50712
125	147		19.85	79.18214	1.136364		-0.62238
150	156		20.05	85.58346	1.363636		-0.71458
175	163		20.2	90.49484	1.590909		-0.78374
200	171		20.4	96.11074	1.818182		-0.87594
225	178		20.6	100.9732	2.045455		-0.96814
250	184		20.77	105.0874	2.272727		-1.04652
275	190		20.9	109.1814	2.5		-1.10645
300	196		21.08	113.2551	2.727273		-1.18943
350	208		21.31	121.3418	3.181818		-1.29547
400	219		21.55	128.6331	3.636364		-1.40611
450	227		21.75	133.7164	4.090909		-1.49832
500	236		21.91	139.4536	4.545455		-1.57208
550	245		22.1	145.1302	5		-1.65967
600	258		22.22	153.5507	5.454545		-1.715
650	261		22.39	154.9058	5.909091		-1.79337
700	268		22.51	159.0182	6.363636		-1.84869
750	275		22.62	163.0835	6.818182		-1.89941
800	285		22.75	169.1646	7.272727		-1.95934
850	291		22.82	172.4411	7.727273		-1.99161
900	297		22.95	175.6772	8.181818		-2.05154
950	301		23	177.5177	8.636364		-2.07459
1000	307		23.1	180.6796	9.090909		-2.1207
1100	320		23.2	187.5494	10		-2.1668
1200	331		23.3	192.9226	10.90909		-2.2129
1300	342		23.38	198.1475	11.81818		-2.24978
1400	349		23.42	200.6352	12.72727		-2.26822
1500	360		23.49	205.5904	13.63636		-2.30049
1600	368		23.5	208.4961	14.54545		-2.3051
1700	376		23.5	211.294	15.45455		-2.3051
1800	385		23.5	214.6042	16.36364		-2.3051
1900	392		23.5	216.566	17.27273		-2.3051
2000	399		23.5	218.4335	18.18182		-2.3051

Table B.5: Triaxial compression on loose oil contaminated sand σ_3=276 kPa

Date of Testing.....:July 18,1988
Tested by.....:Faouzi B. Amor
Type of Sample.....:Loose Sand
Type of test.....:Drained
Confining pressure.....:40 psi
Density.....:1.39 g/cc
Void ratio.....:

Disp reading	Load reading	P.w.P reading	V. chng reading	Dev(kPa) calcul	axStrn %	pwp(kPa) calcul	Volumetri Strain
60	93		17.2	0	0		0
65	97		17.2	2.993878	0.045455		0
70	105		17.2	8.97755	0.090909		0
73	119		17.25	19.44605	0.118182		-0.02332
76	132		17.3	29.16111	0.145455		-0.04663
78	143		17.35	37.37923	0.163636		-0.06995
82	155		17.39	46.33336	0.2		-0.0886
85	164		17.42	53.04467	0.227273		-0.10259
90	178		17.5	63.47525	0.272727		-0.13989
95	187		17.55	70.16417	0.318182		-0.16321
100	196		17.61	76.84696	0.363636		-0.19119
105	205		17.7	83.52362	0.409091		-0.23315
110	213		17.75	89.44875	0.454545		-0.25647
115	221		17.81	95.36843	0.5		-0.28445
120	229		17.9	101.2827	0.545455		-0.32642
125	235		17.95	105.7027	0.590909		-0.34973
130	242		18	110.8627	0.636364		-0.37305
140	253		18.08	118.9382	0.727273		-0.41035
150	265		18.2	127.7415	0.818182		-0.46631
160	275		18.3	135.0445	0.909091		-0.51294
170	285		18.41	142.3338	1		-0.56423
180	294		18.5	148.8689	1.090909		-0.6062
190	302		18.6	154.6517	1.181818		-0.65283
200	309		18.7	159.6844	1.272727		-0.69946
225	328		18.91	173.3308	1.5		-0.79739
250	344		19.1	184.7049	1.727273		-0.88599
275	358		19.3	194.5561	1.954545		-0.97925
300	373		19.5	205.0922	2.181818		-1.07251
350	396		19.8	220.9078	2.636364		-1.2124
400	416		20.1	234.3898	3.090909		-1.3523
450	438		20.37	249.1801	3.545455		-1.4782
500	459		20.61	263.1018	4		-1.59011
550	475		20.85	273.3034	4.454545		-1.70203
600	491		21.05	283.396	4.909091		-1.79529
650	508		21.27	294.0883	5.363636		-1.89788
700	526		21.41	305.3701	5.818182		-1.96316
850	568		21.85	330.1401	7.181818		-2.16834
900	581		21.98	337.5145	7.636364		-2.22896
950	597		22.1	346.8651	8.090909		-2.28491
1000	606		22.15	351.313	8.545455		-2.30823
1100	616		22.2	354.601	9.454545		-2.33155
1200	635		22.3	363.7936	10.36364		-2.37818
1300	652		22.4	371.3988	11.27273		-2.42481
1400	670		22.5	379.4301	12.18182		-2.47144
1500	692		22.5	389.8195	13.09091		-2.47144
1600	705		22.53	394.1136	14		-2.48543
1700	720		22.55	399.5051	14.90909		-2.49475
1800	742		22.57	409.1048	15.81818		-2.50408
1900	752		22.59	410.9224	16.72727		-2.51341
2000	771		22.6	418.1545	17.63636		-2.51807
2100	785		22.6	422.0783	18.54545		-2.51807

Table B.6: Drained triaxial compression on loose oil contaminated sand σ_3=414 kPa

Date of Testing.....:July 7,1988
Tested by.....:Faouzi B. Amor
Type of Sample.....:Loose Sand
Type of test.....:Drained
Confining pressure.....:60 psi
Density.....:1.39 g/cc
Void ratio.....:

Disp reading	Load reading	P.w.P reading	V. chng reading	Dev(kPa) calcul	axStrn %	pwp(kPa) calcul	Volumetri Strain
0	71		8.2	0	0		0
2	73		8.2	1.465086	0.018462		0
5	75		8.21	2.92936	0.046155		-0.00463
7	78		8.22	5.125434	0.064617		-0.00925
10	82		8.22	8.052021	0.092311		-0.00925
13	88		8.23	12.44058	0.120004		-0.01388
15	102		8.24	22.68158	0.138466		-0.01851
17	120		8.25	35.84489	0.156928		-0.02313
20	155		8.3	61.43135	0.184621		-0.04626
25	190		8.4	86.9875	0.230776		-0.09253
30	214		8.45	104.4828	0.276932		-0.11566
35	236		8.51	120.5013	0.323087		-0.14342
40	255		8.57	134.315	0.369242		-0.17118
45	271		8.6	145.9269	0.415397		-0.18506
50	285		8.7	156.0695	0.461553		-0.23132
60	311		8.85	174.8688	0.553863		-0.30072
70	335		8.91	192.1772	0.646174		-0.32848
80	356		9.02	207.2712	0.738484		-0.37937
90	375		9.2	220.8837	0.830795		-0.46264
100	396		9.3	235.9223	0.923105		-0.50891
125	435		9.51	263.6175	1.153882		-0.60606
150	469		9.85	287.5682	1.384658		-0.76336
175	498		10	307.7997	1.615434		-0.83276
200	523		10.2	325.0565	1.846211		-0.92528
225	543		10.4	338.6414	2.076987		-1.01781
250	565		10.55	353.5903	2.307763		-1.08721
275	583		10.75	365.6084	2.53854		-1.17974
300	602		10.9	378.2781	2.769316		-1.24913
350	639		11.15	402.7156	3.230869		-1.36479
400	675		11.45	426.1973	3.692421		-1.50359
450	695		11.65	438.1996	4.153974		-1.59611
500	720		11.9	453.561	4.615527		-1.71177
550	745		12.15	468.7532	5.077079		-1.82743
600	773		12.3	485.8527	5.538632		-1.89683
650	794		12.45	497.9418	6.000185		-1.96623
700	813		12.6	508.5182	6.461737		-2.03562
750	833		12.8	519.648	6.92329		-2.12815
800	857		12.91	533.3569	7.384843		-2.17904
850	876		13.05	543.5275	7.846395		-2.24381
900	893		13.2	552.2259	8.307948		-2.31321
950	909		13.3	560.141	8.769501		-2.35947
1000	927		13.4	569.2779	9.231053		-2.40574
1100	964		13.6	587.8449	10.15416		-2.49827
1200	991		13.7	599.3961	11.07726		-2.54453
1300	1020		13.8	611.8717	12.00037		-2.59079
1400	1042		13.88	619.489	12.92347		-2.6278
1500	1069		14	629.9649	13.84658		-2.68332
1600	1091		14.05	636.9532	14.76969		-2.70645
1700	1112		14.15	643.0263	15.69279		-2.75272
1800	1142		14.25	654.3137	16.6159		-2.79898
1900	1155		14.25	654.9244	17.539		-2.79898
2000	1179		14.25	661.9307	18.46211		-2.79898

Table B.7: Drained triaxial compression on loose clean sand σ_3=138 kPa

Date of Testing.....:June 28,1988
Tested by.....:Faouzi B. Amor
Type of Sample.....:Loose Sand
Type of test.....:Drained
Confining pressure.....:138 kPa, 20 psi
Density.....:1.38 g/cc
Void ratio.....:

Disp reading	Load reading	P.w.P reading	V. chng reading	Dev(kPa) calcul	axStrn %	pwp(kPa) calcul	Volumetri Strain
0	28	76	22.6	0	0		0
1	30		22.6	1.486818	0.009615		0
5	36		22.61	5.944983	0.048077		-0.00489
10	39		22.63	8.17042	0.096154		-0.01466
15	42		22.64	10.39371	0.144231		-0.01955
20	47		22.64	14.09896	0.192308		-0.01955
25	52		22.65	17.80063	0.240385		-0.02444
30	89		22.65	45.22147	0.288462		-0.02444
35	120		22.7	68.16999	0.336538		-0.04888
40	148		22.73	88.87449	0.384615		-0.06354
50	180		22.8	112.4657	0.480769		-0.09776
60	202		22.9	128.6192	0.576923		-0.14664
70	219		22.93	141.0489	0.673077		-0.16131
80	233		23	151.2411	0.769231		-0.19552
90	245	78	23.02	159.9391	0.865385		-0.2053
100	255		23.1	167.1472	0.961538		-0.2444
125	277		23.2	182.9015	1.201923		-0.29328
150	293		23.3	194.1806	1.442308		-0.34216
175	304	78	23.4	201.7477	1.682692		-0.39105
200	315		23.5	209.2754	1.923077		-0.43993
250	333		23.62	221.3105	2.403846		-0.49858
300	350		23.75	232.4949	2.884615		-0.56213
350	365		23.9	242.1208	3.365385		-0.63545
400	378	79	23.98	250.2097	3.846154		-0.67455
450	389		24.01	256.7831	4.326923		-0.68922
500	398	78	24.1	261.8623	4.807692		-0.73321
550	409		24.19	268.2856	5.288462		-0.7772
600	415		24.21	271.1272	5.769231		-0.78698
650	427	79	24.25	278.1081	6.25		-0.80653
700	433		24.3	280.8425	6.730769		-0.83097
750	440	80	24.3	284.2239	7.211538		-0.83097
800	448		24.31	288.2416	7.692308		-0.83586
850	448		24.35	286.7403	8.173077		-0.85541
900	458	79	24.38	292.0305	8.653846		-0.87008
950	463		24.38	293.8713	9.134615		-0.87008
1000	472		24.38	298.3644	9.615385		-0.87008
1100	482		24.31	301.8387	10.57692		-0.83586
1200	490	78	24.3	303.8547	11.53846		-0.83097
1300	503		24.2	309.009	12.5		-0.78209
1400	515		24.13	313.3341	13.46154		-0.74787
1500	521	77	24.1	313.67	14.42308		-0.73321
1600	533		24.05	317.6949	15.38462		-0.70877
1700	544	76	24	320.9261	16.34615		-0.68433
1800	552	75	24	322.1557	17.30769		-0.68433
1900	563		23.92	325.0939	18.26923		-0.64522
2000	568	74	23.9	324.2718	19.23077		-0.63545
2100	578	75	23.8	326.345	20.19231		-0.58657

Table B.8: Drained triaxial compression on loose clean sand σ_3=276 kPa

Date of Testing.....:August 8, 1988
Tested by.....:Faouzi B. Amor
Type of Sample.....:Loose Sand
Type of test.....:Drained
Confining pressure.....:60 psi
Density.....:
Void ratio.....:

Disp reading	Load reading	P.w.P reading	V. chng reading	Dev(kPa) calcul	axStrn %	pwp(kPa) calcul	Volumetri Strain
27	81		12.6	0	0		0
30	85		12.59	3.036869	0.027027		-0.00459
33	93		12.57	9.108143	0.054054		-0.01376
36	101		12.55	15.17613	0.081081		-0.02294
40	123		12.55	31.85839	0.117117		-0.02294
45	172		12.5	68.99537	0.162162		-0.04587
50	211		12.4	98.52035	0.207207		-0.09174
55	256		12.35	132.5637	0.252252		-0.11468
60	291		12.3	159.0046	0.297297		-0.13761
65	324		12.2	183.9079	0.342342		-0.18349
70	350		12.1	203.4933	0.387387		-0.22936
75	375		12	222.3047	0.432432		-0.27523
85	416		11.9	253.0772	0.522523		-0.3211
100	467		11.7	291.2092	0.657658		-0.41284
125	540		11.45	345.4974	0.882883		-0.52752
150	593		11.15	384.5157	1.108108		-0.66514
175	640		10.9	418.8569	1.333333		-0.77982
200	682		10.65	449.2994	1.558559		-0.8945
250	754		10.3	500.8234	2.009009		-1.05505
300	817		10	545.1881	2.459459		-1.19266
350	870		9.65	581.7485	2.90991		-1.35321
400	916		9.3	612.8091	3.36036		-1.51376
450	955		9.1	638.4415	3.810811		-1.6055
500	997		8.8	665.9883	4.261261		-1.74312
550	1031		8.55	687.4586	4.711712		-1.8578
600	1058		8.35	703.6547	5.162162		-1.94954
700	1125		8	744.7668	6.063063		-2.11009
800	1176		7.65	773.6575	6.963964		-2.27064
900	1222		7.35	798.3518	7.864865		-2.40826
1000	1273		7.1	825.881	8.765766		-2.52294
1100	1310		6.85	843.1082	9.666667		-2.63761
1200	1354		6.7	864.5833	10.56757		-2.70642
1300	1390		6.55	880.0777	11.46847		-2.77523
1400	1426		6.35	895.0795	12.36937		-2.86697
1500	1459		6.22	907.6128	13.27027		-2.92661
1600	1487		6.1	916.4355	14.17117		-2.98165
1700	1527		6	932.6146	15.07207		-3.02752
1800	1550		5.95	937.3984	15.97297		-3.05046
1910	1582		5.85	946.522	16.96396		-3.09633
2000	1609		5.8	954.1394	17.77477		-3.11927
2100	1628		5.75	955.4197	18.67568		-3.1422
2200	1658		5.7	963.1582	19.57658		-3.16514

Table B.9: Drained triaxial compression on loose clean sand σ_3=414 kPa

Date of Testing.....:June 24, 1988
Tested by.....:Faouzi B. Amor
Type of Sample.....:Loose Sand
Type of test.....:Drained
Confining pressure.....:138 kPa, 40 psi
Density.....:1.40 g/cc
Void ratio.....:

Disp reading	Load reading	P.w.P reading	V. chng reading	Dev(kPa) calcul	axStrn %	pwp(kPa) calcul	Volumetri Strain
0	30		4.2	0	0		0
1	43		4.22	9.659398	0.009675		0.00983
2	70		4.25	29.71835	0.01935		0.024575
3	83		4.27	39.373	0.029025		0.034405
4	93		4.29	46.79734	0.0387		0.044235
6	114		4.3	62.38438	0.05805		0.04915
8	133		4.32	76.48032	0.077399		0.05898
10	150		4.4	89.08603	0.096749		0.098299
13	174		4.4	106.8722	0.125774		0.098299
16	193		4.4	120.9382	0.154799		0.098299
20	215		4.5	137.208	0.193498		0.147449
25	240		4.55	155.6741	0.241873		0.172024
30	260		4.6	170.4175	0.290248		0.196599
35	275		4.65	181.4436	0.338622		0.221174
40	294		4.7	195.4199	0.386997		0.245749
45	309		4.75	206.423	0.435372		0.270323
50	321		4.75	215.1968	0.483746		0.270323
60	339		4.8	228.2858	0.580495		0.294898
70	359		4.9	242.825	0.677245		0.344048
80	376		4.95	255.1234	0.773994		0.368623
90	389		5	264.4509	0.870743		0.393198
100	405		5.1	275.9674	0.967492		0.442347
125	440		5.2	300.9874	1.209365		0.491497
150	466		5.35	319.2908	1.451238		0.565222
175	488		5.5	334.5786	1.693111		0.638946
200	509		5.55	349.0586	1.934985		0.663521
250	546		5.75	374.1665	2.418731		0.761821
300	577		5.9	394.6792	2.902477		0.835545
350	604		6.1	412.0972	3.386223		0.933844
400	625		6.2	425.0351	3.869969		0.982994
450	646		6.3	437.822	4.353715		1.032144
500	668		6.4	451.165	4.837461		1.081294
550	685		6.5	460.8321	5.321207		1.130443
600	707		6.55	473.8768	5.804954		1.155018
650	722		6.6	481.8888	6.2887		1.179593
710	745		6.7	494.821	6.869195		1.228743
760	758		6.75	501.2008	7.352941		1.253318
810	773		6.8	508.8568	7.836687		1.277892
925	809		6.9	527.0714	8.949303		1.327042
1000	830		6.9	536.9663	9.674923		1.327042
1100	852		6.95	545.8232	10.64241		1.351617
1200	877		6.97	556.3342	11.60991		1.361447
1300	897		6.98	563.2375	12.5774		1.366362
1400	917		6.98	569.8532	13.54489		1.366362
1500	938		6.98	576.8166	14.51238		1.366362
1600	956		6.9	581.5939	15.47988		1.327042
1700	975		6.9	586.7332	16.44737		1.327042
1800	990		6.8	589.1446	17.41486		1.277892
1900	1010		6.8	594.3727	18.38235		1.277892
2000	1022		6.72	594.5188	19.34985		1.238573

Table B.10: Drained triaxial compression on dense clean sand σ_3=138 kPa

Date of Testing.....:August 3, 1988
Tested by.....:Ameir. Altaee
Type of Sample.....:Dense Sand
Type of test.....:Drained
Confining pressure.....:20 psi
Density.....:
Void ratio.....:
Note.....:This test has been repeted because loading ra

Disp reading	Load reading	P.w.P reading	V. chng reading	Dev(kPa) calcul	axStrn %	pwp(kPa) calcul	Volumetri Strain
200	0		10.1	0	0		0
210	43		10.1	73.21466	0.09009		0
220	85		10	144.5961	0.18018		-0.04587
230	118		9.9	200.5523	0.27027		-0.09174
250	158		9.8	268.051	0.45045		-0.13761
275	192		9.9	324.9959	0.675676		-0.09174
300	218		9.8	368.169	0.900901		-0.13761
350	256		9.9	430.38	1.351351		-0.09174
400	283		10.4	473.5992	1.801802		0.137615
450	308		11	513.0722	2.252252		0.412844
500	332		11.6	550.5032	2.702703		0.688073
550	351		12.1	579.3134	3.153153		0.917431
600	368		12.6	604.5464	3.603604		1.146789
650	384		13.1	627.8832	4.054054		1.376147
700	398		13.7	647.7195	4.504505		1.651376
800	422		14.9	680.2989	5.405405		2.201835
900	443		16	707.3512	6.306306		2.706422
1000	462		17.1	730.5959	7.207207		3.211009
1100	471		18.2	737.5969	8.108108		3.715596
1200	482		19.2	747.423	9.009009		4.174312
1300	492		20.2	755.3759	9.90991		4.633028
1400	496		21	753.902	10.81081		5.000000
1500	497		21.8	747.7914	11.71171		5.366972
1600	500		22.5	744.6287	12.61261		5.688073
1700	502		23.2	739.8999	13.51351		6.009174
1800	503		23.7	733.6512	14.41441		6.238532
1900	505		24.2	728.8149	15.31532		6.46789
2000	508		24.7	725.3451	16.21622		6.697248
2100	509		25.2	718.9582	17.11712		6.926606
2200	511		25.7	713.9377	18.01802		7.155963
2300	512		26.1	707.474	18.91892		7.33945
2400	512		26.4	699.6132	19.81982		7.477064

Table B.11: Drained triaxial compression on dense clean sand σ_3=276 kPa

Date of Testing.....:August 4, 1988
Tested by.....:Ameir Altae
Type of Sample.....:Dense Sand
Type of test.....:Drained
Confining pressure.....:40 psi
Density.....:
Void ratio.....:

Disp reading	Load reading	P.w.P reading	V. chng reading	Dev(kPa) calcul	axStrn %	pwp(kPa) calcul	Volumetri Strain
200	0		3.4	0	0		0
220	97		3.4	164.8417	0.18018		0
240	199		3.3	337.5699	0.36036		-0.04587
250	238		3.3	403.3618	0.45045		-0.04587
260	274		3.3	463.9543	0.540541		-0.04587
280	325		3.3	549.3138	0.720721		-0.04587
300	360		3.3	607.3664	0.900901		-0.04587
325	398		3.2	669.9512	1.126126		-0.09174
350	430		3.2	722.1678	1.351351		-0.09174
375	455		3.2	762.4097	1.576577		-0.09174
400	480		3.2	802.4598	1.801802		-0.09174
460	520		3.6	864.5461	2.342342		0.091743
500	552		3.8	914.3625	2.702703		0.183486
550	580		4.1	956.2953	3.153153		0 321101
600	608		4.6	997.7986	3.603604		..550459
650	624		5.1	1019.271	4.054054		0.779817
700	640		5.5	1040.498	4.504505		0.963303
800	668		6.4	1075.775	5.405405		1.376147
900	688		7.3	1097.431	6.306306		1.788991
1000	701		8.3	1107.416	7.207207		2.247706
1100	709		9.3	1109.18	8.108108		2.706422
1200	716		10.2	1109.149	9.009009		3.119266
1300	714		11	1095.1	9.90991		3.486239
1400	711		11.8	1079.594	10.81081		3.853211
1500	708		12.6	1064.179	11.71171		4.220183
1600	704		13.3	1047.37	12.61261		4.541284
1700	702		13.9	1033.627	13.51351		4.816514
1800	698		14.5	1017.032	14.41441		5.091743
1900	695		15	1002.001	15.31532		5.321101
2000	692		15.5	987.0624	16.21622		5.550459
2100	689		15.95	972.2156	17.11712		5.756881
2200	686		16.35	957.4609	18.01802		5.940367
2300	683		16.7	942.7982	18.91892		6.100917
2400	684		17	933.6877	19.81982		6.238532

Table B.12: Drained triaxial compression on dense clean sand σ_3=414 kPa

Date of Testing.....:August 5,1988
Tested by.....:Ameir Altae
Type of Sample.....:Dense Sand
Type of test.....:Drained
Confining pressure.....:60 psi
Density.....:
Void ratio.....:
Note.....:Bedding should be taken into considerations

Disp reading	Load reading	P.w.P reading	V. chng reading	Dev(kPa) calcul	axStrn %	pwp(kPa) calcul	Volumetri Strain
200	0		7	0	0		0
226	120		6.6	203.8174	0.234234		-0.18349
250	245		6.3	415.2254	0.45045		-0.3211
280	340		6.1	574.6667	0.720721		-0.41284
300	410		5.9	691.7228	0.900901		-0.50459
350	530		5.7	890.1138	1.351351		-0.59633
400	612		5.5	1023.136	1.801802		-0.68807
500	726		5.6	1202.585	2.702703		-0.6422
600	809		5.9	1327.663	3.603604		-0.50459
700	872		6.3	1417.679	4.504505		-0.3211
800	920		6.8	1481.606	5.405405		-0.09174
900	954		7.3	1521.729	6.306306		0.137615
1000	982		7.9	1551.33	7.207207		0.412844
1100	1002		8.5	1567.557	8.108108		0.688073
1200	1019		9	1578.524	9.009009		0.917431
1300	1027		9.6	1575.165	9.90991		1.192661
1400	1035		10.2	1571.56	10.81081		1.46789
1500	1035		10.7	1555.686	11.71171		1.697248
1600	1034		11.2	1538.324	12.61261		1.926606
1700	1032		11.7	1519.52	13.51351		2.155963
1800	1030		12.2	1500.778	14.41441		2.385321
1900	1026		12.6	1479.213	15.31532		2.568807
2000	1024		13	1460.624	16.21622		2.752294
2100	1023		13.4	1443.507	17.11712		2.93578
2200	1021		13.8	1425.026	18.01802		3.119266
2300	1018		14.1	1405.225	18.91892		3.256881
2410	1017		14.3	1386.686	19.90991		3.348624

Table B.13: Isotropic compression on dense clean sand

Date of Testing.....:October 13, 1988
Tested by.....:Faouzi Ben Amor
Type of Sample.....:Dense Sand
Type of test.....:Isotropic Compression
Confining pressure.....:
Density.....:1.40 g/cc
Void ratio.....:

Disp reading	Load reading	P.w.P reading	V. chng reading	Dev(kPa) calcul	Isotr press	pwp(kPa) calcul	Volumetri Strain
3		18.4		20.685			0
8		17.9		55.16			0.229358
13		17.7		89.635			0.321101
23		17.4		158.585			0.458716
33		17.1		227.535			0.59633
43		16.85		296.485			0.711009
53		16.65		365.435			0.802752
63		16.5		434.385			0.87156
70		16.4		482.65			0.917431
50		16.7		344.75			0.779817
30		17		206.85			0.642202
10		17.6		68.95			0.366972
5		17.9		34.475			0.229358
3		18.15		20.685			0.114679
8		17.65		55.16			0.344037
13		17.45		89.635			0.43578
23		17.15		158.585			0.573394
33		16.95		227.535			0.665138
43		16.75		296.485			0.756881
53		16.6		365.435			0.825688
63		16.45		434.385			0.894495
70		16.4		482.65			0.917431
80		16.2		551.6			1.009174
90		16.1		620.55			1.055046
70		16.3		482.65			0.963303
50		16.55		344.75			0.848624
30		16.9		206.85			0.688073
10		17.5		68.95			0.412844
5		17.8		34.475			0.275229
3		18.05		20.685			0.16055
50		16.55		344.75			0.848624
70		16.2		482.65			1.009174
90		16		620.55			1.100917
110		15.75		758.45			1.215596
142		15.4		979.09			1.376147
94		15.75		648.13			1.215596
60		16.1		413.7			1.055046
40		16.4		275.8			0.917431
20		16.85		137.9			0.711009
10		17.2		68.95			0.550459
5		17.6		34.475			0.366972
3		17.8		20.685			0.275229

Table B.14: Isotropic compression on loose clean sand

Date of Testing.....:October 20, 1988
Tested by.....:Faouzi B. Amor
Type of Sample.....:Loose Sand
Type of test.....:Isotropic Compression
Confining pressure.....:
Density.....:1.38 g/cc
Void ratio.....:

Disp reading	Load reading	V. chng readng1	V. chng readng2	Dev(kPa) calcul	Isotr Press	Volumetr Strain1	Volumetr Strain2
	3	13.5	12.1		20.94	0	0
	5	13.9	11.75		34.9	0.183486	0.16055
	8	14.2	11.5		55.84	0.321101	0.275229
	13	14.6	11.1		90.74	0.504587	0.458716
	23	15.2	10.6		160.54	0.779817	0.688073
	33	15.5	10.15		230.34	0.917431	0.894495
	43	16	9.85		300.14	1.146789	1.03211
	53	16.3	9.55		369.94	1.284404	1.169725
	63	16.5	9.3		439.74	1.376147	1.284404
	70	16.75	9.1		488.6	1.490826	1.376147
	50	16.35	9.5		349	1.307339	1.192661
	30	15.9	10		209.4	1.100917	0.963303
	10	15	10.8		69.8	0.688073	0.59633
	5	14.4	11.3		34.9	0.412844	0.366972
	3	14	11.75		20.94	0.229358	0.16055
	50	16.4	9.4		349	1.330275	1.238532
	70	16.9	9		488.6	1.559633	1.422018
	90	17.25	8.6		628.2	1.720183	1.605505
	110	17.65	8.15		767.8	1.90367	1.811927
	130	18	7.8		907.4	2.06422	1.972477
	142	18.3	7.6		991.16	2.201835	2.06422
	94	17.8	7.95		656.12	1.972477	1.90367
	60	17.3	8.5		418.8	1.743119	1.651376
	40	16.9	8.9		279.2	1.559633	1.46789
	20	16.15	9.6		139.6	1.215596	1.146789
	10	15.6	10.1		69.8	0.963303	0.917431
	5	15.1	10.7		34.9	0.733945	0.642202
	3	14.65	11.1		20.94	0.527523	0.458716

Table B.15: Isotropic compression on dense oil contaminated sand

Date of Testing.....:November 8, 1988
Tested by.....:Faouzi Ben Amor
Type of Sample.....:Dense Sand
Type of test.....:Isotropic Compression
Confining pressure.....:
Density.....:
Void ratio.....:
Notes.....:Back Pressure applied 17.3 psi around 120 kPa

Disp reading	Load reading	P.w.P reading	V. chng reading	Dev(kPa) calcul	Isotr Press	pwp(kPa) calcul	Volumetri Strain
	20		12.00		18.6165		0
	22		12.20		32.4065		0.091743
	25		12.43		53.0915		0.197248
	30		12.60		87.5665		0.275229
	40		13.00		156.5165		0.458716
	50		13.30		225.4665		0.59633
	60		13.60		294.4165		0.733945
	70		13.80		363.3665		0.825688
	60		13.60		294.4165		0.733945
	50		13.45		225.4665		0.665138
	40		13.22		156.5165		0.559633
	30		13.00		87.5665		0.458716
	25		12.70		53.0915		0.321101
	22		12.50		32.4065		0.229358
	20		12.25		18.6165		0.114679
	67		13.90		342.6815		0.87156
	77		14.05		411.5315		0.940367
	87		14.30		480.5815		1.055046
	97		14.50		549.5315		1.146789
	107		15.20		618.4815		1.46789
	117		15.40		687.4315		1.559633
	127		16.00		756.3815		1.834862
	137		16.30		825.3315		1.972477
	140		16.40		846.0165		2.018349
	94		15.90		528.8465		1.788991
	80		15.60		432.3165		1.651376
	60		14.95		294.4165		1.353211
	50		14.50		225.4665		1.146789
	40		14.10		156.5165		0.963303
	30		13.65		87.5665		0.756881
	25		13.45		53.0915		0.665138
	22		13.20		32.4065		0.550459
	20		12.95		18.6165		0.43578

Table B.16: Isotropic compression on loose oil contaminated sand

Date of Testing.....:November 8, 1988
Tested by.....:Faouzi Ben Amor
Type of Sample.....:Loose sand
Type of test.....:Isotropic Compression
Confining pressure.....:
Density.....:
Void ratio.....:
Notes.....:Back Pressure applied was 10 psi, around 70 k.

Disp reading	Load reading	P.w.P reading	V. chng reading	Dev(kPa) calcul	Isotr Press	pwp(kPa) calcul	Volumetri Strain
	14		11.70		27.580		0
	16		11.95		41.370		0.114679
	20		12.40		68.950		0.321101
	25		13.00		103.425		0.59633
	30		13.55		137.900		0.848624
	40		14.50		206.850		1.284404
	50		15.25		275.800		1.62844
	60		15.95		344.750		1.949541
	70		16.55		413.700		2.224771
	55		16.10		310.275		2.018349
	40		15.70		206.850		1.834862
	25		15.10		103.425		1.559633
	20		14.80		68.950		1.422018
	16		14.50		41.370		1.284404
	14		14.20		27.580		1.146789
	60		16.60		344.750		2.247706
	80		17.50		482.650		2.66055
	100		19.10		620.550		3.394495
	120		19.85		758.450		3.738532
	141		20.55		903.245		4.059633
	94		20.00		579.180		3.807339
	70		19.60		413.700		3.623853
	50		18.70		275.800		3.211009
	30		17.50		137.900		2.66055
	20		16.90		68.950		2.385321
	15		16.40		34.475		2.155963

Table B.17: undrained triaxial compression on loose clean sand σ_3=138 kPa

```
Date of Testing.....:november 14, 1988
Tested by...........:Faouzi B. Amor
Type of  Sample.....:Loose Sand
Type of test........:Undrained Triaxial
Confining pressure..:138 kPa, 20 psi
Density.............:
Void ratio..........:
```

Disp reading	Load reading	P.w.P reading	V. chng reading	Dev(kPa) calcul	axStrn %	pwp(kPa) calcul	Peff calcul
100	67	643		0	0	0	138
105	74	646		5.282586	0.045045	1.449	138.3119
110	79	647		9.051781	0.09009	1.932	139.0853
120	88	650		15.82633	0.18018	3.381	139.8944
130	94	653		20.32978	0.27027	4.83	139.9466
140	98	656		23.32051	0.36036	6.279	139.4945
150	143	668		57.12117	0.45045	12.075	144.9654
160	184	683		87.85696	0.540541	19.32	147.9657
170	207	695		105.0328	0.630631	25.116	147.8949
180	221	704		115.4313	0.720721	29.463	147.0141
200	234	719		124.9483	0.900901	36.708	142.9414
220	240	730		129.2021	1.081081	42.021	139.0464
240	245	738		132.6942	1.261261	45.885	136.3464
260	246	746		133.1961	1.441441	49.749	132.6497
280	250	751		135.9236	1.621622	52.164	131.1439
300	250	756		135.6747	1.801802	54.579	128.6459
320	250	762		135.4257	1.981982	57.477	125.6649
340	251	764		135.9155	2.162162	58.443	124.8622
360	255	766		138.6144	2.342342	59.409	124.7958
380	255	769		138.3587	2.522523	60.858	123.2616
400	253	773		136.6337	2.702703	62.79	120.7546
420	247	778		131.9813	2.882883	65.205	116.7888
460	254	781		136.6052	3.243243	66.654	116.8811
500	258	783		139.0075	3.603604	67.62	116.7158
550	257	788		137.6336	4.054054	70.035	113.8429
600	259	791		138.4294	4.504505	71.484	112.6591
650	260	793		138.494	4.954955	72.45	111.7147
700	262	794		139.266	5.405405	72.933	111.489
750	265	795		140.7352	5.855856	73.416	111.4957
900	252	813		129.6075	7.207207	82.11	99.0925
1000	268	806		139.4497	8.108108	78.729	105.7542
1100	278	802		144.9523	9.009009	76.797	109.5204
1210	264	817		133.8607	10	84.042	98.57822
1300	281	807		144.1021	10.81081	79.212	106.822
1410	291	802		149.1598	11.8018	76.797	110.9229
1500	263	823		129.315	12.61261	89.34	94.16501
1600	290	810		145.6121	13.51351	80.661	105.8764
1720	300	803		150.24	14.59459	77.28	110.8

Table B.18: undrained triaxial compression on loose oil contaminated sand σ_3=138 kPa

```
Date of Testing.....:Mai, 5th 1988
Tested by...........:Faouzi B. Amor
Type of  Sample.....:Loose Sand
Type of test........:Undrained Triaxial
Confining pressure..:138 kPa, 20 psi
Density.............:1.40 g/ccm
Void ratio..........:0.899
```

Disp reading	Load reading	P.w.P reading	V. chng reading	Dev(kPa) calcul	ax-strn %	pwp(kPa) calcul	p eff calcul
0	0.0	238		0.000	0.000	0.0	138.000
30	68.0	259		50.617	0.288	10.5	144.372
50	87.0	286		64.635	0.481	24.0	135.545
80	93.2	316		69.040	0.769	39.0	122.013
100	94.0	329		69.498	0.962	45.5	115.666
110	93.2	338		68.839	1.058	50.0	110.946
120	93.0	342		68.625	1.154	52.0	108.875
130	92.2	348		67.968	1.250	55.0	105.656
140	91.5	353		67.387	1.346	57.5	102.962
150	90.5	357		66.585	1.442	59.5	100.695
170	88.3	366		64.840	1.635	64.0	95.613
200	84.5	376		61.868	1.923	69.0	89.623
250	80.0	389		58.286	2.404	75.5	81.929
300	76.2	397		55.244	2.885	79.5	76.915
350	74.5	403		53.744	3.365	82.5	73.415
400	73.5	408		52.759	3.846	85.0	70.586
450	72.6	412		51.852	4.327	87.0	68.284
500	72.0	415		51.165	4.808	88.5	66.555
550	72.0	417		50.907	5.288	89.5	65.469
600	73.2	417		51.492	5.769	89.5	65.664
650	73.7	418		51.580	6.250	90.0	65.193
700	74.9	419		52.151	6.731	90.5	64.884
750	75.6	419		52.367	7.212	90.5	64.956
800	77.9	419		53.680	7.692	90.5	65.393
858	80.0	419		54.794	8.250	90.5	65.765
900	81.9	419		55.849	8.654	90.5	66.116
950	83.0	419		56.301	9.135	90.5	66.267
1000	84.8	419		57.218	9.615	90.5	66.573
1050	88.0	417		59.061	10.096	89.5	68.187
1100	91.5	416		61.082	10.577	89.0	69.361
1150	94.2	415		62.546	11.058	88.5	70.349
1200	98.1	415		64.783	11.538	88.5	71.094
1250	100.0	413		65.679	12.019	87.5	72.393
1300	102.5	412		66.953	12.500	87.0	73.318
1350	106.5	411		69.184	12.981	86.5	74.561
1400	109.0	410		70.417	13.462	86.0	75.472
1450	111.1	408		71.375	13.942	85.0	76.792
1500	113.5	408		72.509	14.423	85.0	77.170
1550	116.8	407		74.198	14.904	84.5	78.233
1600	120.0	405		75.800	15.385	83.5	79.767
1700	125.8	403		78.561	16.346	82.5	81.687
1750	128.0	401		79.475	16.827	81.5	82.992
1800	131.0	400		80.868	17.308	81.0	83.956
1850	135.5	398		83.159	17.788	80.0	85.720
1900	140.1	397		85.480	18.269	79.5	86.993
1950	143.0	395		86.736	18.750	78.5	88.412
2000	144.0	394		86.826	19.231	78.0	88.942

Table B.19: undrained triaxial compression on dense clean sand σ_3=276 kPa

```
Date of Testing.....:August 8, 1988
Tested by...........:Faouzi B. Amor
Type of  Sample.....:Dense Sand
Type of test........:Undrained Triaxial
Confining pressure..:40 psi
Density.............:
Void ratio..........:
```

Disp reading	Load reading	P.w.P reading	V. chng reading	Dev(kPa) calcul	axStrn %	pwp(kPa) calcul	P effect calcul
100	0	578		0	0	0	276
115	5	584		8.500828	0.135135	2.898	275.9356
120	34	604		57.77956	0.18018	12.558	282.7019
122	52	620		88.35279	0.198198	20.286	285.1649
124	76	637		129.1077	0.216216	28.497	290.5389
126	100	652		169.8479	0.234234	35.742	296.874
128	128	669		217.366	0.252252	43.953	304.5023
130	149	682		252.9819	0.27027	50.232	310.0953
135	176	702		298.6893	0.315315	59.892	315.6711
140	194	717		329.0883	0.36036	67.137	318.5591
150	220	732		372.8555	0.45045	74.382	325.9032
160	242	737		409.7698	0.540541	76.797	335.7929
170	260	735		439.8498	0.630631	75.831	346.7856
180	280	728		473.255	0.720721	72.45	361.3017
190	299	718		504.9101	0.810811	67.62	376.6834
200	317	706		534.8198	0.900901	61.824	392.4493
215	342	686		576.2112	1.036036	52.164	415.9064
235	378	655		635.7055	1.216216	37.191	450.7108
250	406	630		681.8608	1.351351	25.116	478.1709
275	450	586		754.0315	1.576577	3.864	523.4798
300	496	540		829.2085	1.801802	-18.354	570.7568
350	587	445		976.8399	2.252252	-64.239	665.8523
400	679	348		1124.732	2.702703	-111.09	762.0007
450	773	248		1274.511	3.153153	-159.39	860.2269
500	862	152		1414.642	3.603604	-205.758	953.3054
550	950	59		1551.775	4.054054	-250.677	1043.935
600	1030	-28		1674.552	4.504505	-292.698	1126.882
650	1102	-96		1783.157	4.954955	-325.542	1195.928
600	1152	-117		1872.897	4.504505	-335.685	1235.984
750	1183	-117		1896.08	5.855856	-335.685	1243.712
800	1208	-115		1926.885	6.306306	-334.719	1253.014
850	1228	-115		1949.37	6.756757	-334.719	1260.509
900	1242	-115		1962.069	7.207207	-334.719	1264.742
950	1256	-116		1974.554	7.657658	-335.202	1269.387
1000	1267	-117		1982.131	8.108108	-335.685	1272.395
1100	1286	-121		1992.131	9.009009	-337.617	1277.661
1200	1305	-125		2001.548	9.90991	-339.549	1282.732
1300	1319	-128		2002.791	10.81081	-340.998	1284.595
1400	1329	-132		1997.591	11.71171	-342.93	1284.794
1500	1341	-134		1995.06	12.61261	-343.896	1284.916
1600	1352	-137		1990.689	13.51351	-345.345	1284.908
1800	1345	-140		1939.124	15.31532	-346.794	1269.169
1900	1336	-142		1905.658	16.21622	-347.76	1258.979
2000	1323	-142		1866.823	17.11712	-347.76	1246.034
2100	1292	-143		1803.265	18.01802	-348.243	1225.331

Table B.20: undrained triaxial compression on dense oil contaminated sand σ_3=276 kPa

Date of Testing.....:August 8, 1988
Tested by.....:Faouzi B. Amor
Type of Sample.....:Dense Sand
Type of test.....:Undrained Triaxial
Confining pressure.....:40 psi
Density.....:
Void ratio.....:

Disp reading	Load reading	P.w.P reading	V. chng reading	Dev(kPa) calcul	axStrn %	pwp(kPa) calcul	P effect calcul
100	0	579		0	0	0	276
102	5	582		8.510798	0.018018	1.449	277.3879
106	8	583		13.61237	0.054054	1.932	278.6055
110	14	586		23.81306	0.09009	3.381	280.5567
115	32	592		54.4053	0.135135	6.279	287.8561
118	42	596		71.38763	0.162162	8.211	291.5849
120	50	600		84.96994	0.18018	10.143	294.1803
125	88	638		149.4796	0.225225	28.497	297.3295
130	120	671		203.7438	0.27027	44.436	299.4786
140	160	706		271.413	0.36036	61.341	305.13
150	180	721		305.0636	0.45045	68.586	309.1019
160	190	725		321.7201	0.540541	70.518	312.722
170	200	723		338.346	0.630631	69.552	319.23
185	214	714		361.5379	0.765766	65.205	331.3076
200	227	700		382.9782	0.900901	58.443	345.2164
225	251	671		422.5069	1.126126	44.436	372.3996
250	276	635		463.531	1.351351	27.048	403.4623
275	303	598		507.7146	1.576577	9.177	436.0612
300	330	558		551.6911	1.801802	-10.143	470.04
350	386	473		642.3513	2.252252	-51.198	541.3151
400	444	392		735.4654	2.702703	-90.321	611.4761
450	502	315		827.69	3.153153	-127.512	679.4087
500	556	245		912.4606	3.603604	-161.322	741.4755
550	607	177		991.5026	4.054054	-194.166	800.6669
600	656	113		1066.511	4.504505	-225.078	856.5816
700	751	1		1209.441	5.405405	-279.174	958.3211
800	822	-69		1311.175	6.306306	-312.984	1026.042
900	866	-87		1368.077	7.207207	-321.678	1053.704
1000	896	-81		1401.728	8.108108	-318.78	1062.023
1100	920	-79		1425.164	9.009009	-317.814	1068.869
1200	931	-79		1427.924	9.90991	-317.814	1069.789
1300	951	-80		1444.014	10.81081	-318.297	1075.635
1400	962	-82		1445.961	11.71171	-319.263	1077.25
1500	972	-83		1446.084	12.61261	-319.746	1077.774
1600	982	-85		1445.9	13.51351	-320.712	1078.679
1700	990	-87		1442.495	14.41441	-321.678	1078.51
1800	998	-88		1438.845	15.31532	-322.161	1077.776
1900	1005	-90		1433.523	16.21622	-323.127	1076.968
2000	1013	-91		1429.397	17.11712	-323.61	1076.076
2100	1016	-92		1418.047	18.01802	-324.093	1072.775

Appendix C

Interface test results

Table C.1: Direct shear test on clean loose sand σ_n=107 kPa

Date of Testing.....:March 7th, 1989
Tested by.....:Faouzi Ben Amor
Type of Sample.....:Clean Loose Sand
Type of Interface.....:Direct shear
Normal Load.....:62 lbs
Density.....:1.35 g/cc
Void ratio.....:
Dial (2) Constant.....:0.002 mm/div
Dial (3) Constant.....:0.002 mm/div
Proving Ring Constant.....:0.85 lb/div
Notes.....:

(1) Disp reading	(2) Load reading	(3) Vertical reading	(4) Dev(kPa) calcul	(5) Shear Strain	(6) Vol Strain	(7) pwp(kPa) calcul
1831	3	850	3.26	0		
1833	5	850	5.43	0.004		
1839	10	850	10.86	0.016		
1849	15	850	16.30	0.036		
1866	20	850	21.75	0.07		
1888	25	850	27.21	0.114		
1923	30	850	32.69	0.184		
1951	33	850	35.99	0.24		
1964	35	850	38.19	0.266		
2000	38	850	41.51	0.338		
2027	40	850	43.74	0.392		
2078	43	850	47.10	0.494		
2140	45	851	49.40	0.618		
2190	47	851	51.68	0.718		
2310	50	852	55.21	0.958		
2370	51	853	56.43	1.078		
2415	52	854	57.62	1.168		
2650	55	858	61.45	1.638		
2870	58	860	65.30	2.078		
3020	60	860	67.91	2.378		
3200	61	860	69.48	2.738		
3500	61	860	70.23	3.338		
3600	61	860	70.48	3.538		

Table C.2: Direct shear test on clean loose sand σ_n=279 kPa

Date of Testing.....:March 7th, 1989
Tested by.....:Faouzi Ben Amor
Type of Sample.....:Clean Loose Sand
Type of Interface.....:Direct shear
Normal Load.....:162 lbs
Density.....:1.35 g/cc
Void ratio.....:
Dial (2) Constant.....:0.002 mm/div
Dial (3) Constant.....:0.002 mm/div
Proving Ring Constant.....:0.85 lb/div
Notes.....:

(1) Disp reading	(2) Load reading	(3) Vertical reading	(4) Dev(kPa) calcul	(5) Shear Strain	(6) Vol Strain	(7) pwp(kPa) calcul
1900	2	1110	2.19	0		
1901	5	1118	5.47	0.002		
1907	10	1118	10.94	0.014		
1917	20	1118	21.89	0.034		
1928	30	1118	32.85	0.056		
1935	35	1118	38.33	0.07		
1943	40	1118	43.82	0.086		
1953	45	1118	49.32	0.106		
1965	50	1118	54.82	0.13		
1975	55	1118	60.32	0.15		
1985	60	1118	65.83	0.17		
1995	65	1118	71.34	0.19		
2007	70	1118	76.85	0.214		
2028	75	1118	82.40	0.256		
2040	80	1118	87.93	0.28		
2055	85	1118	93.48	0.31		
2075	90	1118	99.04	0.35		
2105	95	1119	104.65	0.41		
2140	100	1120	110.29	0.48		
2170	105	1120	115.92	0.54		
2235	110	1123	121.72	0.67		
2310	115	1125	127.58	0.82		
2411	120	1130	133.59	1.022		
2530	125	1132	139.73	1.26		
2700	130	1133	146.18	1.6		
2900	135	1133	152.86	2		
3100	138	1133	157.36	2.4		
3320	140	1133	160.90	2.84		
3500	140.5	1133	162.51	3.2		

Table C.3: Direct shear test on clean loose sand σ_n=452 kPa

Date of Testing.....:APRIL 6TH, 1989
Tested by.....:Faouzi Ben Amor
Type of Sample.....:Clean Loose Sand
Type of Interface.....:Direct shear
Normal Load.....:262 LBS
Density.....:1.38 G/CC
Void ratio.....:
Dial (2) Constant.....:0.002 mm/div
Dial (3) Constant.....:0.002 mm/div
Proving Ring Constant.....:0.85 lb/div
Notes.....:

(1) Disp reading	(2) Load reading	(3) Vertical reading	(4) Dev(kPa) calcul	(5) Shear Strain	(6) Vol Strain	(7) pwp(kPa) calcul
1880	6	710	6.52	0		
1881	15	710	16.29	0.002		
1881	25	710	27.16	0.002		
1882	35	711	38.02	0.004		
1883	50	711	54.31	0.006		
1885	60	712	65.18	0.01		
1895	75	713	81.50	0.03		
1909	85	715	92.42	0.058		
1927	95	718	103.35	0.094		
1953	105	719	114.33	0.146		
1994	120	719	130.85	0.228		
2028	130	719	141.91	0.296		
2068	140	720	153.04	0.376		
2106	150	723	164.18	0.452		
2150	155	728	169.91	0.54		
2175	160	730	175.54	0.59		
2232	170	738	186.88	0.704		
2300	180	744	198.33	0.84		
2360	190	750	209.79	0.96		
2448	200	756	221.50	1.136		
2532	210	760	233.25	1.304		
2795	220	766	246.61	1.83		
3050	225	771	254.48	2.34		
3300	226	771	257.89	2.84		
3500	226	773	259.74	3.24		

Table C.4: Interface concrete clean loose sand σ_n=107 kPa

Date of Testing.....:March 7th, 1989
Tested by.....:Faouzi Ben Amor
Type of Sample.....:Clean Loose Sand
Type of Interface.....:Concrete
Normal Load.....:62 lbs
Density.....:1.35 g/cc
Void ratio.....:
Dial (2) Constant.....:0.002 mm/div
Dial (3) Constant.....:0.002 mm/div
Proving Ring Constant.....:0.85 lb/div
Notes.....:

(1) Disp reading	(2) Load reading	(3) Vertical reading	(4) Dev(kPa) calcul	(5) Shear Strain	(6) Vol Strain	(7) pwp(kPa) calcul
450	0	1000	0.00	0	0	
480	5	1002	5.44	0.06	0.022	
494	10	1002	10.88	0.088	0.035	
510	15	1003	16.33	0.12	0.04	
529	20	1004	21.78	0.158	0.058	
552	25	1005	27.25	0.204	0.104	
586	30	1007	32.74	0.272	0.172	
655	35	1011	38.28	0.41	0.31	
680	38	1011	41.60	0.46	0.36	
730	42	1014	46.06	0.56	0.46	
810	47	1017	51.68	0.72	0.62	
910	49	1021	54.07	0.92	0.82	
965	50	1021	55.27	1.03	0.93	
1030	52	1021	57.61	1.16	1.06	
1180	54	1022	60.14	1.46	1.36	
1240	57	1022	63.62	1.58	1.48	
1320	58	1022	64.91	1.74	1.64	
1430	59	1022	66.29	1.96	1.86	
1570	59	1022	66.61	2.24	2.14	
1840	61	1022	69.53	2.78	2.68	
2010	61	1022	69.96	3.12	3.02	
2150	61	1022	70.31	3.4	3.3	

Table C.5: Interface concrete clean loose sand σ_n=279 kPa

Date of Testing.....:APRIL 6TH, 1989
Tested by.....:FAOUZI BEN AMOR
Type of Sample.....:CLEAN LOOSE SAND
Type of Interface.....:CONCRETE-CLEAN SAND
Normal Load.....:162 LBS
Density.....:1.39 G/CC
Void ratio.....:
Dial (2) Constant.....:0.002 MM/DIV
Dial (3) Constant.....:0.002 MM/DIV
Proving Ring Constant.....:0.833 LBS/DIV
Notes.....:

(1) Disp reading	(2) Load reading	(3) Vertical reading	(4) Dev(kPa) calcul	(5) Shear Strain	(6) Vol Strain	(7) pwp(kPa) calcul
1720	4	0	4.26	0	0	
1724	20	1	21.30	0.008	0.002	
1732	30	2	31.96	0.024	0.004	
1741	40	4	42.62	0.042	0.008	
1753	50	7	53.30	0.066	0.014	
1778	60	12	64.02	0.116	0.024	
1823	70	24	74.80	0.206	0.048	
1865	80	24	85.61	0.29	0.048	
1919	90	25	96.49	0.398	0.05	
1955	95	26	101.97	0.47	0.052	
2010	100	29	107.54	0.58	0.058	
2035	105	30	113.01	0.63	0.06	
2092	110	37	118.63	0.744	0.074	
2185	115	44	124.42	0.93	0.088	
2255	120	50	130.14	1.07	0.1	
2400	124	66	135.15	1.36	0.132	
2500	126	70	137.81	1.56	0.14	
2570	131	74	143.63	1.7	0.148	
2800	136	81	150.32	2.16	0.162	

Table C.6: Interface concrete clean loose sand σ_n=452 kPa

Date of Testing.....:MARCH 30, 1989
Tested by.....:FAOUZI BEN AMOR
Type of Sample.....:CLEAN LOOSE SAND
Type of Interface.....:CONCRETE-CLEAN SAND
Normal Load.....:262 LBS
Density.....:1.37 G/CC
Void ratio.....:
Dial (2) Constant.....:0.002 MM/DIV
Dial (3) Constant.....:0.002 MM/DIV
Proving Ring Constant.....:0.833 LBS/DIV
Notes.....:

(1) Disp reading	(2) Load reading	(3) Vertical reading	(4) Dev(kPa) calcul	(5) Shear Strain	(6) Vol Strain	(7) pwp,kPa) calcul
6	1935	600	6.39	0	0	
15	1940	600	15.98	0.01	0	
25	1947	600	26.63	0.024	0	
35	1957	601	37.30	0.044	0.002	
50	1975	601	53.31	0.08	0.002	
60	1988	602	64.00	0.106	0.004	
70	2006	603	74.72	0.142	0.006	
80	2027	605	85.45	0.184	0.01	
90	2050	607	96.21	0.23	0.014	
100	2076	610	106.99	0.282	0.02	
110	2108	615	117.82	0.346	0.03	
120	2145	620	128.70	0.42	0.04	
130	2200	630	139.68	0.53	0.06	
140	2260	644	150.74	0.65	0.088	
145	2310	652	156.39	0.75	0.104	
155	2385	661	167.61	0.9	0.122	
161	2450	667	174.48	1.03	0.134	
170	2505	673	184.59	1.14	0.146	
175	2585	682	190.54	1.3	0.164	
180	2660	689	196.50	1.45	0.178	
187	2760	696	204.85	1.65	0.192	
190	2910	706	209.23	1.95	0.212	
192	3000	712	212.11	2.13	0.224	
195	3130	720	216.41	2.39	0.24	
198	3350	728	221.46	2.83	0.256	

Table C.7: Interface concrete-oil cont. loose sand σ_n=107 kPa

```
Date of Testing.....:March 7th, 1989
Tested by...........:Faouzi Ben Amor
Type of  Sample.....:Oil Contaminated Loose Sand
Type of Interface...:Concrete
Normal   Load.......:62 lbs
Density.............:1.35 g/cc
Void ratio..........:
Dial (2) Constant...:0.002 mm/div
Dial (3) Constant...:0.002 mm/div
Proving Ring Constant:0.85 lb/div
Notes...............:
```

(1) Disp reading	(2) Load reading	(3) Vertical reading	(4) Dev(kPa) calcul	(5) Shear Strain	(6) Vol Strain	(7) pwp(kPa) calcul
400	0	2300	0.00	0		
412	10	2300	10.94	0.040067		
436	15	2300	16.43	0.1202		
473	25	2304	27.42	0.24374		
523	30	2310	32.96	0.410684		
610	33	2319	36.36	0.701169		
660	35	2323	38.63	0.868114		
720	38	2325	42.03	1.068447		
805	41	2331	45.48	1.352254		
915	44	2337	48.99	1.719533		
1050	45	2343	50.34	2.170284		
1150	46	2345	51.63	2.504174		
1270	47	2346	52.98	2.904841		
1350	47	2346	53.13	3.171953		
1420	48	2346	54.39	3.405676		
1600	48	2346	54.74	4.006678		

Table C.8: Interface concrete-oil cont. loose sand σ_n=279 kPa

Date of Testing.....:April, 6th, 1989
Tested by.....:FAOUZI BEN AMOR
Type of Sample.....:OIL CONTAMINATED LOOSE
Type of Interface.....:CONCRETE
Normal Load.....:162 LBS
Density.....:1.37 G/CC
Void ratio.....:
Dial (2) Constant.....:0.002 MM/DIV
Dial (3) Constant.....:0.002 MM/DIV
Proving Ring Constant.....:0.85 LB/DIV
Notes.....:

(1) Disp reading	(2) Load reading	(3) Vertical reading	(4) Dev(kPa) calcul	(5) Shear Strain	(6) Vol Strain	(7) pwp(kPa) calcul
1870	3	1100	0.00	0		
1873	30	1100	27.90	0.006		
1887	40	1102	38.25	0.034		
1914	50	1104	48.63	0.088		
1950	60	1105	59.04	0.16		
1990	70	1106	69.49	0.24		
2047	80	1107	80.02	0.354		
2080	85	1109	85.31	0.42		
2122	90	1112	90.64	0.504		
2163	95	1112	95.98	0.586		
2217	100	1112	101.38	0.694		
2312	105	1112	106.95	0.884		
2480	114	1112	117.06	1.22		
2505	115	1112	118.21	1.27		
2640	118	1113	121.94	1.54		
2720	120	1115	124.40	1.7		
3000	126	1120	132.05	2.26		
3250	129	1122	136.45	2.76		
3600	130.5	1122	139.79	3.46		

Table C.9: Interface concrete-oil cont. loose sand σ_n=452 kPa

```
Date of Testing.....:April, 6th, 1989
Tested by...........:FAOUZI BEN AMOR
Type of  Sample.....:OIL CONTAMINATED LOOSE
Type of Interface...:CONCRETE
Normal   Load.......:262 LBS
Density.............:1.40 G/CC
Void ratio..........:
Dial (2) Constant...:0.002 MM/DIV
Dial (3) Constant...:0.002 MM/DIV
Proving Ring Constant:0.85 LB/DIV
Notes...............:
```

(1) Disp reading	(2) Load reading	(3) Vertical reading	(4) Dev(kPa) calcul	(5) Shear Strain	(6) Vol Strain	(7) pwp(kPa) calcul
1741	6	300	3.10	0	0	
1742	10	300	7.23	0.002	0	
1743	30	301	27.89	0.004	0.002	
1746	40	301	38.23	0.01	0.002	
1751	50	302	48.57	0.02	0.004	
1764	60	305	58.93	0.046	0.01	
1784	70	312	69.32	0.086	0.024	
1805	80	317	79.72	0.128	0.034	
1834	90	321	90.16	0.186	0.042	
1868	100	326	100.64	0.254	0.052	
1910	110	331	111.17	0.338	0.062	
1960	120	340	121.76	0.438	0.08	
2020	130	350	132.43	0.558	0.1	
2090	140	357	143.20	0.698	0.114	
2160	150	364	154.02	0.858	0.128	
2260	160	377	165.05	1.038	0.154	
2390	170	390	176.34	1.298	0.18	
2475	175	396	182.15	1.468	0.192	
2590	180	404	188.19	1.698	0.208	
2700	185	413	194.24	1.918	0.226	
2870	190	421	200.75	2.258	0.242	
3180	195	431	208.36	2.878	0.262	
3350	196	435	210.70	3.218	0.27	
3600	196	439	212.58	3.718	0.278	
3700	196.5	441	213.89	3.918	0.282	
3800	196.5	442.5	214.66	4.118	0.285	

Table C.10: Interface steel-clean loose sand σ_n=107 kPa

Date of Testing.....:March 7th, 1989
Tested by.....:Faouzi Ben Amor
Type of Sample.....:Clean Loose Sand
Type of Interface.....:Steel
Normal Load.....:62 lbs
Density.....:1.40 g/cc
Void ratio.....:
Dial (2) Constant.....:0.002 mm/div
Dial (3) Constant.....:0.002 mm/div
Proving Ring Constant.....:0.85 lb/div
Notes.....:

(1) Disp reading	(2) Load reading	(3) Vertical reading	(4) Dev(kPa) calcul	(5) Shear Strain	(6) Vol Strain	(7) pwp(kPa) calcul
1639	3	660	3.28	0		
1691	10	660	10.96	0.173623		
1703	15	658	16.44	0.213689		
1723	20	664	21.94	0.280467		
1751	25	666	27.45	0.373957		
1819	30	666	33.02	0.601002		
2000	35	679	38.75	1.205342		
2145	36	688	40.06	1.689482		
2570	36.5	696	41.21	3.108514		
2730	36.2	700	41.10	3.642738		
3000	36	703	41.26	4.54424		
3200	35.5	704	40.97	5.21202		

Table C.11: Interface steel-clean loose sand σ_n=279 kPa

Date of Testing.....:March 7th, 1989
Tested by.....:Faouzi Ben Amor
Type of Sample.....:Clean Loose Sand
Type of Interface.....:Steel
Normal Load.....:162 lbs
Density.....:1.35 g/cc
Void ratio.....:
Dial (2) Constant.....:0.002 mm/div
Dial (3) Constant.....:0.002 mm/div
Proving Ring Constant.....:0.85 lb/div
Notes.....:

(1) Disp reading	(2) Load reading	(3) Vertical reading	(4) Dev(kPa) calcul	(5) Shear Strain	(6) Vol Strain	(7) pwp(kPa) calcul
1850	5	626	5.47	0.000		
1857	15	626	16.41	0.014		
1858	30	626	32.82	0.016		
1868	40	628	43.77	0.036		
1890	50	628	54.74	0.080		
1923	60	628	65.73	0.146		
1956	65	628	71.26	0.212		
1984	70	630	76.78	0.268		
2017	75	632	82.32	0.334		
2054	80	638	87.87	0.408		
2120	85	645	93.49	0.540		
2180	88	651	96.91	0.660		
2268	90	658	99.28	0.836		
2450	90	667	99.65	1.200		
2510	90.5	669	100.33	1.320		
2570	91	670	101.00	1.440		
2690	90	673	100.14	1.680		
2800	90	675	100.36	1.900		
2875	91.5	677	102.19	2.050		
3015	92	679	103.04	2.330		
3130	91.5	680	102.73	2.560		
3230	91	682	102.37	2.760		

Table C.12: Interface steel-clean loose sand σ_n=452 kPa

```
Date of Testing.....:March 7th, 1989
Tested by...........:Faouzi Ben Amor
Type of  Sample.....:Clean Loose Sand
Type of Interface...:Steel
Normal   Load.......:262 lbs
Density.............:1.33 g/cc
Void ratio..........:
Dial (2) Constant...:0.002 mm/div
Dial (3) Constant...:0.002 mm/div
Proving Ring Constant:0.85 lb/div
Notes...............:
```

(1) Disp reading	(2) Load reading	(3) Vertical reading	(4) Dev(kPa) calcul	(5) Shear Strain	(6) Vol Strain	(7) pwp(kPa) calcul
1850	2	872	2.13	0.000		
1853	10	872	10.65	0.006		
1863	20	872	21.31	0.026		
1866	30	873	31.96	0.032		
1870	40	873	42.62	0.040		
1880	50	873	53.30	0.060		
1888	55	873	58.64	0.076		
1904	65	876	69.34	0.108		
1917	75	876	80.04	0.134		
1935	85	876	90.77	0.170		
1950	90	876	96.16	0.200		
1966	95	876	101.56	0.232		
2000	105	879	112.38	0.300		
2023	110	882	117.82	0.346		
2068	120	886	128.73	0.436		
2100	125	890	134.24	0.500		
2130	130	892	139.75	0.560		
2200	135	900	145.48	0.700		
2270	140	908	151.23	0.840		
2370	142	914	153.92	1.040		
2440	145	918	157.55	1.180		
2510	146	921	159.02	1.320		
2700	145.5	928	159.53	1.700		
2800	146	931	160.64	1.900		
2900	146.5	934	161.76	2.100		

Table C.13: Interface concrete oil cont. loose sand σ_n=107 kPa

Date of Testing.....:March 7th, 1989
Tested by.....:Faouzi Ben Amor
Type of Sample.....:Oil Contaminated Loose Sand
Type of Interface.....:Steel
Normal Load.....:62 lbs
Density.....:1.35 g/cc
Void ratio.....:
Dial (2) Constant.....:0.002 mm/div
Dial (3) Constant.....:0.002 mm/div
Proving Ring Constant.....:0.85 lb/div
Notes.....:

(1) Disp reading	(2) Load reading	(3) Vertical reading	(4) Dev(kPa) calcul	(5) Shear Strain	(6) Vol Strain	(7) pwp(kPa) calcul
1900	2	700	2.19	0		
1913	5	701	5.47	0.044068		
1930	10	701	10.95	0.101695		
1949	15	701	16.44	0.166102		
1980	20	701	21.94	0.271186		
2010	23	701	25.25	0.372881		
2035	25	701	27.47	0.457627		
2078	27	702	29.72	0.60339		
2175	30	707	33.13	0.932203		
2285	32	715	35.47	1.305085		
2382	33	722	36.70	1.633898		
2485	34	727	37.95	1.983051		
2690	35	734	39.34	2.677966		
2900	35	744	39.63	3.389831		
3100	35	753	39.91	4.067797		

Table C.14: Interface steel-oil cont. loose sand σ_n=279 kPa

Date of Testing.....:March 7th, 1989
Tested by.....:Faouzi Ben Amor
Type of Sample.....:Oil Contaminated Loose Sand
Type of Interface.....:Steel
Normal Load.....:162 lbs
Density.....:1.32 g/cc
Void ratio.....:
Dial (2) Constant.....:0.002 mm/div
Dial (3) Constant.....:0.002 mm/div
Proving Ring Constant.....:0.85 lb/div
Notes.....:

(1) Disp reading	(2) Load reading	(3) Vertical reading	(4) Dev(kPa) calcul	(5) Shear Strain	(6) Vol Strain	(7) pwp(kPa) calcul
1220	0	1100	0.00	-0.96		
1770	4	1100	4.26	0		
1775	10	1100	10.65	0.01		
1782	15	1100	15.98	0.024		
1792	25	1100	26.63	0.044		
1800	30	1100	31.96	0.06		
1812	35	1102	37.30	0.084		
1824	40	1103	42.64	0.108		
1835	45	1105	47.98	0.13		
1850	50	1105	53.33	0.16		
1865	55	1106	58.68	0.19		
1905	62	1109	66.20	0.27		
1950	70	1110	74.81	0.36		
1970	73	1111	78.05	0.4		
2000	75	1113	80.23	0.46		
2060	81	1114	86.75	0.58		
2160	86	1114	92.30	0.78		
2210	88	1114	94.54	0.88		
2340	90	1121	96.94	1.14		
2560	92	1125	99.54	1.58		
2700	93	1127	100.91	1.86		
2900	94	1127	102.41	2.26		
3200	94	1127	103.04	2.86		

Table C.15: Interface steel-oil cont. loose sand σ_n=452 kPa

Date of Testing.....:March 7th, 1989
Tested by.....:Faouzi Ben Amor
Type of Sample.....:Oil Contaminated Loose Sand
Type of Interface.....:Steel
Normal Load.....:262 lbs
Density.....:1.35 g/cc
Void ratio.....:
Dial (2) Constant.....:0.002 mm/div
Dial (3) Constant.....:0.002 mm/div
Proving Ring Constant.....:0.85 lb/div
Notes.....:

(1) Disp reading	(2) Load reading	(3) Vertical reading	(4) Dev(kPa) calcul	(5) Shear Strain	(6) Vol Strain	(7) pwp(kPa) calcul
1746	6	1150	6.39	0		
1747	10	1150	10.65	0.002		
1753	15	1150	15.97	0.014		
1757	20	1150	21.30	0.022		
1763	30	1150	31.96	0.034		
1778	40	1150	42.62	0.064		
1797	50	1150	53.30	0.102		
1824	60	1150	63.99	0.156		
1838	65	1150	69.34	0.184		
1852	70	1150	74.70	0.212		
1868	75	1151	80.06	0.244		
1887	80	1194	85.43	0.282		
1930	90	1197	96.19	0.368		
1960	100	1205	106.94	0.428		
2020	110	1210	117.78	0.548		
2060	115	1211	123.23	0.628		
2100	120	1211	128.69	0.708		
2153	125	1211	134.20	0.814		
2200	130	1210	139.70	0.908		
2300	135	1213	145.36	1.108		
2440	140	1222	151.17	1.388		
2600	145	1273	157.08	1.708		
2700	146	1276	158.49	1.908		
2800	148	1279	160.99	2.108		
3000	149.5	1283	163.29	2.508		
3250	150.5	1284	165.23	3.008		